University of Southampton

School of Engineering

Young Researchers Conference 2024

ABSTRACTS

1. **Adnan Akhtar** - Development of La-based perovskite as a plausible oxygen carrier- sorbent for sorption enhanced chemical looping process
2. **Esma Akis** - Objective Measures of Auditory Temporal Resolution Using Auditory Brainstem Response
3. **Ghadah Aljarboa** - Investigating The Effect of Hearing Aid Envelope Distortion on Cortical Responses to Continuous Speech
4. **Ahmed AL-Shuaili** - Ex-post assessment of transport interventions: The case of Southampton and Solent Future Transport Zone (SFTZ) region, using a difference-in-differences quasi-experimental approach
5. **Yousif Alyousif** - Impact of fatigue overloads on crack advancement mechanisms in a polycrystalline nickel-based superalloy
6. **Zia Ullah Arif** - 3D printing of bio-based polymers for lightweight micro-porous structures
7. **Beth Austin** - Active control of a tuned vibration absorber for use in metamaterial applications
8. **Ismail Aydemir** - Reducing the Transport Footprint of Pathology Logistics through Shared-Fleet Passenger and Freight Services: A Case Study on the Isle of Wight, UK
9. **Abigail H. Bateman** - Simplified "*m-θ*" curves for predicting non-linear lateral pile response: incorporating post-peak softening behaviour
10. **Joseph S. P. Binns** - Part-Span Approximation of Non-Linear Tone Noise Propagation in An Aeroengine Intake
11. **Hesam Boroomand** - Dynamic ankle joint angle assessment in daily living activities using the Madgwick algorithm
12. **Lois Brewer** - Developing a modelling framework for the transfer of immunoglobulin G across the human placenta
13. **Fengyuan Cao** - Study of multi-junction Bismuth based perovskite solar cell
14. **Rebecca Cheetham** - Antibody-conjugated Polymersomes for Targeted Antibiotic Delivery to Intracellular B. thailandensis
15. **Bethan Collins** - Tribological testing and crystallographic analysis of high hardness, ultra-low friction Mo-S-C thin film coatings with self-assembling tribolayers
16. **Jamie J. Crispin** - Analytical solution for settlement of pile groups in inhomogeneous soils
17. **Kirstie M. Devin** - Exploration of flexible open-cell mechanical metamaterials
18. **Zizhou Ding** - The application of data-driven methods in assessing and modelling extended endplate connections
19. **Joseph C. Doyle** - Effects of frequency and dwell on the fatigue crack propagation in single crystal Ni-based superalloys CMSX-4 and CMSX-10 at intermediate service temperature
20. **Oliver Gould** - Foam layer composition mechanical properties and the performance implication for wheelchair cushions
21. **Joshua Hooper** - Pipeline Leak Location Using Sensor Arrays
22. **Saeed Hosseinzadeh** - Experimental investigation of the impact of leeway and rudder angles on the yaw moment balance for wind-propelled ships
23. **Matthew Hulbert** - Effects of Build Orientation on Fatigue Crack Growth in Laser Powder Bed Fusion IN718
24. **Kimoon Jang** - Forecasting Transhipment Volume and Analysing Dynamics given Geopolitical and Health Events: A Case Study of the Port of Busan on a Specific Maritime Shipping Route
25. **Karam Kalsi** - Synergy of tidal power and flood alleviation in UK estuaries
26. **Ahmet Nihat Karci** - Investigation of Green Hypergolic Chemical Bipropellant Propulsion Systems
27. **Asadullah Khan** - Development of a low-cost Paper-Based Point of Care Device for Blood Glucose Detection
28. **Bursa Kocak Erdem** - Stimulus Duration Effects on VEMP Responses at 125 Hz and 500 Hz
29. **Dariusz Kosk** - Perfusion chamber for the investigation of microbubble oscillation in bone fractures
30. **Changhoon Lee** - Regional discrepancies of transportation investment appraisal outcomes in South Korea

ABSTRACTS

31. **Yeajin Lee** - Advancing characterisation of fibre break interaction via in situ synchrotron tomography and Digital Volume Correlation
32. **Kenneth Leung** - Vibro-acoustic Metamaterial With an Embedded Helmholtz Resonator
33. **Daniel Li** - A holistic approach towards incorporating and/or improving the green sustainability of chemical process plant systems
34. **Donnchadh MacGarry** - Flow Over an Array of Very Tall Buildings with Random Heights
35. **Imali Manikarachchige** - Integrating Qualitative Content Analysis into Quantitative Systems Modeling: A Methodological Approach for Understanding Dynamics in Fisheries Socio-Ecological Systems
36. **Soumyadeep Mondal** - Active Mechanical Metamaterials: On Optimal Voltage Efficiency
37. **Hamish Moodley** - The tension stiffening behaviour of stainless steel rebar
38. **Thomas F. Munro-O'Brien** - Performance comparison of a novel modular SPT-TAL type Hall effect thruster operating on Krypton
39. **Dibyojyoty Nath** - Ceramic-microbial fuel cell stacks for electricity and liquid fertilizer production for hydroponics
40. **Charalampos Nikolaou** - An investigation into the combination of passive acoustic treatments and active structural acoustic control.
41. **Molly Phillips** - Development of an in situ droplet microfluidic autonomous sensor for wide-range ocean alkalinity
42. **Tararag Pincam** - Conversion of organic wastes into biodegradable plastics: a dual and synergistic solution in a circular economy
43. **Rebecca Presswood** - Abstract: Push-out tests on austenitic stainless steel and carbon steel welded shear studs
44. **Lucas Queiroz Machado** - Ultrasound propagation in materials with elongated grains and preferred orientation
45. **Rosemary Reed** - Investigation into the mechanical performance of aluminium cold spray coated alloys
46. **Greg Sewell -** Predicting UK Domestic Electricity and Gas Consumption between Differing Demographic Household Compositions
47. **Aditi Sharma** - Origami-inspired tubular multi-functional metamaterials
48. **Aradhana Singh -** Electricity generation in Microbial Fuel cell through Biofilm Immobilization Techniques
49. **Sam Sloan** - Using High-Speed Imaging and Digital Image Correlation to Compare Microbubble-Induced Deformation in Stiff and Soft Cells
50. **Yutong Song** - PhD Research Plan: Learning-Based Multi-Agent Marine Vessel Non-Causal Control and Distributed Optimization for Ship Rescue Operations
51. **Katherine Theobald** - Assessing Vibration Risks For Medical Cargoes: A Comparative Analysis Of Electric And Combustion Engine Vans
52. **Ram Kumar Venkateswaran** - Estimation of the relative balance between the rotor and the OGV broadband noise in a turbofan engine
53. **Delin Wang -** What information do road users actually need to know?
54. **Tairan Wang** - Data-driven stochastic model updating with conditional invertible neural networks (cINNs)
55. **Hao Yao Wong** - Validation of Resin Embedding Protocols for Serial Block Face Scanning Electron Microscope of Human Tooth Dentine
56. **Niamh Yates** - Metal organic framework-based microfluidic paper-based analytical devices for detecting nutrients in water
57. **Muhammad Zalkifal** - Bioproducing succinic acid from hydrolysate of biomass waste in a biofilm reactor
58. **Ziliang Zhang** - Probabilistic Assessments of Load Carrying Capacity of Corroded Metallic and Reinforced Concrete (RC) Railway Bridges
59. **Kunyi Zheng** - Load transfer mechanisms for a transfemoral amputee during ambulation

KEYNOTE SPEAKERS

Prof. Stephen Turnock

Head of School of Engineering and Professor of Maritime Fluid Dynamics
University of Southampton

Expertise in the synthesis of computational, experimental and analytical methods applied to marine renewables, performance sport, maritime robotics, hydrodynamics and ship decarbonisation. I joined Ship Science in the University of Southampton in 1988 after a research position at MIT (Aero/Astro) and an engineering degree at Cambridge.

Abstract: Engineering excellence: maximising research impact

Explores how researchers can ensure their research has impact. What choices are made to balance fund raising, research, paper generation and tangible deliverables. Focus is on the UK context of the Research Evaluation Framework and its 7+ year cycle of assessment of outputs from paper quality and number, impact case studies and environmental metrics.

Dr Mark Raiss

MA, MSc, DIC, PhD, FREng, CEng, FICE, FIStructE, HonFRIBA
Consultant at Mark Raiss Consulting

Mark has a particular passion for the timely delivery of economic and buildable engineering solutions. He has extensive experience in major transportation infrastructure projects, both underground and elevated. He has led multi-disciplinary teams on projects in the UK, Ireland, Hong Kong, China, UAE, Saudi Arabia, Singapore and Malaysia. He has a world-class reputation for large and complex infrastructure projects. Mark was AECOM's Programme Director for the design of Crossrail - Europe's largest construction project at the time – including the detailed design of 2 major underground interchange stations, reference design for railway systems and independent checking of tunnels and stations. He was appointed as Managing Director for the AECOM legacy company, URS, in Hong Kong and South East Asia. On returning to the UK, he became AECOM's Programme Director for HS2 in the UK and Engineering Director for AECOM's design of the infrastructure for NEOM – a new city for 9m people in Saudi Arabia. Prior to its acquisition by AECOM, Mark was the Chairman of Benaim which specialised in value engineering, optimising designs and working with contractors. Mark is a Fellow of the Royal Academy of Engineering, an Honorary Fellow of the Royal Institute of British Architects, a Visiting Professor at the University of Bath, an occasional lecturer at the University of Cambridge. He has acted as an Expert on behalf of HS2, London Underground and contractors.

Abstract: Some personal thoughts about the benefits of doing a PhD

After graduating from Cambridge Mark went to work for Arup – sometimes known as the university for practicing engineers. Having spent 6 years working in the UK, Saudia Arabia and Hong Kong, Arup gave Mark leave of absence to undertake a Masters of Concrete Structures and Materials at Imperial College. Whilst he was there, Mark was offered a job to undertake a PhD into the Fracture Mechanics of Concrete – a fairly esoteric subject! The first 10 years of his career was really training for the remainder of his career. On completion of his PhD Mark joined Robert Benaim & Associates - a small offshoot from Arup. Whilst there he worked in the UK and Malaysia and rose to become Chairman of the Group, and, through a Management Buy-out, was a principal shareholder. Mark led the sale of Benaim to Scott Wilson in 2008 and within Scott Wilson he led the tenders for, and then the delivery of, a substantial part of Crossrail (now the Elizabeth Line). Scott Wilson was bought by URS who sent Mark to Hong Kong as MD of Hong Kong and South East Asia. URS was in turn acquired by AECOM and mark returned to the UK, rising to become the Engineering Director, Global Technical Excellence. In September 2024 Mark left AECOM to set up his own small consultancy - markraissconsulting.com.

Dr Sevil Payvandi

Environmental Fate Mechanistic Modeller, Syngenta

I am an environmental fate mechanistic modeller working in Product Safety at Syngenta, specialising in applying analytical and numerical modelling techniques to multidisciplinary challenges. I have an MEng Degree in Biomedical Engineering, and a PhD in mathematical modelling of blood flow in arteries, both conducted at Imperial College London. I continued in academia, first as a PostDoc at the University of Southampton, working on the optimisation of phosphate use in arable farming, and then as a PostDoc at Syngenta, researching modelling bioavailability dynamics within soils. I then became an environmental fate risk assessor and modeller before joining Research Predictive Sciences in 2022.

Abstract: It doesn't matter that plants don't have hearts – how mechanistic modelling can be applied to a variety of biological systems

This talk will provide an overview of the different research topics I have worked on and how the skills learnt from these topics are useful in industry.

In my academic career I have worked on topics ranging from mathematical modelling of flow in curved arteries to optimisation of the use of phosphate fertiliser in wheat plants. Whilst on the face of it these two topics are unrelated, the equations and techniques used to investigate these systems are the same and provided a 'toolbox' of skills useful for research in industry.

At Syngenta Group, which is a leading technology company for sustainable agricultural innovation, I work in Product Safety which is concerned with the safety of plant protection products in the human, ecological, and environmental domains. Within the environmental safety domain we consider the fate of compounds within the soil, groundwater and surface water an air. Modelling is a core part of the safety assessment, and, as an example, I will show a recent model for groundwater leaching screening developed in collaboration with the University of Southampton

KEYNOTE SPEAKERS

1. Development of La-based perovskite as a plausible oxygen carrier-sorbent for sorption enhanced chemical looping process

Adnan Akhtar
School of Chemistry and Chemical Engineering, University of Southampton, SO17 1BJ

Project Objectives and goals

$LaNiO_3$ as a viable Oxygen carrier (OC) has been extensively studied by substituting Ni with Co and Cu (de Santana Santos et al., 2021; Jiang et al., 2020). However, existing literature lacks any insights regarding modification of $LaNiO_3$ to attain the properties of an OC and Dual Functional material (DFM). Therefore, the objectives this work can be described as follows:

- This study aims to synthesize a novel bi-metallic doped $LaNiO_3$ perovskite to enhance its capabilities as hybrid OC-DFM in a sorption-enhanced chemical looping process.
- This research work is aimed to improve the oxygen transfer capacity and stability under several redox cycles by incorporating Mn on the B-site of perovskite.
- Kinetic analysis in isothermal and non-isothermal conditions were employed in this work to predict the reaction mechanism during redox reactions.

Description of method and results

In this study, a novel bi-metallic doped $LaNiO_3$ perovskite was synthesized via conventional sol-gel process, followed by doping with varying compositions of Ca and Mn through wet impregnation method. This tailored perovskite material was specifically designed for the application within sorption-enhanced chemical looping (SE-CL) technique through Reverse Water Gas Shift reaction. The surface area of as-prepared oxy sorbent was analysed using BET while material's morphology was assessed using SEM. Additionally, the crystalline phase pattern and metallic composition were investigated through XRD and EDX respectively. SEM and BET analyses revealed the presence of perovskite and porous structure of oxygen carrier, while EDX analysis indicated the presence of metal doping under varying composition which was also confirmed through ICP analysis. To assess redox properties of catalyst, TGA was used. The metallic doped perovskite material was subjected to 33 consecutive reduction and oxidation cycles in TGA over a range of temperatures (600-900°C). The material demonstrated excellent stability over multiple cycles and exhibited its highest oxygen transfer capacity at 1.745 mmol/g. The material also showed less than 1% degradation under 33 cycles, showing significant improvement over previous work that incorporated La-Ni based perovskites (Zaidi et al., 2024). In addition, this study is also focused on the assessment of kinetics during redox reactions by utilizing as prepared perovskite type under isothermal and non-isothermal conditions. The influence of temperature and composition of gases were investigated, and conversion was assessed with 11 different solid-state models. The findings of kinetic parameters showed that growth nucleation models (Avrami-Erofeev) and Diffusion model (Jander 3D) were in close agreement with experimental data under isothermal and non-isothermal conditions. Therefore, the material indicated its potential as promising oxy sorbent to scale up SE-CL technique which could be further examined on a reactor scale.

References

de Santana Santos, M., Frety, R., Lisi, L., Cimino, S., Teixeira Brandão, S., 2021. LaNi1-xCoxO3 perovskites for methane combustion by chemical looping. Fuel 292, 120187.

Jiang, Q., Cao, Y., Liu, X., Zhang, H., Hong, H., Jin, H., 2020. Chemical Looping Combustion over a Lanthanum Nickel Perovskite-Type Oxygen Carrier with Facilitated O2– Transport. Energy & Fuels 34, 8732–8739.

Zaidi, A., de Leeuwe, C., Spallina, V., 2024. Bi-metallic Ni–Fe LSF perovskite for chemical looping hydrogen application. Powder Technol 436, 119510.

Collaborators

Christopher De Leeuwe (Department of Chemical Engineering, University of Manchester)

Adam Zaidi (Department of Chemical Engineering, University of Manchester)

Further Information

Student: Adnan Akhtar (A.Akhtar@soton.ac.uk)

Supervisor: Dr. Syed Zaheer Abbas (s.z.abbas@soton.ac.uk)

Co-supervisor: Dr Mohamed Hassan- Sayed (M.G.HassanSayed@soton.ac.uk)

2. Objective Measures of Auditory Temporal Resolution Using Auditory Brainstem Response

Esma Akis[1], Steven Bell[1], David Simpson[1]
[1] Institute of Sound and Vibration Research, University of Southampton, Southampton, UK

Project Objectives and Goals:

This study aims to develop objective methods for measuring auditory temporal resolution using Auditory Brainstem Responses (ABR). Temporal resolution, crucial for speech comprehension, is typically reported to range between 2-4 milliseconds in normal-hearing adults (Musiek *et al.*, 2005; Moore, 2012; Filippini *et al.*, 2020). Understanding auditory temporal resolution is especially important for addressing hearing difficulties in noisy environments, which can worsen with age. Traditional hearing tests do not assess temporal resolution, and behavioural tests are impractical for some populations. The primary goal is to investigate forward and backward masking techniques with ABR to provide objective measures of temporal resolution and deepen the understanding of the underlying neural pathways.

Description of Method and Results:

The experiment employed forward and backward masking paradigms in ABR. Silent gaps were introduced between noise and a click stimulus, with epoch durations ranging from 50 to 70 milliseconds. Gap durations varied from 0 to 20 milliseconds for forward masking, and from 0 to 4 milliseconds for backward masking. Data were collected from 20 participants with normal hearing, aged 27.85 ± 3.09 years.

ABR presence was analysed using four statistical detection methods: F_{sp} with bootstrap, Hotelling's T^2 with/without bootstrap, and peak-to-peak amplitude estimation with bootstrap.

Figure 1. A schematic illustration of the ABR paradigms: forward and backward masking.

Results:

In the forward masking condition, the ABR amplitude decreased as gap duration approached temporal resolution thresholds. The average objective threshold for forward masking was 3.30 Ⓟ 1.80 ms, consistent with literature reports of temporal resolution thresholds. Backward masking, however, did not produce significant changes in ABR amplitude across varying gap durations, showing high detection rates regardless of gap duration. This indicates that ABR is not sensitive to backward masking, suggesting that backward masking does not reflect temporal resolution at the brainstem level.

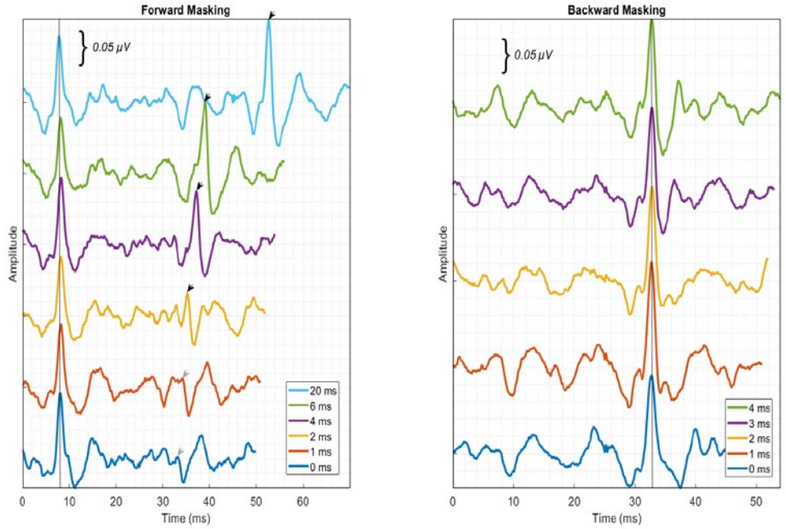

Figure 2. Grand average ABRs for Forward and Backward Masking paradigms across different gap durations. In forward masking, peaks just before 10 ms represent responses to noise onset, and the peaks with a black arrow represent the response to the clicks, which shift to the left and become smaller (due to masking) as the gap duration decreases. In the backward masking plot, peaks represent responses to clicks but no effect of making is seen.

Potential for Application of Results:

These findings hold potential for clinical applications. The forward masking paradigm combined with objective ABR detection methods could become a valuable tool for assessing auditory temporal resolution in populations for whom behavioural tests are impractical, such as children or older adults with cognitive impairments. Developing objective measures of temporal resolution may improve diagnostic capabilities and aid in tailoring auditory interventions, such as hearing aids or cochlear implants, to individual needs. Additionally, a deeper understanding of temporal resolution mechanisms could inform future auditory processing therapies.

References:

Filippini, R. et al. (2020) 'GIN test: a meta-analysis on its neurodiagnostic value', Journal of the American Academy of Audiology, 31(02), pp. 147-157.

Moore, B.C. (2012) An introduction to the psychology of hearing. Brill.

Musiek, F.E. et al. (2005) 'GIN (Gaps-In-Noise) test performance in subjects with confirmed central auditory nervous system involvement', Ear and hearing, 26(6), pp. 608-618.

3. Investigating The Effect of Hearing Aid Envelope Distortion on Cortical Responses to Continuous Speech

Ghadah Aljarboa

Assessing neural responses to continuous speech has gained attention in recent years as an objective tool for evaluating speech perception. However, information on the clinical feasibility of these measurements, particularly for assessing hearing aids, remains limited. While several studies have explored aided neural tracking of speech envelopes in individuals with hearing loss—primarily adults (Petersen et al., 2017, Vanheusden et al., 2020) and recently in children (Van Hirtum et al., 2023)—the specific relationship between envelope distortion and cortical responses has not been previously investigated. This study examines the impact of hearing aid-induced envelope distortion on the detectability of cortical responses to the International Speech Test Signal (ISTS). It also investigates the effects of stimulus intensity and attention on these responses.

Twenty-four normal-hearing adults participated in the study, with EEG data collected using a 32-channel BioSemi system during 15-minute recordings for each condition. ISTS stimuli were prerecorded from a KEMAR ear with and without hearing aids, and four conditions were analysed to assess the effects of hearing aid use with two different envelope diction levels, stimulus intensity, and attention. Neural responses were analysed using single channels through a cross-correlation approach, focusing on two main variables: detection rate and detection time.

Results indicated a significant reduction in response detection rate in the aided 70 dB condition with high envelope distortion (14/24) compared to the unaided 70 dB condition (22/24) (Fig.1). Additionally, detection time was significantly longer in the aided condition with high envelope distortion (11.3 ℗ 6.7 minutes) compared to the unaided condition (7.4 ℗ 6.6 minutes) (Fig 2). However, using the aided signal in the analysis, rather than the unaided signal, improved detectability in the high-distortion condition. No significant effects of attention or intensity level were observed on the measured responses.

In conclusion, cortical responses to continuous ISTS stimuli showed reduced detectability when aided, suggesting that signal processing methods and recording times may still need optimisation. Utilising the speech stimulus from the output of a hearing aid, as opposed to the input signal, shows potential for improving response detectability.

Figure 1: The detection rates of cortical responses measured from Cz Channel for the five conditions in the study.

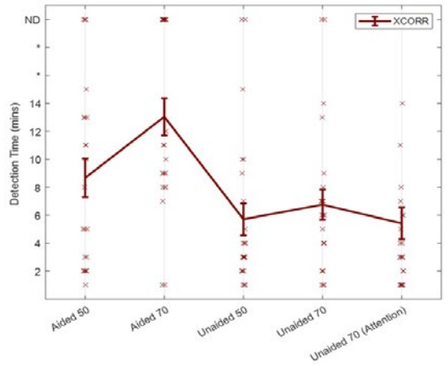

Figure 2: Mean and individual detection times from the XCOR analysis of Cz

Reference:

PETERSEN, E. B., WÖSTMANN, M., OBLESER, J. & LUNNER, T. 2017. Neural tracking of attended versus ignored speech is differentially affected by hearing loss. J Neurophysiol, 117, 18-27.

VAN HIRTUM, T., SOMERS, B., DIEUDONNÉ, B., VERSCHUEREN, E., WOUTERS, J. & FRANCART, T. 2023. Neural envelope tracking predicts speech intelligibility and hearing aid benefit in children with hearing loss. Hearing Research, 439, 108893.

VANHEUSDEN, F. J., KEGLER, M., IRELAND, K., GEORGA, C., SIMPSON, D. M., REICHENBACH, T. & BELL, S. L. 2020. Hearing Aids Do Not Alter Cortical Entrainment to Speech at Audible Levels in Mild-to-Moderately Hearing-Impaired Subjects. Front Hum Neurosci, 14, 109.

4. Ex-post assessment of transport interventions: The case of Southampton and Solent Future Transport Zone (SFTZ) region, using a difference-in-differences quasi-experimental approach

Ahmed AL-Shuaili[a]*, Prof. John Prestona,*
[a] School of Engineering, University of Southampton, Boldrewood Campus, Southampton So16 7QF,United Kingdom

The transport sector in Great Britain has a long history of developing transport interventions to reduce traffic and alleviate its impact; in recent years, much attention has been given to applying more strategies and policies for a more sustainable future. This paper investigates the long-term effects of transport interventions in Southampton and the Solent Future Transport Zone (SFTZ) region via a difference-in-differences (DiD) quasi-experimental approach. The aim is to identify what would happen within the treated area without these interventions and to assess how these initiatives have influenced the region's traffic patterns and sustainability efforts. By comparing Southampton (the intervention-treated area) with Basingstoke and Deane (a control area) following the implementation of the Local Sustainable Transport Fund (LSTF) in 2011 and extending the analysis to the SFTZ initiative that started in 2020—which is done by comparing the Solent region (the treated area) with Bournemouth, Christchurch and Poole (the control area)—this paper offers insights into the outcomes of these intervention policies. The study compares the treated and control groups via statistical methods to interpret two decades of historical data. The results of the counterfactual analysis indicate a notable reduction in traffic compared with what would otherwise have happened. The results highlight the value of such policies in reducing motorised traffic and promoting environmental sustainability. This paper contributes to transport policy evaluation by providing an empirical study to support the importance of such initiatives, highlighting the outcome with the use of a DiD approach.

*Authors E-mail addresses: A.Alshuaili@soton.ac.uk (A.AL-Shuaili), J.M.Preston@soton.ac.uk (Prof.J.Preston)

5. Impact of fatigue overloads on crack advancement mechanisms in a polycrystalline nickel-based superalloy

Y. Alyousif[1] (ya3g19@soton.ac.uk), E.A. Saunders[2] (edward.saunders@rolls-royce.com), S. Taylor[2] (susan.taylor@rolls-royce.com), Dr. J.C. Walker[1] (j.walker@soton.ac.uk), Prof. P.A.S. Reed[1] (P.A.Reed@soton.ac.uk)
[1] Engineering Materials Research Group, School of Engineering, University of Southampton, Highfield, Southampton, SO17 1BJ, UK
[2] Rolls-Royce plc., Materials — Failure Investigation, Bristol BS34 7QE, UK

Fatigue is the most common mode of failure in aerospace components, placing a great demand on the quality and reliability of analytical failure investigations. Fractography continues to be the most effective method of mapping and understanding the propagation history of a fatigue crack, thus motivating the need to further develop the mechanistic understanding of fatigue crack growth at the various stages of fatigue life.

One of the main fractographic markings used to characterise fatigue crack growth (FCG) are striations, where each marking can represent a single loading cycle, with their individual spacing's believed to indicate the local crack growth rate (da/dN). While fatigue striations have been known to be most prominent during stage II of fatigue crack propagation, they can also be observed at the early stages of crack growth, but the validity of assuming their spacing always directly represents da/dN has been questioned when used in failure investigations.

Inconel 718 (IN718) is a cast and wrought Ni-based superalloy commonly used in the manufacturing of high-pressure turbine discs in gas turbine engines due to their strong high temperature performance and excellent corrosion resistance. The temperature of these components can reach 600°C while having to withstand extended service times and high mechanical loads.

The microstructure of IN718 was characterised using optical and scanning electron microscopy (SEM) prior to mechanical testing. A carefully designed testing matrix, exploring different load ratios, loading frequencies and temperatures was employed to provide a variety of fracture surfaces to compare striation morphology and investigate their mechanistic origin. Striations have been measured and assessed using surface tilt reconstructions and sectioning studies.

The results of this work have shown that fatigue striation spacings are indicative of FCG rates in the stable Stage II region of fatigue at relatively high stress-intensity ranges (DK) (Figure 1), however at near threshold and low DK, the striation-like markings observed (Figure 2) bear little relation to loading cycles or FCG rate. These markings can therefore be considered a product of slip processes and be linked to the crystallographic mode of FCG seen at low stress intensity ranges, where the plastic zone size at the crack tip is small in comparison to the grain size of the material.

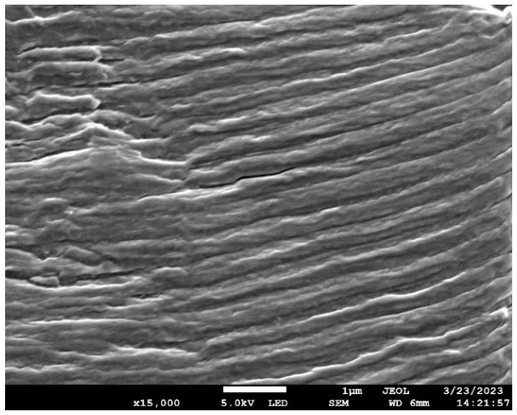

Figure 1: Striations at high ΔK.

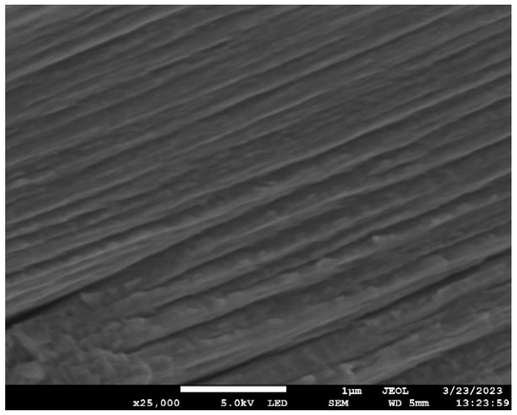

Figure 2: Striations at low ΔK.

6. 3D printing of bio-based polymers for lightweight micro-porous structures

Zia Ullah Arif[1], Andrew R. Hamilton[1]
[1]Department of Mechanical Engineering, School of Engineering, University of Southampton, Southampton, SO17 1BJ, UK
Author(s) email(s): zia.arif@soton.ac.uk; a.r.hamilton@soton.ac.uk

Project description

Petroleum-based materials are environmentally hazardous due to their non-biodegradability. Bio-based polymers, with their accessibility, biodegradability, and low cost, are emerging as sustainable alternatives for construction, shockproof packaging, and biomedical applications (Soykeabkaew et al., 2015; Ortega et al., 2022). Despite these advantages, fabricating customised micro-porous structures in low volumes remains challenging with conventional methods. The combination of 3D printing and bio-based polymers not only enables the fabrication of lightweight micro-porous structures but also promotes environmental sustainability (Andersson et al., 2021; Kalia et al., 2022; Suvanjumrat et al., 2024).

Project objectives and goals

The primary aim of this project is to use bio-based polymers such as starch and cellulose, particularly those derived from industrial and agri-food byproducts, to print in-situ micro-porous structures using a low-cost, easily accessible printer. Additionally, the biodegradable nature of these polymers, as shown in Fig. 1, will promote organic recycling, thereby eliminating associated recycling costs. Moreover, the instant formation of porous structures during printing (in-situ foam printing), as illustrated in Fig. 2, will enhance production speed, and reduce time-related costs.

Description of method and results

The research involves preparing small batches of bio-based formulations by blending starch with glycerol (as a plasticizer) and water (as a blowing agent) at high temperatures to form starch pellets. These pellets are then directly injected into a pellet-based 3D printer to evaluate their suitability for *in-situ* foam printing. Additionally, different bio-based formulations with varying moisture contents will be prepared, and their suitability for printing will be evaluated by assessing their rheological properties through nanoindentation. The extrusion behaviour of the formulations with superior rheological properties will be evaluated using the pellet-based printer. Finally, pellets demonstrating better extrusion performance will be used to print micro-porous structures, and their mechanical, foaming, and biodegradable properties will be investigated to ensure optimal mechanical strength, effective foaming behaviour, and excellent biodegradability suited for cushion-protective packaging.

Potential for application of results

Overall, this research project has the potential to produce customised compostable bio-based foams with good mechanical and foaming properties that will promote circular bioeconomy. In the future, this technology could enable the fabrication of large customised on-demand packaging for ecommerce businesses to protect sensitive equipment during transportation by mounting the pellet extruder on a robotic arm, thus, leading to large-format additive manufacturing.

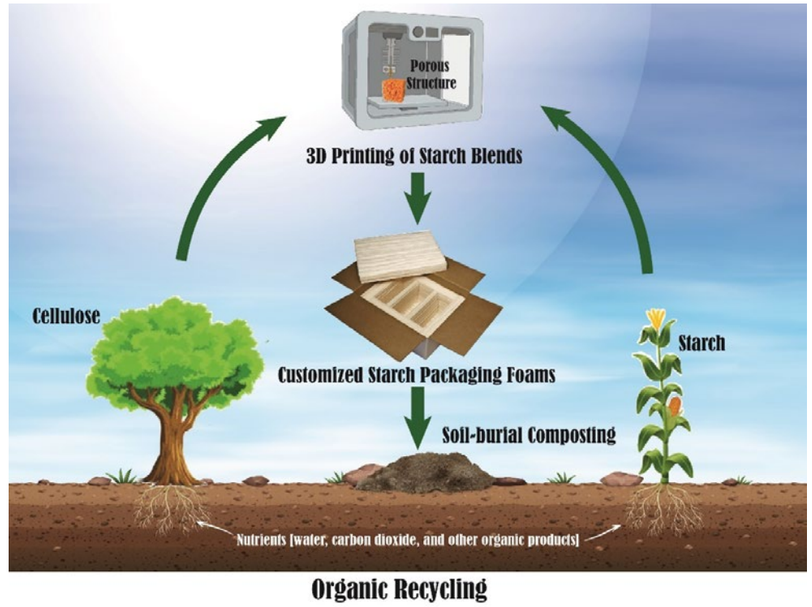

Figure 1: Primary aim of the research project

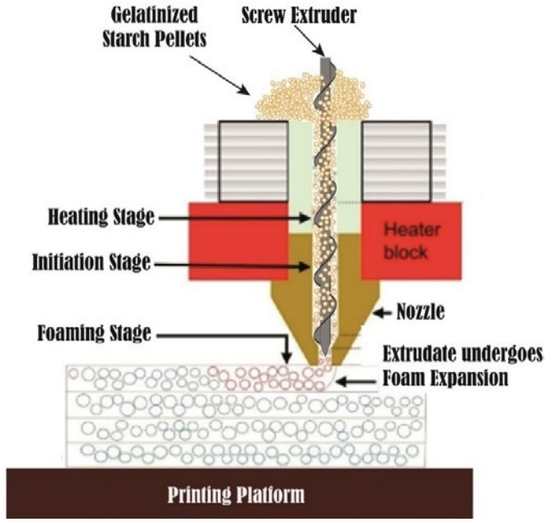

Figure 2: Schematics illustration of in situ fused granulate fabrication foam printing of starch blends

References

Andersson, H. et al. (2021) 'Variable low-density polylactic acid and microsphere composite material for additive manufacturing', Additive Manufacturing, 40, p. 101925.

Kalia, K. et al. (2022) 'In Situ Foam 3D Printing of Microcellular Structures Using Material Extrusion Additive Manufacturing', ACS Applied Materials & Interfaces, 14(19), pp. 22454–22465.

Ortega, F. et al. (2022) 'Biobased composites from agro-industrial wastes and by-products', Emergent Materials, 5(3), pp. 873–921.

Soykeabkaew, N., Thanomsilp, C. and Suwantong, O. (2015) 'A review: Starch-based composite foams', Composites Part A: Applied Science and Manufacturing, 78, pp. 246–263.

Suvanjumrat, C., et al. (2024) 'Additive manufacturing advancement through large-scale screw-extrusion 3D printing for precision parawood powder/PLA furniture production', Cleaner Engineering and Technology, 20, p. 100753.

6. 3D PRINTING OF BIO-BASED POLYMERS FOR LIGHTWEIGHT MICRO-POROUS STRUCTURES

7. Active control of a tuned vibration absorber for use in metamaterial applications

Beth Austin, Jordan Cheer
University of Southampton

Project objectives and goals

Tuned Vibration Absorbers (TVAs) are widely used in vibration control applications where control is required at a known frequency. However, they are ineffective away from this frequency, making them susceptible to issues regarding uncertainty. Prior work by Singleton et al. (2024) used arrays of these TVAs, each tuned to different frequencies, to reduce this problem. This work presented uses active control to change the tuning frequency and damping properties of a single resonator, shown in Fig. 1. The objectives of this work are to:

- Propose a TVA design that can be controlled using commercially available piezoceramic actuators.
- Simulate the response of the design to feedback control.
- Establish the maximum tuning range of the proposed design.

Description of method and results

The proposed TVA was simulated in COMSOL Multiphysics using the solid mechanics and piezoelectricity modules. The piezoceramic actuators were modelled based on the actuators used in the experimental implementation. The passive response of the system and the response to each of the piezo actuators being driven independently were simulated.

These simulated frequency responses were then used to model the response of the TVA to three different feedback regimes: displacement, velocity, and acceleration. MATLAB was used to calculate the closed loop response of the system to each control regime with both positive and negative gains. The limits of stability and the subsequent range of tuning frequencies, fo, and damping ratios, , were established. This range of tuning parameters is presented in Table 1.

Table 1: Tuning parameters at the stability limit of each control regime

Gain	f_0, Hz	ζ
No control	1030	0.024
h_a	660	0.027
$-h_a$	1450	0.015
h_v	1030	-
$-h_v$	1030	0.0015
h_d	1500	0.014
$-h_d$	650	0.030

Velocity feedback only affects damping. Positive gains increase the damping ratio whilst negative gains decrease the damping ratio. Positive feedback velocity control is theoretically unconditionally stable due to the use of collocated sensors and actuators hence there is no known upper limit to the damping ratio. Acceleration and displacement feedback both primarily affect the tuning frequency, with acceleration feedback decreasing this value and displacement feedback increasing it. This provides a theoretical tuning frequency range of 650 – 1500 Hz.

In practice, it will not be possible to perfectly predict the behaviour of the TVA and so it is unwise to run at the extremes of the stable region. Experimental validation is currently underway to validate the simulations presented and establish how close to the theoretical stability limits the system can run, subsequently finding the practically realizable range of tuning parameters.

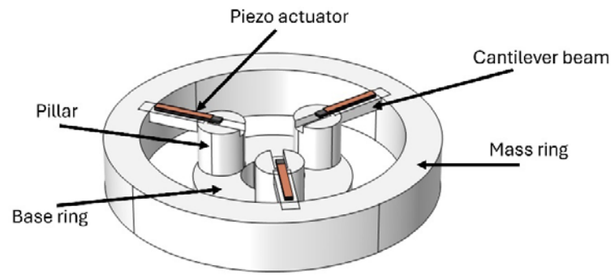

Figure 1 Proposed TVA design

References

Singleton, L., Cheer, J., Bastola, A., Tuck, C., & Daley, S. (2024). A robust optimised multi-material 3D inkjet printed elastic metamaterial. *Applied Acoustics*, *216*, 109796.

Funding body

Intelligent Structures for Low Noise Environments (ISLNE) EPSRC Prosperity Partnership (EP/S03661X/1)

Further information

Beth Austin (b.austin@soton.ac.uk)

Supervisor: Prof Jordan Cheer (j.cheer@soton.ac.uk)

7. ACTIVE CONTROL OF A TUNED VIBRATION ABSORBER FOR USE IN METAMATERIAL APPLICATIONS

8. Reducing the Transport Footprint of Pathology Logistics through Shared-Fleet Passenger and Freight Services: A Case Study on the Isle of Wight, UK

Ismail Aydemir[1], Tom Cherrett[1], Antonio Martinez-Sykora[2], Fraser McLeod[1]
[1] University of Southampton, Transportation Research Group.
[2] University of Southampton, Southampton Business School.

Project Objectives and Goals

This research aims to investigate the feasibility and potential benefits of shared-fleet operations between public sector organisations—the National Health Service (NHS) and the Isle of Wight Council (IWC)—to improve efficiency in healthcare logistics and reduce carbon emissions. By integrating pathology sample collections with IWC's library, school minibus, and cash collection vehicle operations, this study explores the impact on cost, emissions, and operational efficiency in the context of healthcare logistics on the Isle of Wight. The operational area and vehicle stops for the shared-fleet scenario are shown in Fig. 1.

Previous studies have highlighted the importance of last-mile urban freight operations in reducing environmental impacts. Aydemir et al. (2023) emphasised the potential of horizontal collaboration in reducing transport costs and carbon emissions in healthcare settings.

Description of Method and Results

The methodology involved comparing two scenarios: the 'business-as-usual' (BAU) scenario, where only NHS vehicles are used, and the 'intervention scenario', where IWC vehicle routes are integrated with NHS pathology collections. Historical data and an optimisation algorithm were employed to model vehicle movements, evaluating the effectiveness of shared-fleet operations.

The results demonstrated significant improvements in multiple aspects (Table 1):

- 10.6% reduction in CO_2 emissions (644 kg/month)
- 20.2% reduction in working hours (219 hours/month)
- 17.8% reduction in operational costs (GBP 3596/month)
- Potential for IWC to gain an additional annual revenue stream of GBP (£) 54,829, and a 22.4% reduction in logistics costs for the NHS.

Table 1 Monthly statistics for IWC and the NHS in the BAU and the intervention scenarios.

Scenario	Fleet	Distance (km/month)	Working Time (h/month)	Cost (GBP (£)/Month)	CO_2 Emissions (kg)
Business-as-Usual	NHS (3)	7,971	450	8,032	2,232
	Minibuses (6)	11,035	475	9,124	3,090
	Cash Van (1)	1,063	92	1,644	74
	Library Van (1)	1,583	64	1,405	443
	Total	***21,652***	***1,081***	***20,206***	***6,063***
Modelled Shared-Fleet	Minibuses (6)	15,799	670	12,857	4,424
	Cash Van (1)	1,857	116	2,159	130
	Library Van (1)	1,696	76	1,594	475
	Total	***19,352***	***863***	***16,610***	***5,419***
Net Effect (Modelled - BAU)	Minibuses (6)	4,764	195	3,733	1,334
	Cash Van (1)	794	24	515	56
	Library Van (1)	113	12	189	32
	Total	***-2,300 (10.6%)***	***-218 (20.2%)***	***-3,596 (17.8%)***	***-644 (10.6%)***

Potential for Application of Results

The findings highlight significant benefits of collaborative shared-fleet operations between public sector organisations. Cost savings and reduced emissions contribute to both environmental and operational sustainability. Additionally, the collaboration serves as a model for similar initiatives across other regions and public organisations aiming for sustainable logistics management.

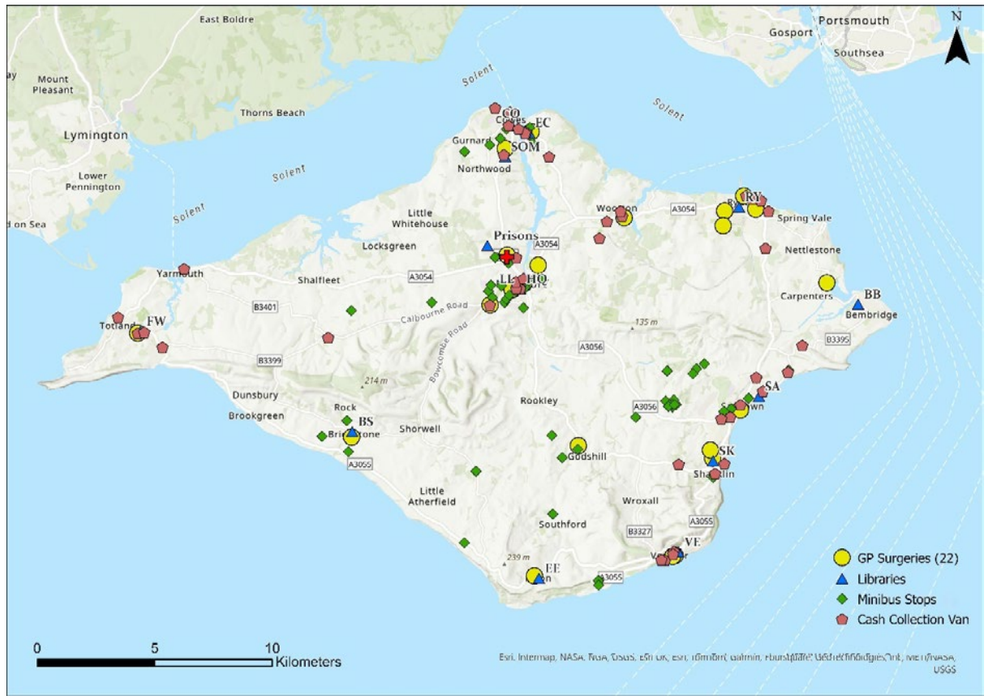

Fig. 1 Map showing location of GP surgeries and the IWC vehicles stops throughout one week. The red cross shows the location of St Mary's Hospital laboratory where samples are delivered for examination

References

Aydemir, I., McLeod, F., Grote, M., and Cherrett, T. (2023). Evaluating the Feasibility of a Shared-Fleet Operation in Healthcare Logistics between Public Organisations. Sustainability, 15(21), 15361. https://doi.org/10.3390/SU152115361.

8. REDUCING THE TRANSPORT FOOTPRINT OF PATHOLOGY LOGISTICS THROUGH SHARED-FLEET PASSENGER AND FREIGHT SERVICES: A CASE STUDY ON THE ISLE OF WIGHT, UK

9. Simplified "*m-θ*" curves for predicting non-linear lateral pile response: incorporating post-peak softening behaviour

Abigail H. Bateman[1], Jamie J. Crispin[2] and George Mylonakis[3]
University of Southampton

Simplified methods to calculate the response of laterally loaded piles discretise the pile into horizontal slices along the pile length and consider multiple soil reaction curves at each depth. Recent research (e.g., on offshore monopile foundations) has demonstrated the importance of considering both the distributed lateral load-displacement response (through *"p-y"* curves) and the corresponding moment-rotation response (through "*m-θ*" curves) to accurately predict horizontal displacements. The latter describes the relationship between the distributed moment acting at the pile-soil interface due to vertical soil tractions and the resulting pile rotation. As the contribution of "*m-θ*" curves has previously been neglected for slender piles, limited solutions are available. However, it is increasingly relevant as design trends are leading to monopiles with lower slenderness. This approach is illustrated in Fig. 1.

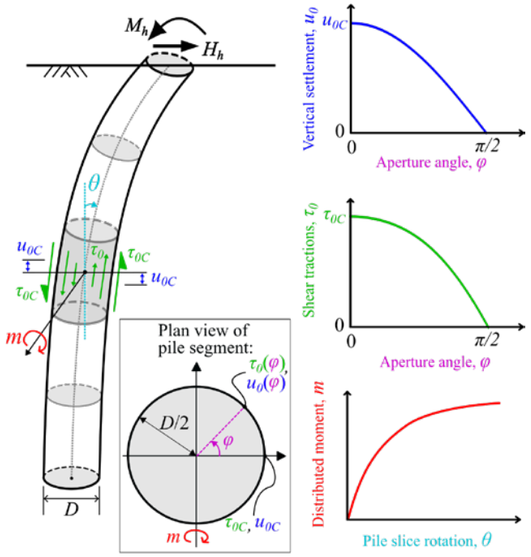

Fig. 1 Development of distributed moment due to rotation of pile segment

One simplified method to derive analytical "*m-θ*" curves integrates the vertical shear tractions at the pile-soil interface around the pile circumference based on solutions for *"t-z"* curves, which describe the vertical soil settlement resulting from uniformly distributed interface shear stresses. Available *"t-z"* curves are collected in Bateman et al. (2022) and have been employed by Bateman et al. (2023) to obtain non-linear "*m-θ*" curves using power-law and hyperbolic soil constitutive models.

However, existing solutions neglect the effect of slip at the pile-soil interface and post-peak behaviour such as softening observed in many clays. This work derives an "*m-θ*" curve from a *"t-z"* curve with an initial parabolic function, followed by strain-softening (originally defined by Randolph 2003). From the *"t-z"* curve, shear stresses around the pile circumference are obtained. Summation of these shear stresses yield the "*m-θ*" curve, shown in Fig 2. The resulting curve allows the distributed moment-rotation response to be considered in design based on routine ground investigation without resorting to complex 3D finite-element analysis. These "*m-θ*" curves can be used in conjunction with available *"p-y"* curves to calculate overall lateral pile response – important in offshore applications.

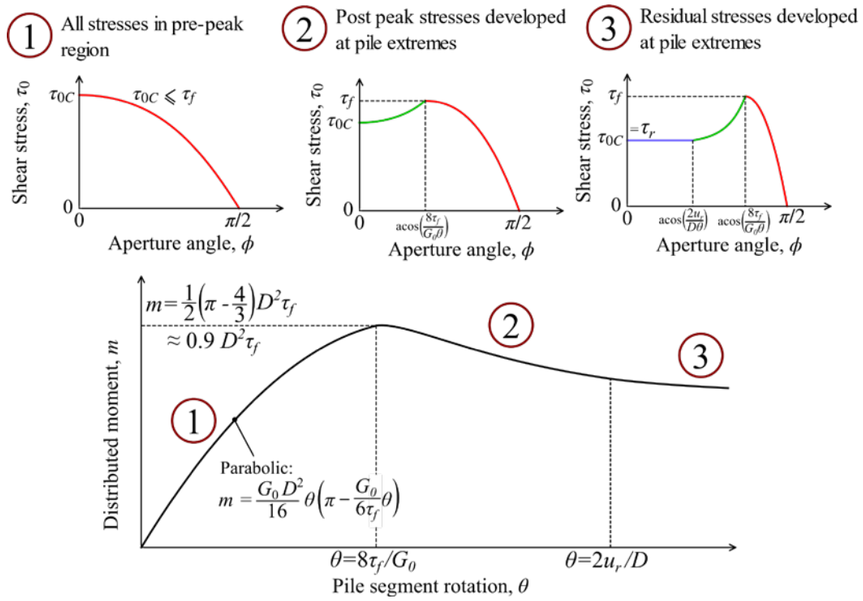

Fig. 2 "*m-θ*" curve obtained from this method and corresponding pile circumference shear stresses.

References

Bateman, A.H., Crispin, J.J., Vardanega, P.J., Mylonakis, G. (2022). Theoretical t-z curves for axially loaded piles. Journal of Geotechnical and Geoenvironmental Engineering, ASCE, 148, 04022052.

Bateman, A. H., Mylonakis, G. and Crispin, J.J. (2023). Simplified Analytical *"m-θ"* Curves for Predicting Nonlinear Lateral Pile Response. In 9th International Site Investigation and Geotechnics Conference. London, UK.

Byrne, B. W., Houlsby, G.T., Burd, H.J., Gavin, K.G., Igoe, D.J.P., Jardine, R.J., Martin, C.M., McAdam, R.A., Potts, D.M., Taborda, D.M.G. and Zdravkovic, L. (2020). PISA Design Model for Monopiles for Offshore Wind Turbines: Application to a Stiff Glacial Clay Till. Géotechnique 70(11): 1030–47.

Randolph, M. F. (2003). Load transfer analysis of axially loaded piles. RATZ manual version 4.2. University of Western Australia.

Funding body

This work was financially supported by the Engineering and Physical Sciences Research Council (EPSRC; grant number EP/T517872/1).

Further Information

1. Abigail .H. Bateman, Postdoctoral Research Assistant, University of Southampton, Southampton, UK, a.bateman@soton.ac.uk.
2. Jamie J. Crispin, Lecturer, University of Southampton, Southampton, UK.
3. George Mylonakis, Professor, Khalifa University, UAE; University Chair in Geotechnics and Soil Structure Interaction, University of Bristol, Bristol, UK.

10. Part-Span Approximation of Non-Linear Tone Noise Propagation in An Aeroengine Intake

Joseph S. P. Binns
ISVR, University of Southampton

Project Motivation

Computational methods for predicting the tonal acoustic field in aeroengine intake ducts are currently too costly for iterative design use. With increasingly strict noise emission regulations (UK Civil Aviation Authority, 2023), both research and industry need more efficient computational tools to address modern aeroengine noise challenges.

To improve fuel efficiency, the next generation of turbofan engines will feature Ultra High Bypass Ratio (UHBR) designs (Moreau, 2019; Rolls-Royce plc., 2024), which increase Bypass Ratio (BPR) and decrease Fan Pressure Ratio (FPR). This is expected to result in greater inflow distortion and impact the upstream propagation of fan-related tonal noise. Specifically, mode scattering due to distortion has been observed (Daroukh et al., 2016; Daroukh et al., 2019; Winkler et al., 2014; Prinn et al., 2016; Wu and Wilson, 2024), often resulting in an overall increase in Sound Pressure Level (SPL).

Methods

Given the high cost of accurate computational methods, this study investigates the feasibility of a novel 'part-span' methodology, first explored by Binns et al. (2024*a*,*b*). The upstream non-linear propagation of shock-associated tonal noise (buzz-saw noise) from the fan is considered using a Computational Fluid Dynamics (CFD) approach, specifically the Unsteady Reynolds-Averaged Navier-Stokes (URANS) method in Fluent. Similar methods have been validated in related contexts (Doherty and Namgoong, 2016). Two methodologies are explored:

1. Conventional full-span approach (datum)
2. Novel 'part-span' approach

For fan rotor tone noise and rotor-stator interaction tones, most acoustic energy is concentrated near the outer wall of the duct. This presents the opportunity to reduce the computational cost by neglecting low-span regions. The part-span domain is defined by an inviscid streamtube boundary with hub-tip ratio at the source plane.

Results & Conclusions

Applying the part-span approximation, much of the propagated buzz-saw spectrum can be predicted within 4 dB of the datum case, as highlighted in Figure 1.

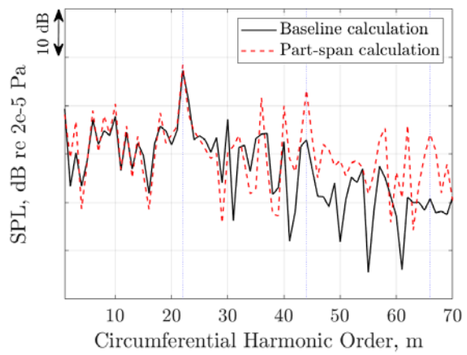

Figure 1: A spatial Fourier transform at 95% span and upstream by 50% duct radius.

To appreciate if the methodology can be applied to understand the mode scattering effect, known to occur for distorted inflows, a relative mode distribution at the first blade passing frequency (BPF) is shown in Figure 2 for the same position as in Figure 1. This is obtained by completing a temporal Fourier transform over a single cycle of the fan and then completing a spatial Fourier transform azimuthally according to the Fourier coefficients at the BPF.

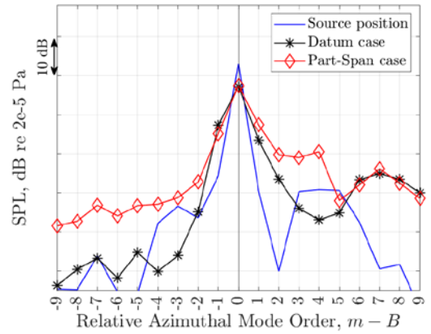

Figure 1: Relative mode at 95% span and upstream by 50% duct radius for the first BPF. The source data highlights the scattering effect, identified by both calculations.

The part-span approximation was applied to an axisymmetric intake with non-uniform inflow and accurately captured the most significant effects of distortion. The highest amplitude scattered modes were predicted to be within around 4 dB of the datum case but the detailed behaviour, partly due to the radial phasing of the modes, was less accurate.

The part-span approximation reduces the mesh count in the intake domain by around 30%. Applied with a two-part calculation methodology, a computational saving of up to 60% is expected.

Acknowledgements

This PhD work is financially supported by the University of Southampton and Rolls-Royce plc. Howoong Namgoong, the wider noise team and the CFD team at Rolls-Royce are acknowledged for their continued support and technical discussion.

References

Binns, J. S. P., Wu, L. & Wilson, A. G. (2024a), 'Part-span approximation of tone noise propagation in an aeroengine intake. Part I: Linear propagation', 30th AIAA/CEAS Aeroacoustics Conference, 2024.

Binns, J. S. P., Wu, L. & Wilson, A. G. (2024b), 'Part-span approximation of tone noise propagation in an aeroengine intake. Part II: Non-linear propagation', 30th AIAA/CEAS Aeroacoustics Conference, 2024

Daroukh, M., Moreau, S., Gourdain, N., Boussuge, J. F. & Sensiau, C. (2016), 'Influence of distortion on fan tonal noise', 22nd AIAA/CEAS Aeroacoustics Conference, 2016 .

Daroukh, M., Moreau, S., Gourdain, N., Boussuge, J. F. & Sensiau, C. (2019), 'Tonal noise prediction of a modern turbofan engine with large upstream and downstream distortion', Journal of Turbomachinery 141(2).

Doherty, M. & Namgoong, H. (2016), 'Impact of turbofan intake distortion on fan noise propagation and generation', 22nd AIAA/CEAS Aeroacoustics Conference, 2016 pp. 1–18.URL: http://dx.doi.org/10.2514/6.2016-2841

Moreau, S. (2019), 'Turbomachinery Noise Predictions: Present and Future', Acoustics 1(1), 92–116.

Prinn, A. G., Sugimoto, R. & Jeremy Astley, R. J. (2016), 'The effect of steady flow distortion on noise propagation in turbofan intakes', 22nd AIAA/CEAS Aeroacoustics Conference, 2016 pp. 1–14.

Rolls-Royce UltraFan (2024). URL: https://www.rolls-royce.com/innovation/ultrafan.aspx

UK-Civil-Aviation-Authority (2023), 'Aviation noise and health; the effects of aviation noise'. Accessed on 12/05/2023. URL: https://www.caa.co.uk/consumers/environment/noise/aviation-noise-and-health/

Winkler, J., Aaron Reimann, C., Reba, R. & Gilson, J. (2014), 'Turbofan inlet distortion noise prediction with a hybrid CFD-CAA approach', 20th AIAA/CEAS Aeroacoustics Conference 3(June).

Wu, L. & Wilson, A. G. (2024), 'Fan buzz-saw noise under intake flow distortion: a computational study', 30th AIAA/CEAS Aeroacoustics Conference, 2024.

11. Dynamic ankle joint angle assessment in daily living activities using the Madgwick algorithm

Hesam Boroomand, Jinghua Tang, Liudi Jiang
University of Southampton

Project objectives and goals

Measuring joint angles for individuals with different physical conditions during various activities is of significant importance in monitoring mobility, especially for people suffering from neurological disorders. Inertial Measurement Units (IMU) can measure accelerations and angular velocities. Therefore, to obtain the angles or positions of these sensors, the integration of these signals is required. Various techniques have been reported to reduce drift which is a well-known issue affecting data quality. The Madgwick algorithm utilizes the quaternion representation of orientation, which helps prevent singularity-related issues in Euler angles (Madgwick et al, 2011). However, the optimal sensor fusion parameter needs to be found for different activities.

The primary aim of this work is to calculate drift-free ankle joint angles in the sagittal plane during ambulation. Objectives include:

- → Collect lower limb IMU data in daily living activities
- → Finding the optimal parameter and process for dynamic ankle joint measurements

Description of method and results (Ethic ID: 93856)

Multiple IMU sensors (WitMotion WT9011DCL) were placed on the lower limbs of a healthy participant. In this study, only data from IMUs attached to the foot and shank were utilized. The participant was asked to walk at a self-selected speed, 10% faster and 10% slower speeds respectively, as well as ascending and descending stairs. IMU data at a frequency of 100 Hz were collected.

After resampling signals and separating the signals corresponding to each activity, an algorithm based on the identified mid-swing points in the shank gyroscope signal was used to identify two important gait events: heel strike and toe-off. Each gait cycle is defined between two sequential heel strikes. By mapping these identified points onto the angular velocity of the foot and comparing them with gait events identified in the literature, the signals were manually synchronized (Wu et al. 2021). The optimal value for the sensor fusion parameter of the Madgwick algorithm was determined to calculate drift-free angles. Figure 1 shows the drift-corrected and drifted foot angle for consecutive gait cycles.

By using the optimal values for different activities, the ankle angle joint will be derived (figure 2).

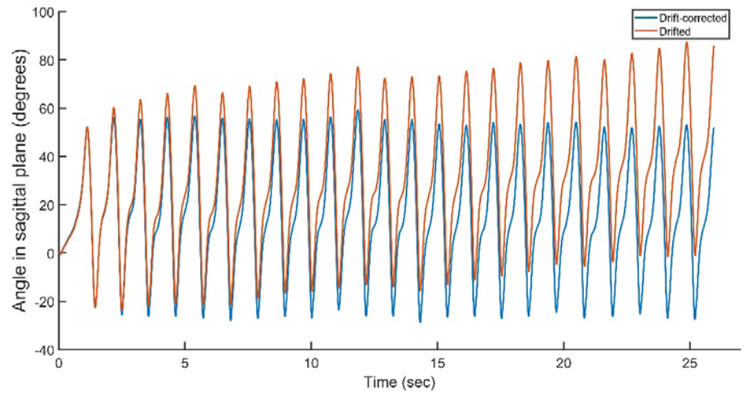

Figure 1- Drifted and drift-corrected angles

11. DYNAMIC ANKLE JOINT ANGLE ASSESSMENT IN DAILY LIVING ACTIVITIES USING THE MADGWICK ALGORITHM

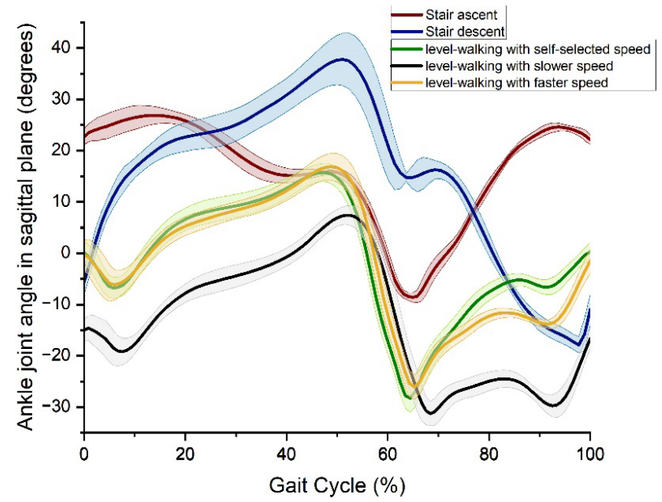

Figure 2- Ankle joint angle for different activities

Discussion and future work

The Madgwick algorithm-based IMU data processing was established to extract key kinematic information from various activities. The real-time monitoring of these biomechanical measures such as ankle angles, and range of motion of the ankle joint could be utilized to assess limb motion for pathological individuals compared with health groups, in particular, in out-of-lab daily living settings, which will be a focus of future work.

References

S Madgwick, A Harrison, and R Vaidyanathan (2011). Estimation of IMU and MARG orientation using a gradient descent algorithm, IEEE International Conference on Rehabilitation Robotics (2011), 1-7

J Wu et al (2021). An intelligent in-shoe system for gait monitoring and analysis with optimized sampling and real-time visualization capabilities, Sensors 21(8), 2869

11. DYNAMIC ANKLE JOINT ANGLE ASSESSMENT IN DAILY LIVING ACTIVITIES USING THE MADGWICK ALGORITHM

12. Developing a modelling framework for the transfer of immunoglobulin G across the human placenta

Lois Brewer, Christine E. Jones, Rohan M. Lewis, Bram G. Sengers
University of Southampton
Email: L.L.Brewer@soton.ac.uk

Project Objectives

Antibody transfer, more specifically immunoglobulin G (IgG), across the placenta is essential for providing protection against infection in the first weeks of a newborn's life. Out of the five antibody subclasses, only IgG and its subclasses are known to cross the main layers of the placenta, including the syncytiotrophoblast (STB), stroma, and fetal capillary endothelial cells (FCECs) (Sand et al., 2022). While it is widely accepted that IgG interacts with the neonatal Fc receptor (FcRn) within the STB, our understanding of IgG transfer across the other layers remains limited. The transfer of IgG across the FCECs is thought to be partially mediated by the low-affinity immunoglobulin gamma Fc receptor IIb (FcGR2b), although the underlying mechanisms are unclear.

This project aims to:

- Develop a computational model to simulate and explore the mechanisms underlying transplacental IgG transfer, particularly in the context of:
  - Ex-vivo placental perfusion experiments.
  - Transwell models.
- Use this model to investigate:
  - IgG subclass competition.
  - IgG glycosylation.
  - Maternal disease, especially the impact of HIV+ patients on IgG transplacental transfer and hypergammaglobulinemia (high maternal IgG levels - observed in malaria).

Method and Results

Our in-silico approach uses a 3-layer compartmental model to simulate the transfer of IgG in an ex-vivo placental perfusion context based on our previous modelling work (Panitchob et al., 2016). These layers include the intervillous space (IVS), STB, and the fetal capillaries, simulating the uptake of IgG from the IVS into the STB, which then binds to FcRn at a low physiological pH. IgG undergoes transcytosis across the STB, dissociates from FcRn and enters the fetal capillaries.

The model was extended to include the stromal and FCEC layers, which considers binding to FcRn and FcGR2b to transport IgG across the FCECs. A global sensitivity analysis was conducted to assess which parameters have a direct influence on the total transferred IgG concentration.

The model was successfully applied to several ex-vivo placental perfusion studies from existing literature to capture the mechanisms behind IgG subclass and IgG-based drug (such as infliximab) transfer across the placental layers. Results from the global sensitivity analysis confirm the central role of FcRn binding in placental IgG transfer, with physiological FcRn concentrations just below the point of FcRn saturation within the STB. Levels higher than this had a limited impact on the total IgG transfer.

Additionally, a multivariate analysis revealed how the interactions between parameters could be rate-limiting under different scenarios.

References

Sand K.M.K. et al (2022). Contribution of the ex vivo placental perfusion model in understanding transplacental immunoglobulin G transfer, Placenta 2022; 127:p77-87.

Panitchob N. et al. (2016). Computational modelling of placental amino acid transfer as an integrated system, Biochimica Biophysica Acta (BBA) - Biomembranes 2016; 1858:p1451-1461.

13. Study of multi-junction Bismuth based perovskite solar cell

Fengyuan Cao
University of Southampton

Project objectives and goals

The project aims to find the method of multi-junction solar cell fabrication using novel type of Bi-Based perovskite semiconductor and increase its efficiency by optimizing its composition and structure.

- Increase the thickness of the film.
- Study the formation mechanism of $Cs_3Bi_2BrxI_{9-x}$.
- Comparation of optimal bandgap.

Previous work by Dr.Selma et al (2023),and Dr.Bavykin led to design the experiment increase the thickness of the film and measure the corresponding energy gap of $Cs_3Bi_2BrxI_{9-x}$.

Description of method and results

CsI, BiI_3, CsBr, $BiBr_3$, and DMF (anhydrous, 99.8%) are used in the $Cs_3Bi_2I_9$ perovskite layer. CsI (0.775g) and BiI_3 (1.175g) were combined in DMF (10ml) for 24 hours at 70°C to achieve a concentration of 0.1M. This procedure necessitates the employment of magnetic stirrers on the hot plate to ensure that the final liquid is uniformly mixed. This solution is reddish brown in color. Similarly, CsBr (0.635g) and $BiBr_3$ (0.895g) were combined in DMF (10ml) for 24 hours at 70 °C to generate $Cs_3Bi_2I_9$ at a concentration of 0.1M.

$$3CsI + 2BiI_3 \rightarrow Cs_3Bi_2I_9 \qquad (1)$$

The Caesium Bismuth Iodide perovskite solution was created using Eq. 1.

$$3CsBr + 2BiBr_3 \rightarrow Cs_3Bi_2Br_9 \qquad (2)$$

The Caesium Bismuth Bromine perovskite solution was created using Eq. 2.

Since Dr. Stranks found that high-concentration perovskite solutions react too violently under ultraviolet and visible light, the perovskite solution needs to be diluted to 3mM.

Figure 1 shows the absorption characteristics of perovskite for different wavelengths of light when Br/I is different, thus reflecting its optical properties. Figure 2 shows the process of obtaining its energy gap using $Cs_3Bi_2I_9$ solution as an example.

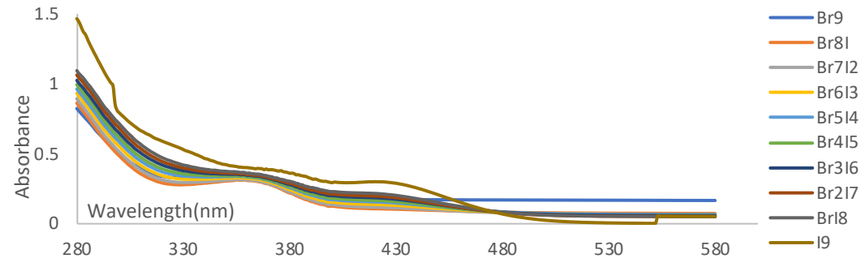

Figure 1 shows absorbance and wavelength diagram of $Cs_3Bi_2BrxI_{9-x}$.

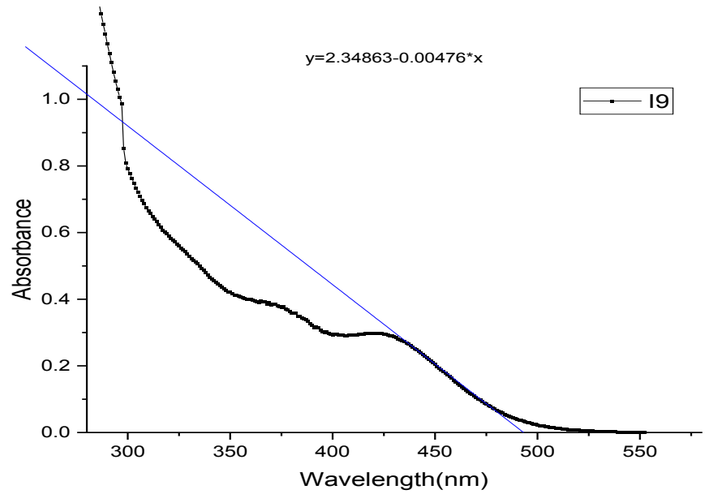

Figure 2 shows how to determine the energy gap of perovskite layer material.

$$E_g = \frac{1240}{Wavelength(nm)}\ ev \qquad (3)$$

Eq. 3 shows how to calculate the energy gap of different perovskite solutions.

Table 1 shows the energy gap of $Cs_3Bi_2BrxI_{9-x}$.

$Cs_3Bi_2I_9$	$Cs_3Bi_2BrI_8$	$Cs_3Bi_2Br_2I_7$	$Cs_3Bi_2Br_3I_6$	$Cs_3Bi_2Br_4I_5$	$Cs_3Bi_2Br_5I_4$	$Cs_3Bi_2Br_6I_3$	$Cs_3Bi_2Br_7I_2$	$Cs_3Bi_2Br_8I$	$Cs_3Bi_2Br_9$
2.52ev	2.60ev	2.88ev	2.90ev	2.92ev	2.94ev	2.95ev	2.98ev	3.04ev	3.10ev
493nm	477nm	431nm	428nm	423nm	422nm	420nm	416nm	408nm	400nm

Potential for application of results

- By optimizing the film thickness, the conversion efficiency of perovskite solar cells can be significantly improved, promoting their competitiveness in commercial applications.
- $Cs_3Bi_2BrxI_{9-x}$ as absorber layer for solar cells, improving energy conversion efficiency.
- Multi-junction perovskite solar cells show significant advantages in the design of optimal band gaps, which can improve light absorption efficiency and overall cell efficiency and enhance stability.

References

[1] S.Durak, Organic and Inorganic Perovskite Solar Cells: Design, Fabrication and Performance Analysis, Southampton: University of Southampton, Faculty of Engineering and Physical Sciences School of Engineering, 2023.

[2] Stranks, S.D. and Snaith, H.J. (2015). Metal-halide perovskites for photovoltaic and light-emitting devices. Nature Nanotechnology, 10(5), pp.391–402. Doi: https://doi.org/10.1038/nnano.2015.90.

14. Antibody-conjugated Polymersomes for Targeted Antibiotic Delivery to Intracellular B. thailandensis

RM Cheetham, AW Taylor[2], TA Newman[1], SS Lee[1], S Mahajan[1]; AO Whelan[2], ND Evans[1]

[1] University of Southampton, United Kingdom

[2] DSTL-Porton Down, Salisbury, United Kingdom

Polymeric nanoparticles, polymersomes, may improve antibiotic delivery and clearance of difficult-totreat, facultative intracellular Burkholderia pseudomallei. Polymersomes target bacteria, occupying the protective intracellular niche, by retaining antibiotic payload until internalisation by cells, however their targeting is not pathogen-specific. In this study, we hypothesised that antibody could be covalently linked to polymersomes and modifying polymersomes with B. pseudomallei anti-capsular polysaccharide monoclonal antibody (3VIE5) would enhance Burkholderia thailandensis (HG2 surrogate organism) interaction, improving inhibition of intracellular infection.

Aminated polymersomes, loaded with doxycycline, were fabricated by nanoprecipitation of 15 mg/mL polymer-DMF solution (PEO(5k)-b-PCL(18k) and H2N-PEO(5k)-b-PCL(17k), mass%=50/50) in aqueous antibiotic receiver solution. Dynamic light scattering measured nanoparticle size. Crosslinker, sulfo-SMCC, activated NH2-polymersomes were reacted to TCEP-reduced fluorescent antibody for 6-hours prior to dialysis and centrifugation. Fluorescence intensity (FI) was measured to assess conjugation. Coherent anti-stokes Raman scattering (CARS) tuned to the Raman CH-stretch region produced label-free, chemically-informative images of RAW264.7 cells incubated with or without polymersomes.

Polymersomes were uniform and ≈100 nm in diameter. The FI of cross-linked polymersomes was greater than control suspensions, polymersomes omitting cross-linker and antibody-alone ($p<0.001$). The linear antibody-FI standard curve indicated a conjugated antibody concentration of 1.5 gg/mL. CARS imaging revealed greater signal from CH-stretch in cells treated with polymersomes compared to controls, suggesting intracellular polymersome uptake.

These data suggest sulfo-SMCC conjugates antibody to polymersomes. This methodology may now be used to fabricate B. pseudomallei-specific antibody-polymersome conjugates, assessing conjugation using ELISAs. Ongoing work will investigate the antimicrobial activity of the novel targeted treatment using B. thailandensis in vitro infection assays.

Funding Body:

DSTL

EPSRC

Further information:

Applicant: RM Cheetham r.m.cheetham@soton.ac.uk

Primary Supervisor: ND Evans n.d.evans@soton.ac.uk

15. Tribological testing and crystallographic analysis of high hardness, ultra-low friction Mo-S-C thin film coatings with self-assembling tribolayers

Bethan Collins
University of Southampton

Project objectives and goals

The aim of this project is to tribologically test and analyse the crystalline structure of carbon-doped molybdenum disulphide solid lubricant coatings that provide ultra-low friction at maximum material hardness created with chemical compositions informed by the results of molecular dynamics simulations.

Transition metal dichalcogenides (TMD) are a group of materials that are well-known for their low friction properties. The weak van der Waals forces between layers of covalently bonded atoms gives rise to easy shear and can therefore provide very low friction. These materials, however, have low hardness, meaning that in their pure form they display high wear rates. To improve their material properties, TMD coatings can be deposited with a doping element, which leads to the production of amorphous coatings with significantly increased hardness and density (Polcar and Cavaleiro 2011).

Although the as-deposited coatings do not initially feature the crystals responsible for the ultra-low friction properties of pure TMDs, the application of frictional forces leads to the creation of crystalline regions, or a 'tribolayer'. It has been shown via sliding wear tests that these coatings display an initial coefficient of friction (COF) of around 0.3, which rapidly reduces and can reach steady state values of as low as 0.025 at room temperature (Vitu et al. 2021).

Method and Results

Molecular dynamic simulations were used to model the process of tribolayer formation to find the optimal carbon content that should provide the maximum hardness whilst still allowing for the creation of the tribolayer. This composition was then used to deposit the Mo-S-C coatings studied in this project. The coatings were deposited via magnetron sputtering, a physical vapour deposition (PVD) process, using the industrial deposition chamber Oerlikon Balzers in high power impulse magnetron sputtering (HIPMS) mode. The as-deposited coatings had a hardness of 8.1GPa.

The coatings were tribologically tested using a Plint TE77 linear reciprocating tribometer. A range of sliding conditions were used: applied load ranging from 5-20N, sliding frequency ranging from 1-20Hz and sample temperature ranging from 20-150°C. The tribological results showed COF ranging from 0.035 to 0.05, and specific wear rates averaging 5E-10 mm^3/Nmm.

The wear tracks were analysed using scanning electron microscopy with energy-dispersive X-ray spectroscopy (SEM-EDS), and Raman spectroscopy to search for crystalline regions within the wear tracks as evidence of tribolayer formation. Most of the wear track remained amorphous, however an area of crystalline MoS2 was discovered. High resolution transmission electron microscopy was also employed to investigate the layer adhered onto the ball used in the wear tests, in which MoS_2 platelets were found although no compact tribolayer was present.

References

Polcar, T. and Cavaleiro, A., 2011. Self-adaptive low friction coatings based on transition metal dichalcogenides. Thin Solid Films, 519(12), pp.4037-4044.

Vitu, T., Huminiuc, T., Doll, G., Bousser, E., Matthews, A. and Polcar, T., 2021. Tribological properties of Mo-SC coating deposited by pulsed dc magnetron sputtering. Wear, 480, p.203939.

Funding body

DSTL

16. Analytical solution for settlement of pile groups in inhomogeneous soils

Jamie J. Crispin
University of Southampton

Project objectives and goals

Pile group foundations are used to limit the settlement of structures due to vertical loads. However, the proximity of piles to others in the group introduces interaction effects. These reduce the overall efficiency of the foundation compared to single piles spaced further apart. To select appropriate pile dimensions and group configurations, designers need to predict settlements by incorporating this interaction effect. This is a complex three-dimensional problem which often necessitates numerical analysis. However, selecting dimensions and configurations requires many analyses be completed to optimise the design. Closed-form solutions are therefore desired as an alternative to significantly reduce analysis time. Currently, closed-form solutions are available for homogeneous soils, but many realistic soil profiles have properties that vary with depth. In this work, solutions are developed for a number of these soil profiles.

Description of method and results

Poulos (1968) introduced interaction factors that allow the superposition of the effects of each pile on another (in pairs) to get the overall group response. This reduces the problem to only two piles at a time. The problem was further simplified by Mylonakis and Gazetas (1998), who developed the three-step model for calculating the interaction factor in closed form. This method, shown in Fig. 1, incorporates both the attenuation of displacement from a single "source" pile and the reinforcing effect of a second "receiver" pile.

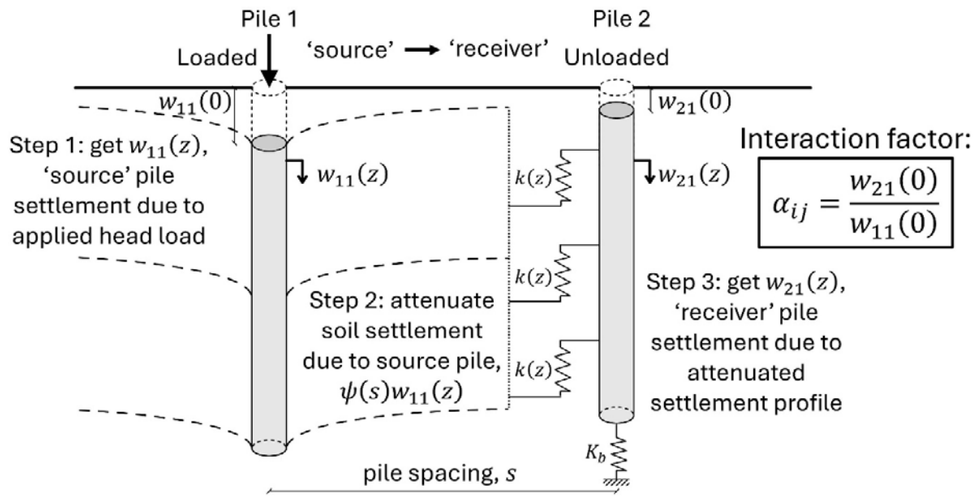

Fig. 1 Three step model proposed by Mylonakis and Gazetas (1998).

This solution was previously limited to homogeneous soils. Extension of this model to inhomogeneous soils was achieved by solving the governing differential equation for the receiver pile in closed-form. The resulting interaction factors are calculated from the diffraction factor shown in Fig. 2. Dimensionless design charts such as these can be used for hand calculations, and approximate expressions are provided that can be used in simple spreadsheet calculations.

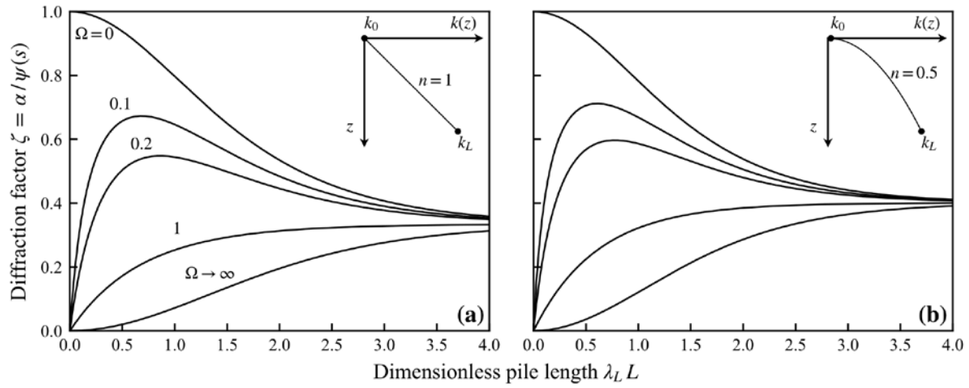

Fig. 2 Resulting reinforcing effect of the second pile calculated for two inhomogeneous soil profiles. Reproduced from Crispin and Leahy (2019).

References

Crispin, J.J. and Leahy, C.P. (2019) The Journal of the Deep Foundations Institute, 12:3, 163-170.

Mylonakis, G. and Gazetas, G. (1998) Settlement and additional internal forces of grouped piles in layered soil. Géotechnique, 48:1, 55–72

Poulos, H.G. (1968) Analysis of the settlement of pile groups. Géotechnique, 18:4, 449–471.

Further Information

Jamie J. Crispin, Lecturer, University of Southampton, Southampton, UK.
j.j.crispin@soton.ac.uk

Collaborations

This work was conducted in collaboration with Colm Leahy and Prof. George Mylonakis at the University of Bristol.

Funding body

This work was financially supported by the Engineering and Physical Sciences Research Council (EPSRC; grant number EP/N509619/1).

17. Exploration of flexible open-cell mechanical metamaterials

Kirstie M. Devin (kirstie.devin@soton.ac.uk), Jinghua Tang, David Moser, Liudi Jiang (L.Jiang@soton.ac.uk)
School of Engineering, Mechanical Engineering, University of Southampton

Introduction

Advancements in 3D-printing technology with elastomeric materials have facilitated the fabrication of complex architectures, unlocking new possibilities in the design of mechanical metamaterials (Jiao et al, 2023). Among these, some metamaterials are characterised by their tuneable mechanical properties (e.g., stiffness, flexibility, energy absorption), which exhibit significant potential across various applications (Maiti et al., 2016), including soft robotics, wearables, automotive components, adaptive cushioning systems and architectural designs. This work explores select unit cell designs that could be leveraged for such applications.

Aim and objectives

The primary aim of this work is to assess different elastomeric open-cell metamaterials designs. Objectives include:

- → Explore open-cell metamaterials of varying size and pore shape.
- → Design and develop open-cell units with focus on tuneability of stress-strain relationship.
- → Evaluate design configurations with potential applications in mind.

Methods and results

Unit cells were modelled using SolidWorks 2021 (Dassault Systèmes, Cambridge). FEA was used for preliminary evaluation of metamaterials made of Elastic 50A (EL50). Examples of unit cells explored are shown in Fig 1. Select metamaterial samples of 20x20x20mm (Design A and B in Fig 1) were fabricated using a Form 3 (FormlabsTM, Germany) table-top 3D-printer, using EL50 as the base material (E=2.63MPa).

Theoretical porosity (φT) of metamaterials Design A and B were evaluated using Eq. 1, where VP represents the volume of pores and Vs is the solid volume:

$$\varphi_T = \frac{V_P}{V_P + V_S} \times 100\%$$

Unit cell parameters and corresponding φT are listed in Table 1. Mechanical tests were performed applying compressive force of up to 200N.

Table 1. Parameters assigned to design A and B unit cells.

Design	u (mm)	r (mm)	L x w (mm)	φ_T (%)
A1	5	1.5	-	83
A2	5	1.37	-	76
A3	5	1.00	-	50
A4	5	0.80	-	35
B1	5	-	3 x 2	65
B2	2.5	-	1.1 x 0.8	45
B3	4	-	2.25 x 1.5	60
B4	4	-	2 x 1	40

Fig 2 shows stress-strain profiles and respective effective Young's modulus (E). While further variation of design A parameters could achieve similar E-values to that of design B, use of ovular pores may produce different stress-strain behaviours under higher loads, as indicated by comparison of designs A2 (E=0.24MPa) and B3 (E=0.29MPa).

Future work

Future work should evaluate design B subjected to shear load; this may potentially yield greater differences in stress-strain behaviour, particularly under higher loads. Assessment of different unit designs/configurations with constant φT is needed. Nevertheless, preliminary findings indicate such elastomeric open-cell metamaterials could be promising for different applications.

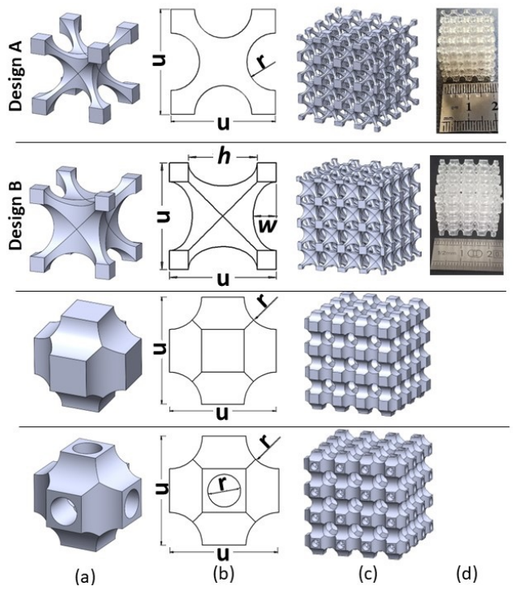

Fig 1. Schematics showing (a) 3D unit designs, (b) cross-sectional view of units, (c) metamaterials formed by stacking 3D cellular units and (d) examples of 3D-printed metamaterials.

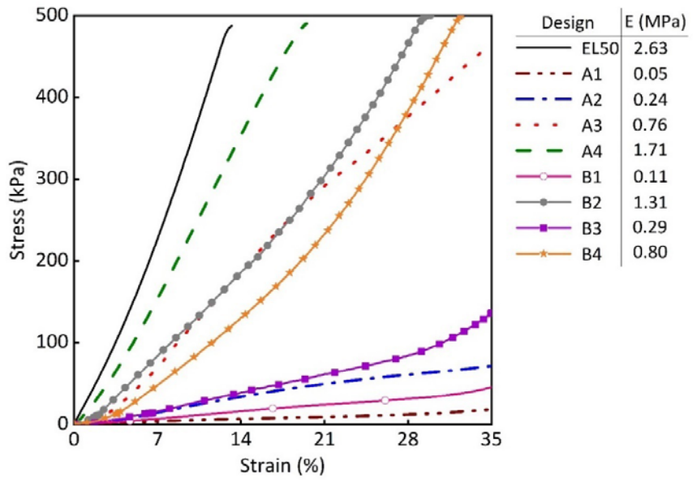

Fig 2. Stress-strain for design A and B metamaterials, with E-values indicated.

References

Jiao et al, 2023. Vol.14, 6004. DOI: 10.1038/s41467-023-41679-8.

Maiti et al, 2016. Vol.6, 24871. DOI: 10.1038/srep24871

18. Abstract: The application of data-driven methods in assessing and modelling extended endplate connections

Zizhou Ding
University of Southampton

Project objectives and goals

Extended endplate connections (EEPCs) are widely used in practice to connect beams and columns as part of the wind/seismic design of moment-frame buildings. These connections are designed as either fully rigid (FR) or semi-rigid (SR). The moment-rotation response and deformation mode behaviours of EEPCs are complicated. This is mainly dependent on the rigidity classification and the complex interactions between each component, such as the endplate, column flange, and column web panel zone. Several studies have investigated EEPCs' moment-rotation response and deformation modes (CEN, 2005, Kozlowski et al., 2008, Eatherton et al., 2021). However, these existing models do not always provide reliable predictions and cannot predict the full-scale EEPCs' behaviour. This is mainly attributed to the limited numbers of predictors, small datasets (limited applicability range), or non-generalised assumptions. This paper aims to address the problems above using a comprehensive database and advanced numerical methods. The research's objectives are as follows:

- → Develop a comprehensive multi-attribute experimental database for the bare steel EEPCs.
- → Develop robust numerical models for predicting the full-scale moment rotation response and deformation mode of EEPCs.

Description of method and results

A comprehensive database with over 800 specimens was established as the data resource for developing the predictive models for EEPCs. This database includes multi-attribute parameters, mainly the test/specimen attributes, geometrical properties, material properties, and reported deformation modes. For EEPC's moment-rotation response, several targeted parameters need to be predicted, which are the elastic stiffness (Ke), plastic strength (Mye), ultimate strength (Mu), and maximum rotation (c). A bilinear curve was used to present the full-scale EEPC's behaviour with the target predicted parameters. The target response parameters were predicted by training the multiple linear regression (MLR) and artificial neural network (ANN) models. The developed models can provide an accurate and robust prediction with a P20 larger than 0.9, see an example of the unstiffened EEPCs in Fig. 1 (a).

Several primary deformation modes were determined for EEPCs, which include endplate bending (EPB), column flange bending (CFB), panel zone in shear (CWS), and beam buckling (BB). The random forest (RF) model was trained to predict the determined primary deformation mode of EEPCs. The trained RF model can reach an accuracy of over 90%, see the performance of the testing set in Fig. 1

(b). To ensure the robustness and reliability of the developed RF model, the probability of each primary deformation mode was also predicted. This can address the issues caused by material uncertainty and geometrical imperfection.

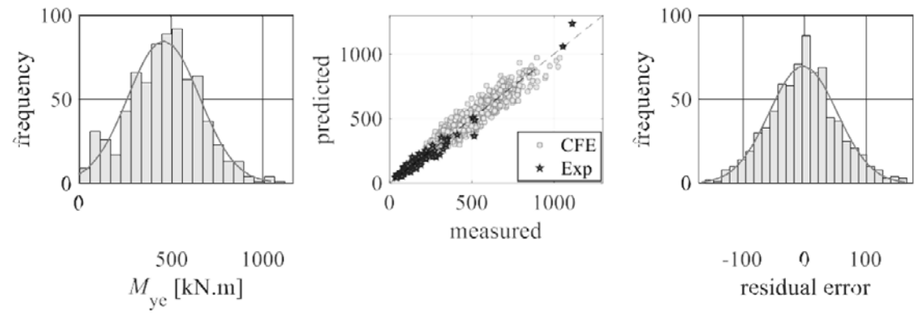

(a) Example of Mye prediction of the MLR model for unstiffened EEPCs

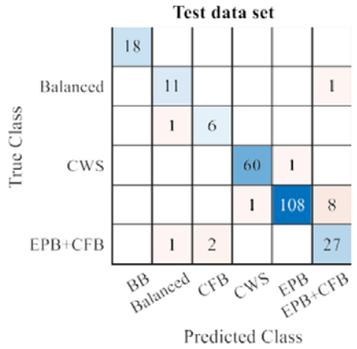

Fig. 1 Model performance of the MLR and RF model for EEPC

(b) Confusion matrix of the RF model for the EEPCs with the testing set

Potential for application of results

The developed models can effectively predict the moment-rotation response and corresponding deformation mode of an EEPC. This can be used as the part of the performance-based design to assess the acceptable design criteria.

References

CEN 2005. Eurocode 3 - Design of Steel Structures, Part 1-8: Design of Joints. Brussels, Belgium: European Committee for Standardization.

EATHERTON, M. R., NGUYEN, T. N. & MURRAY, T. M. 2021. Yield line patterns for end-plate moment connections.

KOZLOWSKI, A., KOWALCZYK, R. & GIZEJOWSKI, M. Estimation of the initial stiffness and moment resistance of steel and composite joints. CTBUH 8th World Congress, Dubai, 2008.

19. Effects of frequency and dwell on the fatigue crack propagation in single crystal Ni-based superalloys CMSX-4 and CMSX-10 at intermediate service temperature

J.C. Doyle1 (J.C.Doyle@soton.ac.uk), A. Evangelou1,2 (A.Evangelou@soton.ac.uk), E.A. Saunders3 (Edward.Saunders@rolls-royce.com), J.M. Woolrich4 (Jane.Woolrich@rolls-royce.com), N. Gao1 (N.Gao@soton.ac.uk), P.A.S. Reed1 (P.A.Reed@soton.ac.uk)

[1]Engineering Materials Research Group, School of Engineering, University of Southampton, Highfield, Southampton, SO17 1BJ, UK

[2]Engineering Powder Technology Laboratory, Department of Mechanical and Manufacturing, University of Cyprus

[3]Rolls-Royce plc., Materials — Failure Investigation, Bristol BS34 7QE, UK

[4]Rolls-Royce plc., Materials — Failure Investigation, Derby DE24 8BJ, UK

Ni-based single crystal superalloys are used in turbine blades due to their excellent combination of high temperature mechanical properties and corrosion resistance. Although service temperatures in the turbine gas stream of a jet engine can exceed 1000°C, a large temperature gradient is experienced across the blade with the cooler regions towards the blade root where intermediate service temperatures (450-650°C) are observed. Often, blade aerofoils are coated to help protect from high temperature oxidation. However, where the blade is exposed to intermediate temperatures towards the root, the blade is commonly left uncoated so is directly exposed to oxidation damage and oxidation-fatigue mechanisms.

The effects of oxidation and dwell will influence fatigue crack propagation rates and damage mechanisms at elevated temperatures. In this work the effects of frequency on the fatigue crack growth rate have been studied on CMSX-4 and CMSX-10 at an intermediate service temperature 550°C through a series of frequency scan tests to obtain the transition from cycle to time dependent crack growth; as well as constant load testing where the loading waveform was kept constant. Tests were conducted on single edge notched bend bar specimens in air at a load ratio of 0.1. Frequencies tested range from high frequency 5Hz to a low frequency 90s dwell waveform. The effects of frequency on crack growth rate are shown in Figure 1. Fatigue crack propagation mechanisms have been compared between each frequency using a combination of optical microscopy, scanning electron microscopy and Alicona IFM (Infinite Focus Microscope) to characterise the fracture surfaces and assess fatigue and time dependent failure mechanisms.

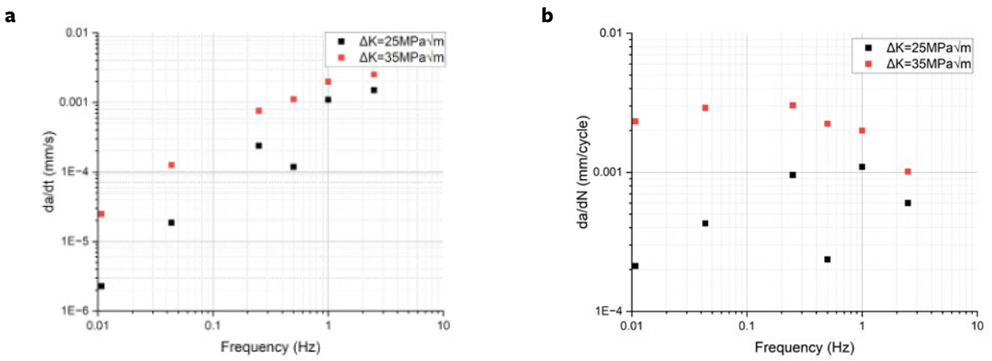

Figure 1 – Effect of frequency on the crack growth rate of CMSX-4 at 550°C (at constant JK=25MPa√m and 35MPa√m) with respect to a) time and b) cycles

20. Foam layer composition mechanical properties and the performance implication for wheelchair cushions

Oliver Gould, Engineering Materials Research Group, Department of Mechanical Engineering, University of Southampton.
Supervisors: Prof. Liudi Jiang, Prof. Pete Worsley, Dr. Andrew R. Hamilton.

Pressure ulcers are wounds that are caused by extended durations or magnitudes of force onto the soft tissues of a body, for example they can develop under the ischium when a person is seated for long durations without relief. If left untreated they can break the skin and pose a huge infection risk and may take months to heal fully. Pressure ulcer prevalence is directly related to the quality of body support materials. Long periods of time spent with force on soft tissues causes localised hypoxia and the development of a pressure ulcer. Body support materials, like wheelchair cushions, aim to reduce the pressure on soft tissues to prevent the formation of pressure ulcers. These cushions are frequently made up of multiple layers of soft foams with different densities and therefore different mechanical properties. Therefore, understanding the mechanical behaviour of multi-layer cushions for use as body-support materials is essential for improving user comfort and outcomes. The indentation force deflection (IFD) is the applied force at an indentation depth of 25mm, and it is used by manufacturers as a measure of the firmness and an indicator of the magnitude of pressure experienced by supported soft tissue. The aim of this project is to improve the understanding of different foams and multi-layer foam combinations on the mechanical response and cushion performance, as characterised by IFD and peak surface pressure reduction capabilities.

Indentation tests using a range of anatomical indenters (to replicate different geometries common within the population) were performed on multi-layer foam cushions made from three types of commonly used densities of ethyl vinyl acetate (EVA) foams (25, 35, and 40 kg/m3). Finite element models were created to analyse the stress distribution in and between layers. An external surface pressure array was used in an additional long duration test to observe the changing surface pressure distribution for each sample to simulate the long periods of sitting common in users. The results indicate that changing the number of layers affected the overall response of the material. Splitting a monolithic block of the lowest density foam into two layers of the same foam resulted in a 1.8% decrease in IFD whilst three layers reduced the IFD by 9.8%. The force displacement behaviour of these samples is shown figure 1. Using adhesive tape to attach the two layers together resulted in a 4% increase in IFD over a single layer block of the same foam, whilst attaching the three-layer sample's layers together resulted in a 3.75% decrease in IFD when compared to the single layer block of foam. The results indicate the magnitude of reductions in IFD that can be expected for layered configurations of these EVA foams with densities typically used in cushions. Future work will aim to link the IFD to real world surface pressure reducing metrics using the pressure sensing array.

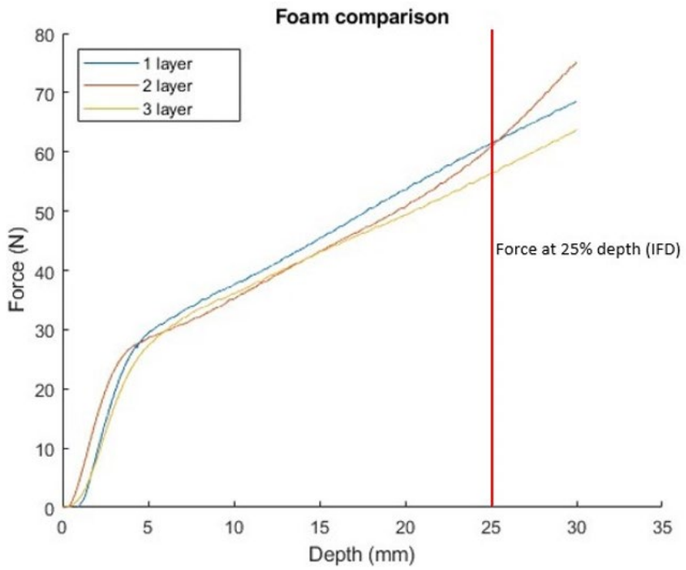

Figure 1: Average Force-Depth graph for single, double, and triple layer samples Keywords: foam, multi-layer foam, indentation, soft materials, wheelchair cushions, layer attachment

Table 1 Indentation force deflection (IFD) for single and multi-layer foams with percentage difference to the single layer

Sample	IFD (N)	% difference to single layer
Single layer	62.01	-
Two-layer	60.92	-1.76
Three-layer	55.96	-9.76
Two-layer taped	64.54	4.08
Three-layer taped	59.68	-3.75

20. FOAM LAYER COMPOSITION MECHANICAL PROPERTIES AND THE PERFORMANCE IMPLICATION FOR WHEELCHAIR CUSHIONS

21. Pipeline Leak Location Using Sensor Arrays

Joshua Hooper
University of Southampton

Project objectives and goals

Leaks in water distribution mains have been a problem for many years, and continue to be even more so as infrastructure ages and the security of water supply in many countries becomes more unstable. Correlation-based (vibro-) acoustic methods have provided an accurate and non-invasive way of detecting and locating these leaks for several decades; this has typically been using two sensors. This project is investigating the use of a discrete sensor array along the pipe as an improvement to enable multiple leaks to be found. This has involved the transferal of source localisation methods from array processing literature to the problem of leak detection. In particular, the MUSIC algorithm has been selected.

The goal of the project is to first demonstrate that this method works to locate leaks, using both simulated data and an experimental test rig, 42 m in length (see Fig. 1). Then, aside from a basic validation, we are assessing the accuracy and robustness with some theoretical analysis and Monte Carlo simulations.

Description of method and results

Simulated data is generated using a simple, infinite pipe propagation model with a dispersion relation supplied from Pinnington and Briscoe (1994) with a leak represented by Gaussian white noise. Comparing the root-mean-squared error (RMSE) of the estimates across a range of signal-to-noise ratios (SNRs), the MUSIC-based leak location maintains an accuracy of < 1 m up to -10 dB SNR, whereas the two-sensor cross-correlation method fails to resolve leak locations below 0 dB SNR.

Because the MUSIC method, as with time delay estimation, requires an accurate value of the wavespeed/wavenumber in the computation, this is a large source of error. Fig. 2 shows that for a wavespeed mismatch of more than , the average error is over . Since an accurate value is difficult to measure, this is likely to be an issue in practice.

Furthermore, this method is affected by any model mismatch, not just the wavespeed, so for example the practical test rig in Fig. 1 has multiple junctions and joints which will cause scattering and reflection of waves. The method so far has not incorporated a way of factoring in these effects generally, since any theoretical expression (e.g. adding end reflections) would be limited in scope. A planned piece of future work concerns using measured responses to a known excitation to interpolate the response of the pipe to a hypothetical noise source location, which could be directly used in the MUSIC computation.

Fig. 1 Test rig set up

21. PIPELINE LEAK LOCATION USING SENSOR ARRAYS

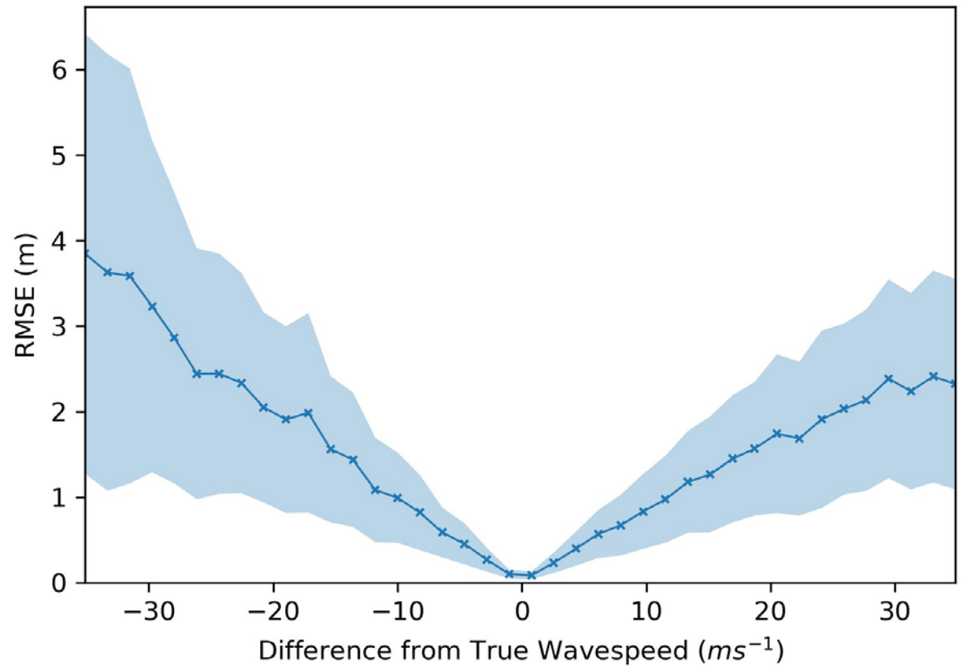

Fig. 2 RMSE vs wavespeed mismatch for a plastic (MDPE) pipe, 200 m in length; 8 equally-spaced sensors, 40 dB SNR.

References

R. J. Pinnington and A. R. Briscoe. Externally applied sensor for axisymmetric waves in a fluid filled pipe. Journal of Sound and Vibration, 173(4), 1994

Funding body

Engineering and Physical Sciences Research Council (EPSRC)

Further Information

Joshua Hooper (Email: J.Z.Hooper@soton.ac.uk)
Supervisors: Jen Muggleton, Michal Kalkowski
(Email: jmm@isvr.soton.ac.uk, m.kalkowski@soton.ac.uk)

22. Experimental investigation of the impact of leeway and rudder angles on the yaw moment balance for wind-propelled ships

Saeed Hosseinzadeh
University of Southampton

Wind propulsion offers a promising solution to rapidly reduce commercial ships' CO_2 emissions. This two-year project develops software to predict the performance of vessels with wind sail technologies, focusing on Smart Green Shipping's FastRig wing-sails. We aim to test a retractable 20-meter FastRig wing-sail on a commercial ship using innovative numerical simulations (Zhang, et al. 2024) and experiments (Turnock et al., 2024) to assess emission reduction potential.

Project objectives

- Research and predict the aerodynamic and hydrodynamic forces acting on wind-assisted ships.
- Analyse and understand the complex interactions between wing sails, hull, propeller, and rudder.
- Develop efficient methods for predicting wind-assisted vessel performance.
- Contribute to the advancement of wind-assisted propulsion technology in modern shipping.

- Main Results

Efficient prediction of wind-assisted vessel performance is crucial for maximizing the savings achieved through route optimisation. This presents an opportunity to combine high-performance sailing prediction techniques with recent ship resistance and propulsion research to develop effective tools for commercial wind-assisted vessels.

Using a self-propelled KCS model, we experimentally investigated the complex interactions between hull, rudder, and propeller under varying rudder and leeway angle conditions. Our findings revealed intricate relationships among these factors and wind assistance levels. The total tow force coefficient increased with both rudder angle magnitude and leeway angle, showing a more pronounced effect at negative leeway angles. This asymmetry highlights the importance of flow field dynamics, particularly around the transom and propeller. Analysis of drift-induced resistance provided valuable insights into efficiency trade-offs in wind-assisted propulsion systems. The side force coefficient (Fig. 1) and yaw moment studies demonstrated clear interactions between rudder and leeway angles. Notably, our results showed that larger leeway angle magnitudes require increased rudder angles to maintain balance, with the specific angle varying based on wind assistance level (Fig. 2).

Potential application

This study establishes a robust framework for understanding the hydrodynamic complexities of wind-assisted propulsion in modern shipping. Our findings significantly advance the development of performance prediction algorithms, providing a foundation for more accurate modelling and optimization of wind-assisted vessels. The experimental results improve the prediction algorithm, enabling precise forecasts of vessel performance that will be validated against a demonstration vessel within the project scope. This project is crucial for independently verifying the fuel savings of wind-assist technologies, accelerating their market readiness, and contributing to the creation of quieter, emission-free ships that benefit ocean environments and improve air quality in ports and coastal cities.

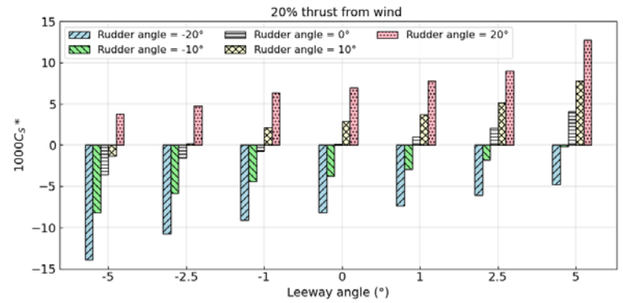

Fig. 1 Influence of combined rudder and leeway angles on side force coefficient.

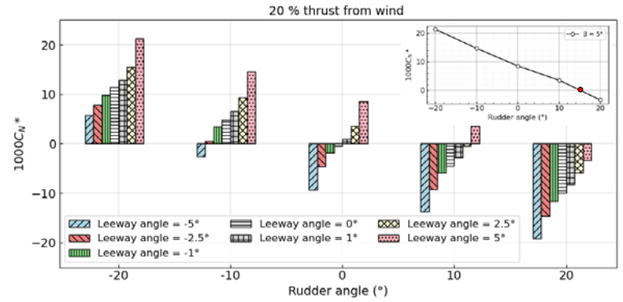

Fig. 2 Effect of combined rudder and leeway angles on yaw moment coefficient.

References

Y Zhang, et al. (2024). Influence of drift angle on the propulsive efficiency of a fully appended container ship (KCS) using Computational Fluid Dynamics." Ocean Engineering 292: 116537.

S Turnock, et al. (2024). Hull-propeller-rudder interactions: Time-accurate data of a scaled model ship in waves. Ocean Engineering, 312, 119258.

Funding body

This work was conducted as part of the Winds of Change Clean Maritime Demonstration project funded by UKShore and Innovate UK.

Further information

This research includes experimental studies, numerical simulations, and a prediction algorithm, carried out by a team of researchers listed below from Maritime Engineering (MarEng) group at the University of Southampton.

Joseph Banks – j.banks@soton.ac.uk
Saeed Hosseinzadeh – s.hosseinzadeh@soton.ac.uk
Yifu Zhang, Andhini Zurman-Nasution, Dominic Hudson, Stephen Turnock, Martyn Prince

Collaborations

Wolfson Unit: https://www.wumtia.soton.ac.uk/
Smart Green Shipping: https://smartgreenshipping.com/

22. EXPERIMENTAL INVESTIGATION OF THE IMPACT OF LEEWAY AND RUDDER ANGLES ON THE YAW MOMENT BALANCE FOR WIND-PROPELLED SHIPS

23. Effects of Build Orientation on Fatigue Crack Growth in Laser Powder Bed Fusion IN718

Matthew Hulbert[1], Philippa Reed1 & Andrew Hamilton[1]
[1] Engineering Materials Research Group, School of Engineering, University of Southampton, Highfield, Southampton, SO17 1BJ, UK

Project Background and Goals

Inconel 718 is a nickel-based superalloy commonly used in aerospace engine technology due to the stability of its mechanical performance up to temperatures of ~650°C. The weldability of this material, along with the increasing complexity of aerospace engines, makes it a good choice for Laser Powder Bed Fusion (LPBF) manufacturing. However, when understanding the fatigue performance, significant complications arise due to the unique microstructure formed as a result of the thermal conditions during the manufacturing process. In particular, a predominantly columnar microstructure, aligned parallel with the build direction, is characteristic of parts manufactured in this way. This gives rise to anisotropic properties within the material. Therefore, this study considers the effect of build direction on the fatigue response at high temperatures.

Discussion of Methods and Results

At these high temperatures, the anisotropic effects of the microstructure are amplified due to the grain boundaries providing preferential crack paths through the component. This results in significantly different crack behaviour between build orientations. Within this study, Single Edge Notch Bend (SENB) specimens, printed in vertical and horizontal orientations, were tested at elevated temperatures of 650°C. Tests were conducted at constant load and a frequency of 0.25Hz, with data recorded using a Direct Current Potential Drop (DCPD) approach. The resultant data was calibrated and compared between the two build orientations, and various techniques were employed to gather further information from the fracture surfaces. These techniques included optical microscopy and macroscopy of the fracture surface, crack path, and crack tip (where applicable). In addition, Alicona Infinite Focus Microscope (IFM) scans and Scanning Electron Microscope (SEM) imaging of the samples were also used.

Crack growth rates were observed to be an order of magnitude higher when the crack grew perpendicular to the grain direction than when growing parallel, contrary to findings within the literature. Additionally, the perpendicular crack growth showed significant deflection from the crack path with maximum bending moment – growing under mixed mode conditions. This suggests a susceptibility to shear (mode 2) loading causing accelerated crack growth. Again, contrasting expected results, crack growth parallel to the grain direction was observed to be interrupted, presenting relatively consistently spaced crack arrests at low DK values. These results further emphasise the importance of fully understanding the micromechanisms behind crack growth at high temperature through this anisotropic microstructure.

Further Research

Further investigation at room temperature, including a comparison of crack propagation behaviour in equivalent samples, may aid in developing the understanding of the complex and unique crack paths observed as a part of this study. Furthermore, repeat tests under pure mode 1 loading, and a controlled ratio of mode 1 to mode 2 tests could help further explain the dependability of fatigue crack growth on mixed mode loading conditions.

24. Forecasting Transhipment Volume and Analysing Dynamics given Geopolitical and Health Events: A Case Study of the Port of Busan on a Specific Maritime Shipping Route

Kimoon Jang
University of Engineering

Project objectives and goals

The aim of this study is to develop a forecasting model for container transhipment volume (CTV) at the Port of Busan on the maritime route from China to the U.S. The study has three main objectives: to investigate the background of the case study by analysing past and recent trends in relevant industries, focusing on transhipment hub ports (THP); to derive an accurate forecasting model using various methods; and to examine the dynamics surrounding CTV.

Description of method and results

Three methods were employed to model CTV: multiple regression analysis (MRA), autoregressive integrated moving average with exogenous variables (ARIMAX), and explainable boosting machine (EBM). EBM, a machine learning method based on a gradient boosting algorithm, enables glass-box modelling that offers insights into the dynamics surrounding CTV (Nori et al. (2019)).

We obtained 12 datasets from various sources, including governments and global analysis institutions, defining 8 variables: 1 dependent variable (CTV (TEU, Twenty-foot Equivalent Units)) and 7 independent variables, such as U.S. imports from China (USD), ship voyage duration (days), and port congestion levels (dimensionless), spanning January 2016 to May 2024 (101 months), with the first 89 months for model fitting and the remaining 12 months for validation.

The EBM model demonstrated superior performance during both fitting and validation periods, with Mean Absolute Percentage Errors of 2.9% and 7.4%, and R-squared values of 0.95 and 0.68, respectively. Korean industry experts assessed these results as satisfactory for forecasting CTV.
External events significantly impacted THP activities. The U.S.-China trade war, a geopolitical issue, led to supply chain restructuring, including reshoring and nearshoring (Moehr (2018)), affecting CTV at Busan. The COVID-19 pandemic, a health issue, caused further disruptions, with shipping liners favouring direct shipping over transhipment due to severe congestion in global maritime logistics (Reuters (2021)). During the validation period, conflicts involving Houthi rebels led to an unexpected increase in CTV at Busan from Chinese ports.

Potential for application of results

From a research perspective, this study collected a dataset that reflects real-world industry conditions and developed a CTV forecasting model. This approach underscores the originality of the study and demonstrates that complex CTV dynamics can be effectively examined using limited data, highlighting potential for future research.

From a policy standpoint, the results emphasise the vulnerability of transhipment logistics to external factors and the importance of adaptability in port management. The study's forecasting capabilities enable efficient port facility investments and proactive operational measures for both public and private sectors. Insights from the analysis of dynamics among variables can assist in predicting future unexpected events.

The research contributes to academia and industry, providing valuable tools for decision-making in an increasingly complex global shipping environment.

References

Nori, H., Jenkins, S., Koch, P. and Caruana, R., (2019). InterpretML: A unified framework for machine learning interpretability. arXiv preprint arXiv:1909.09223.

Moehr, O., (2018). Trade Disrupted: US and China Need More Than a Truce. Atlantic Council.

Reuters, (2021). South Korea's container squeeze throws exporters into costly gridlock. *Reuters*, 9 July. [Online] Available at: https://www.reuters.com/business/south-koreas-container-squeeze-throws-exporters-into-costly-gridlock-2021-07-09/

25. Synergy of tidal power and flood alleviation in UK estuaries

Karam Kalsi, Luke Blunden and AbuBakr S Bahaj
Energy and Climate Change Division, Sustainable Energy Research Group, University of Southampton

Project objectives and goals

Many UK estuaries present both tidal power potential and significant risk of coastal flooding, which is being exacerbated by climate induced sea-level rise. This project investigates the potential synergy between tidal power generation (through turbine arrays or barrages) and flood prevention through surge barriers. By exploring the integration of renewable energy production with flood protection.

The research aims to undertake:

- Desk study to review overlap between literature and UK datasets covering tides and surges in estuaries, tidal power potential, flooding and sea-level rise.
- Case study future-scenario modelling of the River Itchen mixed-use scheme using field data on tidal elevations and with flood prevention under long term future climate change & sea-level scenarios.
- Techno-economic feasibility assessment of such multi-use schemes, enhanced with bathymetric data, tidal measurements and recent cost estimates.

Description of method and results

Hydrographic and official data layers were combined to identify areas of high flood risk and population density as potential sites for tidal power installations around the UK (Fig.1). Bathymetric data from the S-100 trial [Admiralty,2024] was used to calculate the depth of the estuaries such that the cross-sectional area of a potential barrage may be derived.

As a case study, a hypothetical barrage was simulated in the River Itchen (Southampton UK, (Fig.1)), where the black box represents the Itchen Bridge, the location selected for the case study).

Tidal elevation data from Southampton Port [Admiralty,2024] was used to model a tidal barrage operating in ebb flow generation. This is illustrated in Fig.2, where a time-stepping loop waits until sufficient head difference is reached before generating electricity until the basin level and the sea-level are equal, all based on a fixed discharge coefficient. Power is calculated by time-stepping Eq.1 following identification of generation periods [Pugh, D.T.,1993].

$$Potential\ Energy\ Change\ per\ Tidal\ Cycle = \frac{1}{2}\,\rho\, g\, Area\, \Delta H^2$$

Equation 1

Initial results indicate a modest annual potential of 3.5 GWh, accounting for the entire electrical demand of Southampton 033B LSOA which has 1200 electrical meters [GOV.UK,2024].

Potential for application of results

Future development of the model will introduce additional complexities, including sluicing, holding and generating, and will account for variations in tidal range, river flow, storm surges etc. Machine learning techniques could be applied to optimise the predictive operation of tidal barrages.

The time stepping model was effective in modelling the Solent's complex tidal dynamics, including its double high-water phenomenon, with the developed methods robustly applicable for other estuaries with similar characteristics.

Acknowledgement

Funding from 2023/24 SMMI HEIF fund, supported by Energy and Climate Change Division.

25. SYNERGY OF TIDAL POWER AND FLOOD ALLEVIATION IN UK ESTUARIES

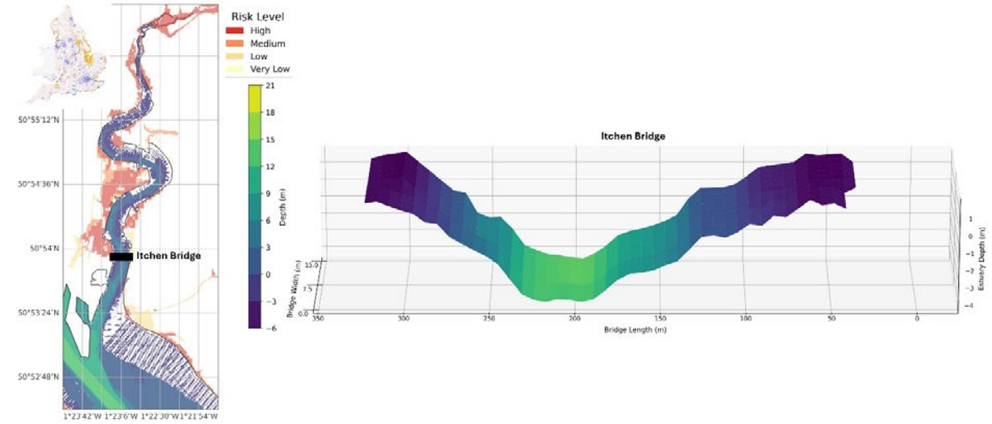

Fig.1 Mapping the Flood Risk, Population Density and Bathymetry for UK Estuaries

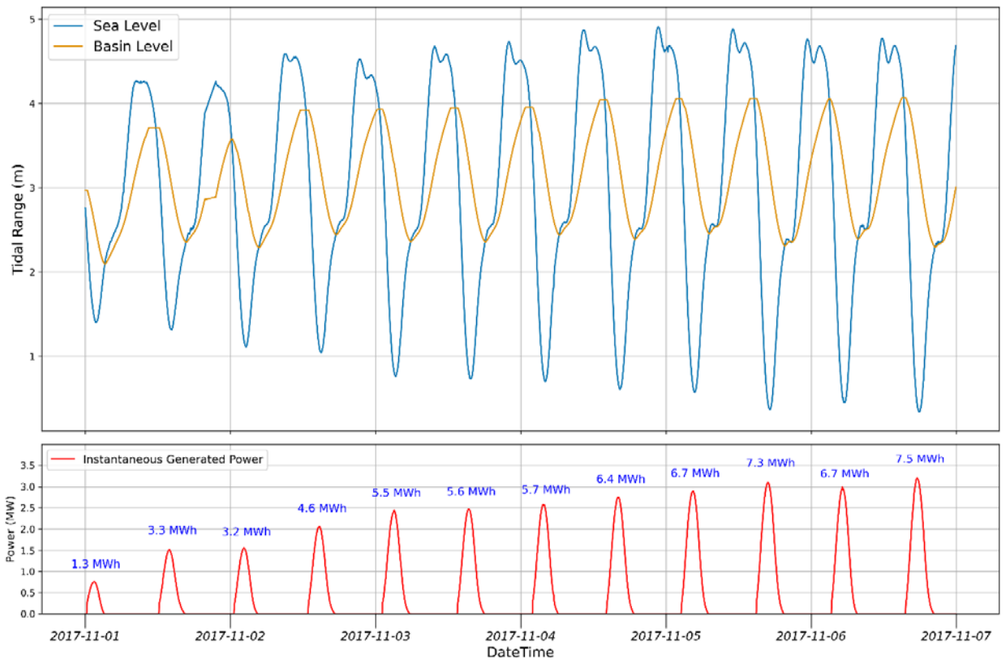

Fig.2 Tidal Range and Barrage Modelling with Power Generation for the Itchen Bridge

References

Soton Met. (2024). Tidal Data. https://www.sotonmet.co.uk/(S(e2yprs55kizvnsyqfpo1zfau))/default.aspx

GOV.UK (2024) Lower and Middle Super Output Areas electricity consumptionhttps://www.gov.uk/government/statistics/lower-and-middle-super-output-areas-electricity-consumption

Data.gov.uk (2024) Risk of flooding from multiple sources risk band. https://www.data.gov.uk/dataset/0afc0a17-cb2c-4221-bcb8-947e61ac30f0/risk-of-flooding-from-multiple-sources-risk-band

Admiralty (2024) Access data S-100. https://www.admiralty.co.uk/access-data/s-100

Pugh, D.T. (1993) Tides, Surges and Mean Sea-Level. Chichester: Wiley.

26. Investigation of Green Hypergolic Chemical Bipropellant Propulsion Systems

Ahmet Nihat Karci(1), Charlie Ryan(2)
Faculty of Engineering and Physical Sciences, Southampton, United Kingdom
(1)a.n.karci@soton.ac.uk, (2)c.n.ryan@soton.ac.uk

Project objectives and goals

Traditional hypergolic bipropellant propulsion systems in spacecraft use toxic and hazardous propellants such as monomethyl hydrazine(MMH) and dinitrogen tetroxide(NTO). These substances require stringent safety measures and incur high costs. Research is now focused on developing safer, environmentally friendly hypergolic propellants with similar performance to address these issues. The goal is to reduce health and environmental risks while cutting production and handling expenses associated with spacecraft propulsion.

Description of method and results

High-Test Peroxide (HTP), with a concentration of 95.4 wt%, is used as the green oxidizer in this project. Various alternative fuels were evaluated for their hypergolicity with HTP using drop tests, which were recorded with a high-speed camera to measure ignition delay time (IDT). A target IDT of approximately 15 ms was set for rapid, repeatable ignition, based on literature (Austin et al., 2012; Lauck et al., 2021). The results of the drop tests are given in Table 1.

Table 1 - Drop Test Results

Fuel	Fuel Proportion (wt%)	Additive	Additive Proportion (wt%)	Average IDT (ms)
EMIM SCN	100	-	-	41.11
EMIM SCN	99.5	$CuCl_2$	0.5	21.56
EMIM SCN	99	$CuCl_2$	1	21.00
EMIM SCN	97	$CuCl_2$	3	14.44
EMIM SCN	95	$CuCl_2$	5	12.00
N-Methylformamide	100	-	-	-
N-Methylformamide	99	$NaBH_4$	1	-
N-Methylformamide	97	$NaBH_4$	3	15.56
N-Methylformamide	95	$NaBH_4$	5	10.89
Pyridine	100	-	-	-
Pyridine	98.01	$NaBH_4$	1.99	-
Pyridine	94.17	$NaBH_4$	5.83	11.33
NN-Dimethylthioformamide	100	-	-	27.33

Results indicated that 1-Ethyl-3-methylimidazolium thiocyanate (EMIM SCN) is hypergolic with HTP but has a longer IDT. However, adding copper(II) chloride as an additive significantly reduced the IDT to 12.00 ms. For N-Methylformamide and pyridine, which were not inherently hypergolic with HTP, the inclusion of sodium borohydride ($NaBH_4$) achieved sufficiently short IDTs, with N-Methylformamide reaching 10.89 ms and pyridine reaching 11.33 ms. NN-Dimethylthioformamide was also hypergolic with HTP, and shorter IDTs can be attained using additives.

Potential for application of results

These results demonstrate the potential of selected green fuels for spacecraft propulsion systems. The next phase involves integrating these fuels into a propellant delivery system, thruster, and cooling system for impingement and thruster testing. If these evaluations are successful, the green propellant system could be refined into a final product suitable for spacecraft propulsion, with the possibility of extending its application to launch vehicles.

References

Austin, B. L., Heister, S. D., & Anderson, W. E. (2012). Characterization of Pintle Engine Performance for Nontoxic Hypergolic Bipropellants. Https://Doi.Org/10.2514/1.7988, 21(4), 627–635. https://doi.org/10.2514/1.7988

Lauck, F., Balkenhohl, J., Negri, M., Freudenmann, D., & Schlechtriem, S. (2021). Green bipropellant development – A study on the hypergolicity of imidazole thiocyanate ionic liquids with hydrogen peroxide in an automated drop test setup. Combustion and Flame, 226, 87–97. https://doi.org/10.1016/J.COMBUSTFLAME.2020.11.033

26. INVESTIGATION OF GREEN HYPERGOLIC CHEMICAL BIPROPELLANT PROPULSION SYSTEMS

27. Development of a low-cost Paper-Based Point of Care Device for Blood Glucose Detection

Asadullah Khan

In recent years, point-of-care testing (POCT) devices have revolutionized fields such as medical diagnostics, food safety, and environmental monitoring by providing rapid and convenient analysis, enabling timely decision-making. Despite these advancements, the need for low-cost, portable, and user-friendly diagnostic tools remains critical, especially in resource-limited settings.

This paper presents a novel, low-cost, 3D-printed device designed for the quantitative determination of blood glucose levels. Central to our innovation is a universal clamp, compatible with any mobile phone, which harnesses the phone's display screen brightness to illuminate a sample on a paper microfluidic strip. This paper-based analytical device is engineered to slide seamlessly into the 3D-printed structure, allowing the mobile phone's camera to capture colorimetric data.

Utilizing principles of the Beer-Lambert law, the device accurately quantifies glucose concentrations, transforming the mobile phone into a sophisticated diagnostic tool. This integration of paper microfluidics with mobile phone technology offers a cost-effective and accessible solution for glucose monitoring, particularly beneficial for managing diabetes and other metabolic disorders.

Our research delves into the design, feasibility, and performance of this innovative diagnostic platform. By combining advancements in 3D printing, microfluidics, and optical sensing, we aim to enhance the accessibility of essential diagnostic tools. This study underscores the potential of our device to expand point-of-care diagnostics, providing a significant contribution to healthcare, food safety, and environmental monitoring.

Our findings suggest that this low-cost, portable diagnostic tool not only meets the immediate needs of healthcare providers and patients but also paves the way for future innovations in the field of POCT devices.

28. Stimulus Duration Effects on VEMP Responses at 125 Hz and 500 Hz

Kocak Erdem B[1], Bell SL[1], Ye Y[1]
1 Institute of Sound and Vibration Research, University of Southampton, Southampton, UK

Project Objectives and Goals:

This study aims to investigate the effects of different stimulus types and durations on Vestibular Evoked Myogenic Potentials (VEMPs) to better understand the response characteristics of the saccule and utricle at 125 Hz and 500 Hz frequencies. The project utilizes traditional air-conducted (AC) and bone-conducted (BC) sounds (BEST, and B81 transducers), along with vibration-based stimuli using Mini-shaker. Previous research (Cheng, Wu, and Lee, 2012; Lim et al., 2013; Parker-George, Bell, and Griffin, 2016) has examined the influence of stimulus types on VEMP responses. However, there is a lack of systematic investigation on the interaction between different durations and methods of stimulation at these specific frequencies.

Description of Method and Results

Eighteen healthy participants (10 females, 8 males) aged between 23-41 years were included in this study. VEMP responses were collected with four different transducers (AC, B81, BEST and mini-shaker) and different stimulus durations (1:2:1, 1:4:1, 1:8:1) (1 cycle rise/fall and 2,4,8 cycles plateau), at 125 and 500 Hz frequencies. At 500 Hz, both cVEMP and oVEMP responses showed consistent behaviour across different stimulus durations. Shorter durations, such as 4 and 6 cycles, produced comparable latency and amplitude values, whereas a 10-cycle stimulus resulted in a significant reduction in amplitude, indicating that longer durations may not be optimal for eliciting robust responses. For 125 Hz stimuli, the B81 transducer showed increased susceptibility to stimulus artefacts, making it less suitable for clinical applications at 125 Hz due to potential compromises in response quality and reliability. In contrast, oVEMP responses to mini-shaker stimulation at 125 Hz were duration-dependent, with increasing stimulus duration resulting in increased mean Fsp values and p-p amplitude, suggesting that temporal properties may effect the vestibular response.

Potential for application of results

At 500 Hz, shorter durations are recommended for saccular-based assessments, particularly in conditions like Meniere's disease, where saccular dysfunction is common. Longer durations are recommended for utricle-specific testing at 125 Hz, as they produce stronger and more consistent responses, which can be useful in diagnosing utricular pathologies such as superior canal dehiscence syndrome. These insights can inform clinical protocols by tailoring VEMP parameters to better distinguish between utricular and saccular dysfunctions, ultimately contributing to a more comprehensive understanding of vestibular function and its underlying mechanisms.

References

Cheng, Y. L., Wu, H. J., & Lee, G. S. (2012). Effects of plateau time and ramp time on ocular vestibular evoked myogenic potentials. Journal of Vestibular Research, 22(1), 33-39.

Lim, L. J., Dennis, D. L., Govender, S., & Colebatch, J. G. (2013). Differential effects of duration for ocular and cervical vestibular evoked myogenic potentials evoked by air-and bone-conducted stimuli. Experimental brain research, 224, 437-445.

Parker-George, J. C., Bell, S. L., & Griffin, M. J. (2016). Ocular vestibular evoked myogenic potentials elicited with vibration applied to the teeth. Clinical Neurophysiology, 127(1), 833-841.

29. Perfusion chamber for the investigation of microbubble oscillation in bone fractures

Dariusz Kosk[1], Meng Chen Michelle Li[1], Shemaal Parry[1], Richard OC Oreffo[2], Eleanor Stride[3], Dario Carugo[3], Janos Kanczler[2], Nicholas D Evans[2]
[1] Faculty of Engineering and Physical Sciences, University of Southampton, Southampton, UK; [2] Faculty of Medicine, University of Southampton, Southampton, UK; [3] Nuffield Department of Orthopaedics, Rheumatology and Musculoskeletal Sciences (NDORMS), University of Oxford, Oxford, UK.
Corresponding author: dkk1e21@soton.ac.uk – PhD student (2nd year), Supervisor email: N.D.Evans@soton.ac.uk

Project objectives and goals

Approximately 2-10% of bone fractures result in delayed or non-union healing. The associated complications have a significant negative impact on patients' lives and surgery carries a high risk of disease transmission. Gas-filled microbubbles (MBs) perfusing the vasculature can be stimulated to oscillate by remote application of ultrasound and are therefore a potential minimally-invasive drug delivery system for bone fracture treatment. However, there is a lack of in-vitro models recapitulating the physical and geometrical properties of bone fractures, which could be employed in laboratory-scale research on novel ultrasound-mediated therapies. The aim of this study was to develop a perfusion chamber to study the behaviour of ultrasound-stimulated microbubbles.

Description of method and results

MBs were formulated by sonication of suspensions of 1,2-distearoyl-sn-glycero-3-phosphocholine (DSPC), polyoxyethylene (40) stearate (PEG(40)s) at molar ratios of 9:1.

Perfusion chambers were manufactured via replica moulding, coupled with 3D printed parts. The device design comprised a 2 mm wide channel passing through a series of bone fracture geometries. Positive moulds were designed in SolidWorks and 3D printed using stereolithography. Upon fabrication, moulds were baked in the oven at 120 for 120 min and exposed to ultraviolet light for 120 min. Subsequently, the moulds were filled with liquid polydimethylsiloxane in 10:1 ratio, cured and then bonded together with inlet-outlet structure.

MBs were perfused through system, after its placement in custom designed ultrasound stimulation chamber, employed for the in-vitro testing with a passive cavitation detection (PCD) device placed on the opposite side of a transducer (operating at 1.0 MPa, 1000 kHz frequency and duty cycle of 30%). MBs concentration varied within the range of 1.271x106 to 1.27 x107 MBs/mL. PCD device and TiePie were used to detect and record acoustic emissions. COMSOL 6.1 with frequency-domain simulations were carried out to model the ultrasound pressure field within the device, as a function of bone geometry.

The total power of the acoustic emissions generated by MBs under ultrasound stimulation increased with MBs concentration. COMSOL simulations showed increased acoustic pressure magnitude in the focus point of the transducer (placement of MBs channel) from 0.97 MPa to 1.41 MPa when the fracture gap width was set to 0.5 mm and 4.0 mm, respectively. Fracture gap simulations predicted higher peak pressures in the whole volume of in-vitro system, located out of the focus zone of the transducer, reaching 2.28 MPa for the 0.5 mm fracture model. Physical obstruction created by a narrow fracture gap below 1.5 mm, reduces ultrasound pressure field in the transducer focus. This is a very important finding for selecting appropriate MB concentrations and US parameters for specific fracture geometries.

Potential for application of results

As would be expected the concentration of MBs has a significant impact on their activity upon ultrasound stimulation in a non-obstructed system. We also found that increased ultrasound pressure caused by the bone geometry has a high impact on MB cavitation due to lower acoustic pressure, and it could potentially impact MB detection and biological effects such as sonoporation, due to high pressure generated on the side of the transducer by reflected ultrasound waves.

30. Regional discrepancies of transportation investment appraisal outcomes in South Korea

Changhoon Lee
Transport Research Group, University of Southampton
Supervisors: Prof. John Preston, Dr Shahram Heydari

Project objectives and goals

This study examines the regional disparities in transportation investment appraisal outcomes in South Korea, focusing on the impact of the Preliminary Feasibility Study (PFS) system introduced in 1999. The PFS was designed to assess large-scale infrastructure projects, integrating economic feasibility, policy objectives and regional balance using the Analytic Hierarchy Process (AHP) that originates with Saaty (1980). This research aims to determine whether the inclusion of regional balance considerations in the PFS framework has effectively fostered regional balance between developed and less developed regions.

Description of method and results

The analysis utilizes data from 484 PFS cases conducted between 2002 and 2023, covering road and railway projects. A panel regression model is employed to control for temporal dependencies and regional variations Hsiao (2020). Key variables include the Benefit-Cost Ratio (BCR), project type, project cost, weights of assessment criteria (w_brd), and regional socioeconomic indicators, such as population density. The analysis results are shown in Table 1. These results indicate that less developed areas receive higher scores in the PFS, supporting investments despite lower economic feasibility. In contrast, major cities outside the Seoul capital area, such as Busan and Daegu, experience disadvantages in scoring compared to rural areas and the Seoul metropolitan region.

Table 1: Analysis results

Variables	Model 1	Model 2	Model 3	Model 4
Bcr	1.041***	1.130***	1.109***	1.087***
w_brd	1.593***	-	0.613*	0.858**
Region (ref=Seoul)				
Incheon	-	-	-	-
Gyeonggi	-	-0.114***	-	-
Gangwon	-	0.196***	-	-
S. Chungcheong	-	-	-	-
N. Chungcheong	-	-	-	-
Daejeon	-	-0.235***	-	-
N. Jeolla	-	0.160***	-	-
S. Jeolla	-	0.134***	-	-
Gwangju	-	-0.154**	-	-
N. Gyeongsang	-	0.0779**	-	-
S. Gyeongsang	-	-	-	-
Daegu	-	-0.117**	-	-
Ulsan	-	-0.138**	-	-
Busan	-	-0.198***	-	-
Jeju	-	-	-	-
ln_pop_den	-	-	-0.0657***	-
Region (ref=Seoul Metropolitan)				
Other major cities	-	-	-	-0.105***
Provincial areas	-	-	-	0.112***
Constant	-1.128***	-0.877***	-1.024***	-1.065***
AIC	131.328	68.581	95.784	98.016
BIC	152.239	127.130	120.876	127.291

Note.
* p < 0.1, ** p < 0.05, *** p < 0.01. AIC (Akaike Information Criterion) and BIC (Bayesian Information Criterion) assess model fit, with low values indicating better fit.

Potential for application results

This study found that the inclusion of balanced development initiatives in the PFS positively impacted decision-making regarding transportation investments in underdeveloped areas, while major cities outside the metropolitan area were excluded from these benefits. Based on these conclusions, future research will explore how much transportation investments resulting from the current PFS approach have improved regional balance, utilizing econometric methodologies such as the production function model.

References

Saaty, T.L. (1980). The Analytic Hierarchy Process, McGraw-Hill, New York.

Hsiao, C. (2022). Analysis of panel data, Cambridge University Press.

Further information

Changhoon Lee (Changhoon.Lee@soton.ac.uk)

Supervised by Professor John Preston (J.M.Preston@soton.ac.uk) and Dr Shahram Heydari (S.Heydari@soton.ac.uk)

31. Advancing characterisation of fibre break interaction via *in situ* synchrotron tomography and Digital Volume Correlation

Yeajin Lee, Mark N. Mavrogordato, S. Mark Spearing, Ian Sinclair

g-VIS X-ray Imaging Centre, University of Southampton, UK

Research background

The overarching goal of this study is to achieve a detailed understanding of the longitudinal tensile failure of carbon fibre composites at the micrometre scale. Even though various failure modes can be observed in unidirectional composites, their final failure is often associated with the failure of the load-bearing 0-degree fibre plies. Therefore, this study focuses on characterising the accumulation of fibre breaks and their interaction with local microstructural damages, until the occurrence of final failure.

A crucial factor in determining fibre break development is the load redistribution from a broken fibre to surrounding intact fibres through the matrix. As consecutive fibre breaks accumulate steadily and exponentially, large regions of the remaining intact fibres become overloaded with significant stress concentrations. These affected fibre bundles reach a critical state when saturated with individual breaks and groups of clustered breaks, potentially triggering final failure. This scenario of longitudinal tensile failure has been widely accepted and studied in literature and fibre break models to elucidate the interaction between load redistribution and cluster formation. Nevertheless, discrepancies between experimental observations and models persist, highlighting the necessity to develop approaches for a more reliable and detailed understanding of the longitudinal tensile failure processes.

Description of research goals, methods, and results

To pave the way for more reliable failure predictions, this study fully leverages the potential of *in situ* damage monitoring, enabled by state-of-the-art ultrafast synchrotron radiation computed tomography combined with *in situ* mechanical testing and digital volume correlation (DVC) [1,2]. This approach first provides an opportunity to monitor the accumulation of fibre breaks in relation to longitudinal debonds, matrix cracks, and local morphologies, such as fibre misalignment. Additionally, the integration of DVC with the acquired *in situ* scans facilitates the monitoring of load redistribution around fibre breaks by mapping 3D local fibre-level strains around fibre breaks along the fibre direction. The results and findings shed new light on fibre break development and highlight the importance of accounting for load redistribution varied by cluster patterns and local microstructural damages, for a reliable understanding of longitudinal tensile failure processes.

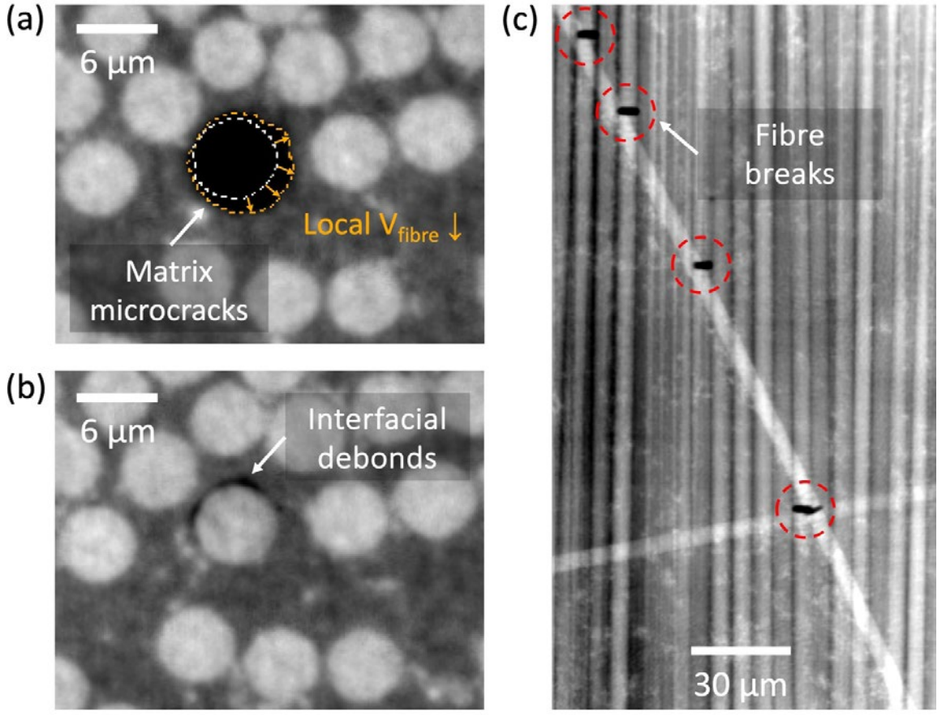

Fig 1. Formation of fibre breaks in relation to (a) matrix micro-cracks, (b) interfacial debonds, and (c) fibre misalignment, as captured by in situ synchrotron holotomography at a 150 nm pixel size.

References

[1] Schöberl, E., et al. "Fibre-direction strain measurement in a composite ply under quasi-static tensile loading using Digital Volume Correlation and in situ Synchrotron Radiation Computed Tomography." Composites Part A: Applied Science and Manufacturing 137 (2020): 105935.

[2] Lee, Y., et al. "Internal strain sensing in carbon fibre composites via digital volume correlation and in situ synchrotron computed tomography." ICCM23 International Conference on Composite Materials (2023)

Collaborators

European Synchrotron Radiation Facility (ID16B/ID19 beamline), Grenoble, France

https://www.esrf.fr/UsersAndScience/Experiments/XNP/ID16B

https://www.esrf.fr/home/UsersAndScience/Experiments/StructMaterials/ID19.html

Department of Materials Engineering, KU Leuven, Belgium

https://www.mtm.kuleuven.be/english/research/scalint/cmg

Funding body

Mitsubishi Chemical Corporation https://www.mcgc.com/english/group/outline/mcc/

32. Vibro-acoustic Metamaterial With an Embedded Helmholtz Resonator

Kenneth Leung
University of Southampton

Project Objectives and goals

Acoustic metamaterials (AMM), which are artificial structures that are composed periodically arranged subwavelength resonant unit-cells, display superior sound transmission loss (TL) capabilities that are not achievable with their constitutive materials alone. Such characteristics of AMM have led them to emerge as potential future technology for lightweight sound insulation. Previous work by Van Belle et al. (2019) have proposed a cantilever AMM design, which had gain research interest due to its simple design and manufacturability. However, this AMM design only provides a TL improvement in a limited frequency bandwidth and introduces a region of TL deficit at higher frequencies in comparison to the well-known mass-law. My work aims to reduce the TL deficit and expand the bandwidth of TL improvement by embedding a Helmholtz resonator in the cantilever design, as shown in Fig. 1a.

Description of method and results

The predicted TL of the proposed AMM is simulated in a finite-element model using the COMSOL commercial package, with the set-up shown in Fig. 1.b. To increase computational efficiency, a single AMM unit-cell is modelled, with Bloch-Floquet periodic conditions imposed on the edges of the unit cell to simulate an infinitely large partition. The AMM cell is subjected to an incident sound wave of 1 Pa amplitude. The sound power of both the incident sound wave and the transmitted sound wave are calculated to obtain the AMM TL performance.

The TL of the proposed AMM design is plotted in the blue curve in Fig. 2. The figure shows a TL improvement compared to the mass-law (Fig. 2 yellow curve) due to the structural resonance (CL) at 310 Hz and the Helmholtz resonance (HR) at 340 Hz. The HR resonance frequency is tuned to both extend the bandwidth of TL improvement and reduce the TL dip. The improvement can be seen by contrasting behaviour to the same AMM design with a deactivated HR, as shown by comparing the blue and red curves in Fig. 2. By embedding the HR, the bandwidth is extended by 25 Hz and the TL dip is reduced by 2 dB.

Potential for applications of results

Despite only emerging as a research field from the early 2000s, the research on AMM for lightweight sound insulation applications is becoming one of the hottest topics of acoustic research. AMM is also appearing as sound insulation solutions in aerospace, automotive and architectural industries, and have huge potential on industrial applications when problems such as limited bandwidths and mass-production manufacturability are tackled.

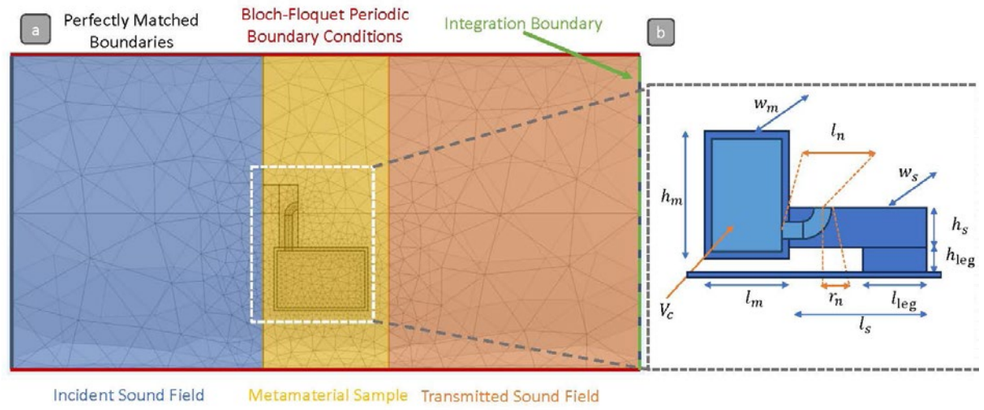

Fig 1. Finite-element simulation set-up of a unit-cell of the proposed AMM. (a) AMM design. (b) Simulation set-up.

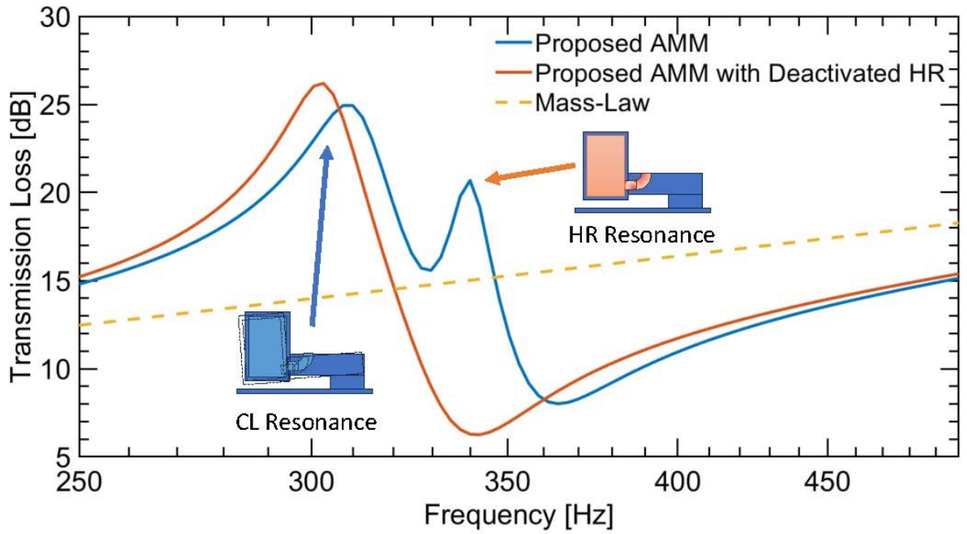

Fig 2. Sound transmission loss of proposed acoustic metamaterial (blue), in comparison to acoustic metamaterial with a deactivated Helmholtz resonator (red) and corresponding mass-law (yellow).

References

L Van Belle et al (2019). The impact of damping on the sound transmission loss of locally resonant metamaterial plates, Journal of sound and vibration 461(114909).

33. A holistic approach towards incorporating and/or improving the green sustainability of chemical process plant systems

Daniel Li
University of Southampton

Project objectives and goals

Truly holistically green sustainability has yet to be fully implemented, particularly from a social dimension beyond safety (Guati-Rojo et al., 2021). Multi-criteria Decision Making (MCDM) with process systems engineering (PSE) tools, such as life cycle assessment (LCA) and life cycle cost analysis (LCCA), could be the key towards holistically green sustainability, particularly in the context of small-scale, modular chemical process plants (CPPs).

- The project proposes the utilisation of MCDM frameworks for holistically green sustainability in CPPs, compared to previous literature (Jamwal et al., 2021)
- Four case studies were examined, with increasing framework complexity: sustainable water desalination, isopropanol via isopropyl acetate, green ammonia production, and bioethanol production. Each case study had pathways that were ranked based on (green) sustainability
- Bioethanol production serves to validate the proposed methodology framework(s), beyond a purely simulation-based level
- Outline the methodology of PSE tools (LCAs and LCCAs, theoretically along with social-LCAs), and how they have/can be integrated with MCDM via literature and PSE software (i.e. SimaPro) to determine specified sub-criteria

Description of methods and results

Table 1 summarises the overall methodology framework(s), pathways, and rankings for each case study. Each case study utilises a methodology framework of increasing complexity via the integration of one or more MCDM methods to remove/mitigate individual limitations/weaknesses (Jamwal et al., 2021). This provides a more reliable and accurate overall ranking of potential pathways, which validates the implementation of integrated MCDM frameworks over individual methods (Vakilipour et al., 2021).

Table 1. Methodology with increasing MCDM complexity (descending), pathways, and highest- and lowest-ranked pathway

Case study	Potential pathways	Methodology	Overall rankings (Highest>Lowest)
Sustainable water desalination (energy configuration; capacity)	100% diesel, 75% diesel / 25% solar, and 60% -- / 40% -- energy configurations + 50, 100, 200, and 1000 m^3/day capacities e.g. A1=100% diesel; 50 m^3/day A2=75% diesel / 25% solar; 50 m^3/day Total pathways=12 (3x4)	FAHP	A3>A2>A1>A6>A9>A5>A12>A8>A11>A7>A4>A10
Isopropanol production	Direct Propylene Hydration (PH) Propylene Indirect Hydration (IAH) Acetone Hydrogenation (AH)	FAHP-TOPSIS	IAH>PH>AH
Green NH_3 production	Wind turbine electrolysis (WGEA) Solar photovoltaic electrolysis (PVEA) Hydropower electrolysis (HPEA) Biomass gasification electrolysis (BGEA) Nuclear high temperature electrolysis (NTEA)	FAHP-TOPSIS FAHP-VIKOR with PROMETHEE-II	HPEA>WGEA>PVEA/BGEA>NTEA
Bioethanol production (alpha-amylase, mL / glucoamylase, gms / fermentation period, days)	Round 1 (R1): 0.3/5/3 R2: 2/16/3 R3: 1.15/10.5/8	LCA-LCCA + FAHP-VIKOR with PROMETHEE-II	R2>R3>R1

References

GUATI-ROJO, A., DEMSKI, C., POORTINGA, W. & VALERA-MEDINA, A. 2021. Public Attitudes and Concerns about Ammonia as an Energy Vector. Energies, 14, 7296

JAMWAL, A., AGRAWAL, R., SHARMA, M. & KUMAR, V. 2021. Review on multi-criteria decision analysis in sustainable manufacturing decision making. International Journal of Sustainable Engineering, 14, 202-225

VAKILIPOUR, S., SADEGHI-NIARAKI, A., GHODOUSI, M. & CHOI, S.-M. 2021. Comparison between Multi-Criteria Decision-Making Methods and Evaluating the Quality of Life at Different Spatial Levels. Sustainability, 13

Contact information:

Daniel Li (dd1r22@soton.ac.uk); Mohamed G. Hassan-Sayed (m.g.hassansayed@soton.ac.uk); Nuno Bimbo (n.bimbo@soton.ac.uk)

Collaborators

School of Chemistry, University of Southampton, SO17 1BJ.

34. Flow Over an Array of Very Tall Buildings with Random Heights

Donnchadh MacGarry, Zheng-Tong Xie and Christina Vanderwel

Department of Aeronautics and Astronautics, University of Southampton

Large-Eddy Simulations (LES) in PALM-4U were used to investigate building slenderness effects. A staggered array of cuboid buildings with random heights was selected for the investigation (Cheng & Castro, 2002). Defining the aspect ratio (AR) as the ratio of the building width to the height, these buildings have an AR= 1 on average. The aspect ratio was then modified to AR = 0.25, while maintaining the same packing density as the AR = 1 building array, as well as the same normalised maximum building height and standard deviation of the heights. A cyclic inlet-outlet boundary condition was used in the validation and verification of the simulation design. It was then used in the comparison of the slenderness effects and approaching wind direction effects. A synthetic turbulence generation (STG) inlet condition was used to verify those results, and to conduct turbulence length-scale analysis in the wake.

Results from the cyclic inlet-outlet gave near identical results in the flow for both AR = 0.25 designs, giving evidence that the changes to the flow are purely due to the aspect ratio of the buildings. The vertical profiles of the spatially averaged velocity and turbulent quantities normalised by the friction velocity were smaller in magnitude within the canopy layer for the AR = 0.25 buildings. A cause of this was due to a skimming regime that was occurring over these high-rise buildings. Adjusting the approaching wind direction produced a notably larger spread in these profiles for the AR = 1 buildings than it did for the AR = 0.25 buildings. Furthermore, it was seen that the spatially averaged deflection angle of the flow around buildings was reduced for the AR = 0.25 buildings. The slenderer buildings were notably less sensitive to wind direction effects. A possible cause for this was due to the height dimension being significantly longer than the cross-section dimensions, thus reducing the influence that the shape of the cross-section has on the flow. Turbulence integral lengthscale analysis in the wake of the buildings when using the STG inlet provided further insight into this observation. The integral length-scales observed in the wake of the AR = 0.25 buildings were notably larger than those for the AR= 1 buildings and were also much larger than the building's cross section size. Thus, the energetic eddies were less affected by the cross-section geometry. This helps explain why the slenderer buildings were less sensitive to the various approaching wind directions tested in the simulations with the cyclic inlet-outlet. Castro et al. (2006) stated that the integral length scales in the wake can be approximated by the building's width. However, the integral length scales estimated in this current study suggest that height of the building must be accounted for as well. Further work in this investigation is currently on-going, using wavelet analysis to understand vortex shedding and examining the dispersive shear stress in the flow.

References

Castro IP, Cheng H, & Reynolds R, 2006, Turbulence over urban-type roughness: deductions from wind-tunnel measurements. Bound.-Layer Met., 118, pp.109-131. Cheng H & Cast

35. Integrating Qualitative Content Analysis into Quantitative Systems Modeling: A Methodological Approach for Understanding Dynamics in Fisheries Socio-Ecological Systems

Imali Manikarachchige, Paul Kemp, Bindi Shah, Jonathan Hare
University of Southampton

Project objectives and goals

Information collection is essential to gain a comprehensive understanding of complex issues and provide the fundamental evidence needed to inform sound decision-making. Evidence synthesis is vital in various fields including engineering, healthcare, and multidisciplinary studies, which relys on technical literature to justify contemporary research and innovation needs.

Qualitative approaches have been historically neglected in technical fields, however, this trend is now shifting more towards mixed method research. Qualitative measures have more power in theory constructions (Vogelsang et al., 2013) and are now embraced in studies focusing on the socio-cultural aspects of technical phenomena (Crosbie, 2006). The objective of this paper is to demonstrate how content analysis, a qualitative research approach, can be effectively used to inform quantitative systems modeling in a socio-ecological systems paradigm.

Description of method and results

A research gap was identified asserting that there is a need to predict the dynamics of vulnerabilities of fisheries socio-ecological systems (SES). An SES is a complex and dynamic structure with an interdependent connection between the ecological and social components through a flow of material and information and the system can be vulnerable to various external stressors, shattering the delicate balance between the two components. A research question was developed to (i) identify multifaceted stressors in fisheries SES and (ii) understand how they infiltrate into the social and ecological components, triggering vulnerabilities. To answer the first part of the research question, a systematic review of peer-reviewed scholarly articles was carried out. The SPIDER framework was used to select the relevant articles, and a content analysis was performed to identify themes and patterns of information using Nvivo 14. Information that supported answering the research question was highlighted and referenced into thematic codes, which enabled the recognition of recurring patterns and data-driven insights.

The content analysis identified five main themes of stressor categories, namely biophysical, economic, social, technological, and governance stressors. Under each theme, a set of subthemes depicting the type of stressors and their impacts on fisheries SES were identified (Figure 1). The second part of the research question involves mapping the dynamics of the system using Causal Loop Diagrams (CLD). Articles were reviewed for Information that described causal relationships among different variables and how they behave under different stressors. This information was contained in "relationship codes", enabled in the software, which helps to visualize the influence of one variable on another (Figure 2).

Potential for application of results

At this point, both parts of the research question were answered, and the research momentum can be extended toward a quantitative systems modeling. The mapped systems exposed to different stressors can be operationalized with real-time numerical data collected from field surveys. Likewise, qualitative content analysis can be a powerful approach to explore technical literature and propose innovative solutions to present-day problems.

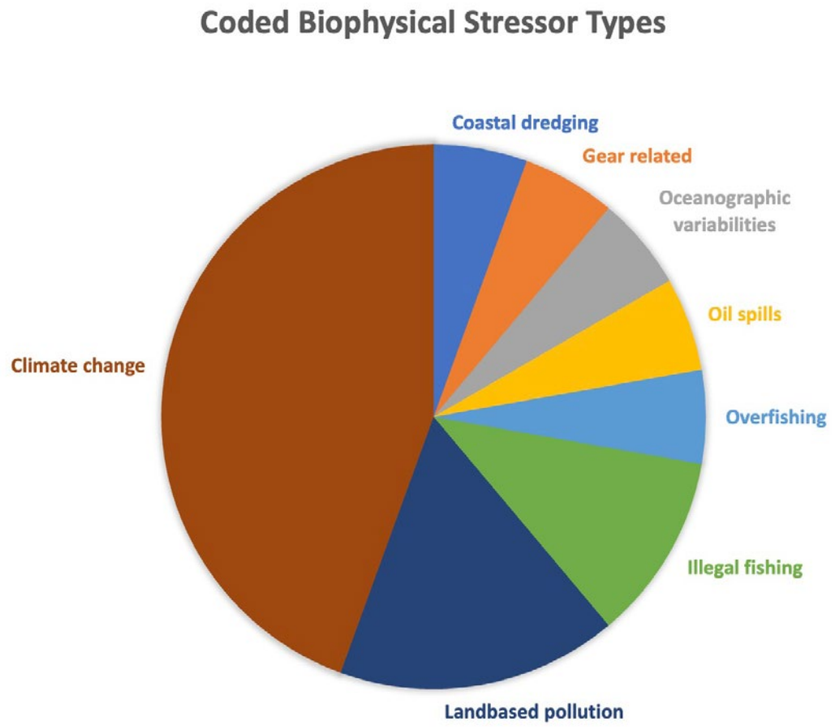

Fig. 1 Coded subthemes under the theme "biophysical stressors"

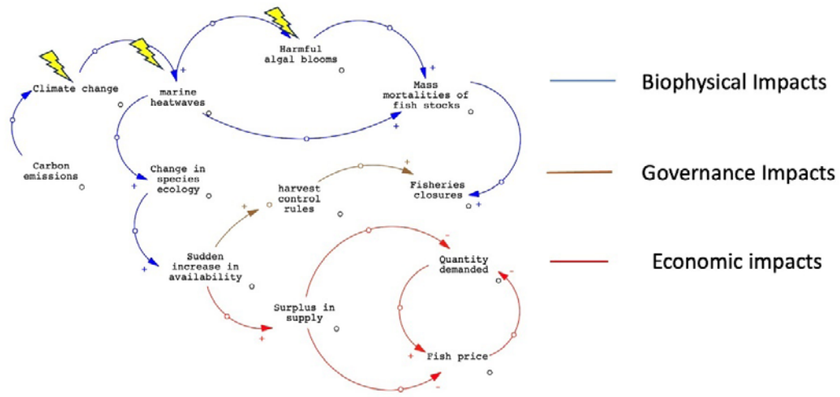

Fig. 2 CLD showing the systems map of fisheries SES, impacted by biophysical stressors

References

Crosbie, T. (2006). 'Household Energy Studies: The Gap between Theory and Method', Energy & Environment, 17, pp. 735–753.

Vogelsang, K., Steinhüser, M. and Hoppe, U.A. (2013) 'A Qualitative Approach to Examine Technology Acceptance', in International Conference on Interaction Sciences.

Funding Body

University of Southampton

Further Information

Imali Manikarachchige (E: i.u.m.manikarachchige@soton.ac.uk)

35. INTEGRATING QUALITATIVE CONTENT ANALYSIS INTO QUANTITATIVE SYSTEMS MODELING: A METHODOLOGICAL APPROACH FOR UNDERSTANDING DYNAMICS IN FISHERIES SOCIO-ECOLOGICAL SYSTEMS

36. Active Mechanical Metamaterials: On Optimal Voltage Efficiency

Soumyadeep Mondal[1,*], Tanmoy Mukhopadhyay[2] and Susmita Naskar[3]

[1] Faculty of Engineering and Physical Sciences, University of Southampton, Southampton, UK, Email: S.Mondal@soton.ac.uk
[2] Faculty of Engineering and Physical Sciences, University of Southampton, Southampton, UK,
Email: T.Mukhopadhyay@soton.ac.uk
[3] Faculty of Engineering and Physical Sciences, University of Southampton, Southampton, UK, Email: S.Naskar@soton.ac.uk

Project objectives and goals

This study proposes an optimized configuration for two-dimensional honeycomb lattices with piezoelectric patches embedded in their cell walls. The elastic properties are evaluated at the lattice level by combining a bottom-up mechanics-based approach with an RVE-based finite-element model. A key advantage of this optimal piezoelectric patch lay- out is its enhanced voltage sensitivity, outperforming current lattices [1-3] with standard piezoelectric patches. Various lattice geometries, including both auxetic and non-auxetic designs, with differing height ratios and piezoelectric patch thicknesses, are explored to assess the potential for real-time adjustment of equivalent elastic constants. This flexibility in tailoring active properties in real-time allows for customization of mechanical characteristics based on different working conditions and applications, such as morphing structures, wearable technologies, and soft robotics, among others.

Description of method and results

A hybrid alternating tri-layered piezo-metallic strip architecture for the cell members (including slant as well as upright members) of honeycomb lattice metamaterial is proposed (refer to 1a).

Mechanics based bottom-up beam-based bi-level framework is carried out at the level of the cell wall as well as the level of the unit cell to obtain closed-form expressions of effective material characteristics (Young and shear modulus).

Achieved an active and on-demand stiffness modulation: During operation of aircraft, with more wind load, more stiffness is needed which can be actively increased as required.

Exhibits higher voltage sensitivities of its effective properties than existing piezo- electric honeycombs (refer to 1b)

On-demand property modulation in real-time with greater external stimuli sensitivity.

Alternating tri-layered piezo-metallic strip architecture of honeycomb unit cell

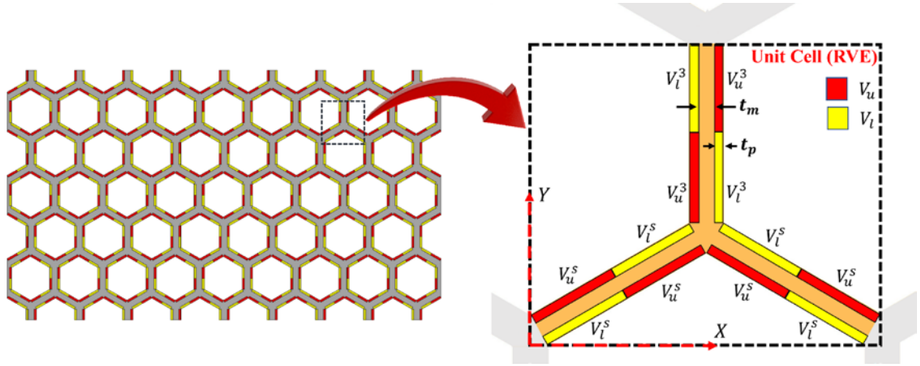

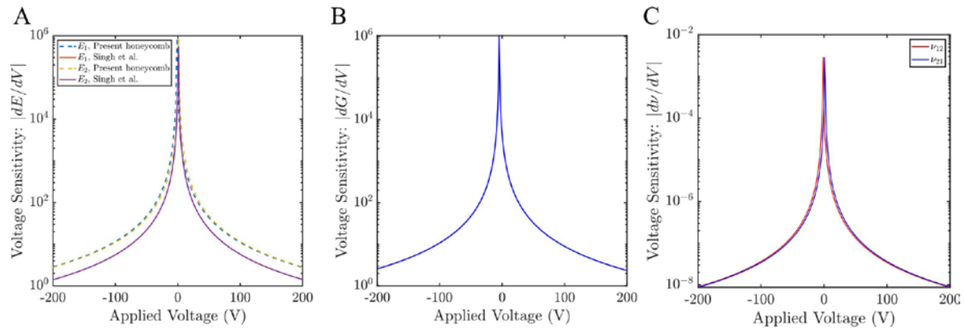

Effect of cell-wall architectures on sensitivity of overall elastic properties of regular honeycomb lattice

Figure 1: A summary of the active honeycomb design and its improved voltage sensitivity.

References

[1] Singh, A., Mukhopadhyay, T., Adhikari, S., Bhattacharya, B. (2021). Voltage- dependent modulation of elastic moduli in lattice metamaterials: Emergence of a programmable state-transition capability. International Journal of Solids and Structures, 208, 31-48.

[2] Sinha P., Mukhopadhyay T. (2023) Programmable multi-physical mechanics of mechanical metamaterials, Materials Science and Engineering R, 155 100745.

[3] Kundu D., Ghuku S., Naskar S. Mukhopadhyay T. (2023) Extreme specific stiffness through interactive cellular networks in bi-level micro-topology architected metamaterials, Advanced Engineering Materials, 2201407.

Collaborators

Department of Aeronautics and Astronautics, University of Southampton.

36. ACTIVE MECHANICAL METAMATERIALS: ON OPTIMAL VOLTAGE EFFICIENCY

37. The tension stiffening behaviour of stainless steel rebar

Hamish Moodley
University of Southampton

Project objectives and goals

The stress-strain behaviour of stainless steel rebars differs from carbon steel rebars, with a highly non-linear response, no clear yielding point, high ductility, and significant strain hardening. These material differences impact the behaviour and failure modes of stainless steel reinforced concrete, including crack formation and growth. Tension stiffening, where concrete between cracks adds stiffness due to the bond with steel, has not been studied in round-ribbed stainless steel rebars. This study aims to:

- Characterise the tension stiffening behaviour of stainless steel rebars, and
- Assess the suitability of existing codified tension stiffening models for stainless steel rebars.

Description of method and results

An extensive experimental program was conducted at the University of Southampton to characterise the tension stiffening behaviour of stainless steel rebars. Twelve specimens were tested, including 12mm and 16mm diameter carbon steel, 12mm diameter austenitic stainless steel, and 16mm diameter lean-duplex stainless steel rebars. All specimens were of the same dimensions and tested using a Schenck servo-hydraulic machine with a strain rate of 0.00025 strain/s [1]. Mean strain was measured over 450mm using two LVDTs, and crack development was monitored via Digital Image Correlation (DIC). The adopted test setup is shown in Fig. 1. Three analytical models (Model Code 1990 [2], Fib Bulletin 51 [3], and Eurocode 2 [4]) were also examined.

Key results include:

- Stainless steel specimens exhibited similar tension stiffening behaviour to carbon steel up to the first cracking stress, with differences emerging afterwards due to the nonlinear stress-strain response of stainless steel (see Fig. 2).
- The codified tension-stiffening models commonly used were compared with the experimental results. The models were shown to generally be in good agreement with the carbon steel rebar experimental responses during the crack stabilisation stage, while for the stainless steel rebars, the models were not capable of accurately capturing the nonlinear effects of the material and modifications may be necessary as part of future works.

Potential for application of results

The results of this work provide an experimental data set from which future modifications to the current codified analytical models for tension stiffening could be derived.

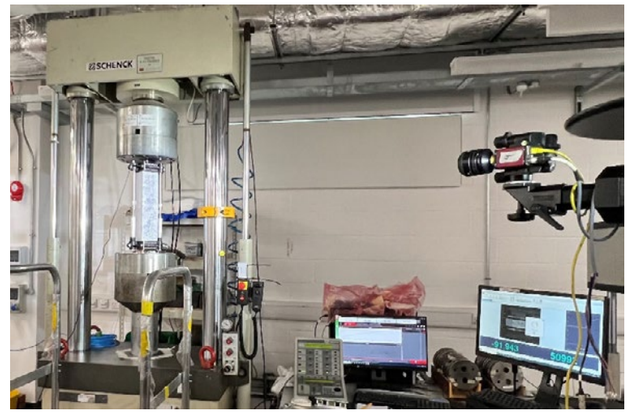

Fig. 1. Experimental tension stiffening test setup

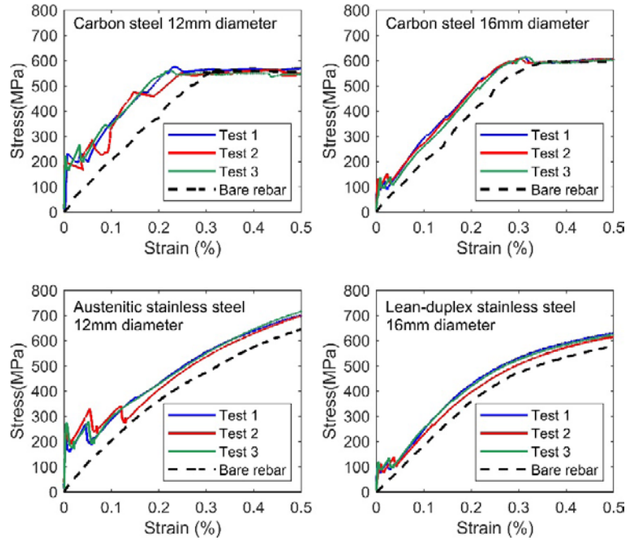

Fig. 2. Tension stiffening responses of the tested carbon steel and stainless steel tension stiffening specimens.

References

[1] CEN, "EN ISO 6892-2016. Metallic materials. Tensile testing. Method of test at room temperature.," 2016, Brussels, Belgium.

[2] CEB-FIP, "CEB-FIP Model Code 1990 - Design Code.," 1993, The International Federation for Structural Concrete, Switzerland.

[3] Fib, Structural Concrete Textbook on behaviour, design and performance, Second edition Volume 1: Design of concrete structures, conceptual design, materials. fib Bulletin No. 51. Switzerland: The International Federation for Structural Concrete, 2009.

[4] CEN, "EN 1992-1-1 Eurocode 2: Design of concrete structures General rules and rules for buildings. Standard," 2004, CEN, Brussels.

Funding

Funded by Network Rail.

37. THE TENSION STIFFENING BEHAVIOUR OF STAINLESS STEEL REBAR

38. Performance comparison of a novel modular SPT-TAL type Hall effect thruster operating on Krypton

Thomas F. Munro-O'Brien, Charles N. Ryan
University of Southampton

In the quest for more efficient and sustainable space propulsion, Hall effect thrusters have proven to be highly effective, especially in long-term space missions. Traditionally, these thrusters use xenon as fuel, but due to the rising cost of xenon, the space industry is now exploring alternative options. This study focuses on investigating krypton as a potential replacement for xenon in Thrusters with Anode Layer (TAL), a type of Hall thruster, and compares its performance with a similar type of thruster called a Stationary Plasma Thruster (SPT), both operating on krypton.

The experiments were conducted using a medium-power thruster (1.35 kW) that can operate in both TAL and SPT modes with the same design. Key measurements included direct thrust readings using a specialized thrust stand, along with monitoring the electrical signals from the thruster's various components. This research is one of the first to deeply examine the performance of TAL thrusters using krypton, and the findings are expected to provide valuable insights for the future design of high-power propulsion systems, which are crucial for space exploration.

By comparing the two thruster types, this study hopes to contribute to a better understanding of the unique characteristics of TAL thrusters and pave the way for more versatile and cost-effective propulsion solutions.

39. Ceramic-microbial fuel cell stacks for electricity and liquid fertilizer production for hydroponics

Dibyojyoty Nath1, and Yannis Ieropoulos1
[1] Water & Environmental Engineering Group, University of Southampton, England, SO16 7QF, UK
Author email: D.Nath@soton.uk.ac, i.ieropoulos@soton.ac.uk

Project Objectives and Goals:

Wastewater (sewage) is replete with organic matter (mostly carbon and nitrogen). Thus, recovery and reuse of these nutrients could be a promising solution instead of their treatment through conventional processes.

Previously, catholyte was collected from MFCs fed with urine and observed to contain highly concentrated nitrogen and phosphate sources, which could be used as liquid fertilizer to grow plants1. However, this concept has not been scaled up to produce liquid fertilizer from sewage. Here, we developed stacking microbial fuel cells (MFC) to produce electricity and liquid fertilizer directly from raw sewage at the cathode.

Methods:

The ceramic MFCs are fabricated using cylindrical ceramic structures acting as membranes for ion exchange. The outer surface of the ceramic pot is wrapped with a carbon veil and used as anode. Similarly, stainless-steel mesh coated with PTFE-blended with activated carbon is fixed tightly on the inside of the cylinders, as cathodes. Plastic containers have been populated with 20 ceramic MFCs, where all units share the same anolyte and, therefore, are electrically connected in parallel. Two MFC trays (40 MFCs) have been fabricated and stacked in a cascade manner to run continuously using raw sewage. The fresh sewage is collected from the nearest wastewater treatment plant (Millbrook Water Works, Southampton) and fed to these two MFCs through gravity. The effluent from the second MFC-Tray is also recycled to the feeding chamber using a peristaltic pump.

Results:

MFC tray-1 generates 320 mV (against 4.7 Ohms), resulting in a current of 68 mA, whereas MFC tray-2 generates 303 mV, 64 mA, across 4.7 Ohms load. The catholyte is collected at the cathode from each MFC, and it is observed that 1 L of catholyte/day is generated when 2.5 L of sewage is fed in the anodic chamber. The catholyte acts as a liquid fertilizer and hence could be used to grow plants in a hydroponic system, which is the main subject of study of the Microbial Hydroponics (Mi-Hy) project. Therefore, MFCs can be integrated with hydroponics to grow vegetables while recovering nutrients and electricity from sewage. The electricity from MFCs will be used to power LEDs/aeration pumps as part of the ongoing investigation.

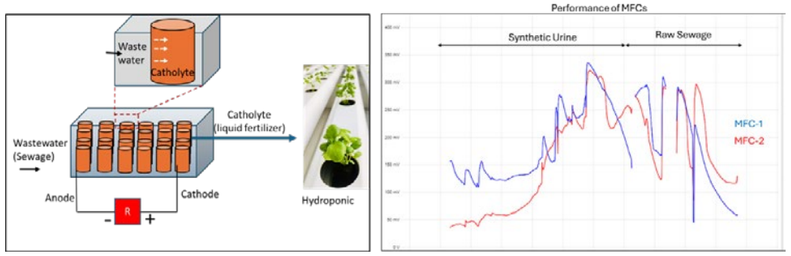

Fig. 1: Schematic of ceramic MFCs producing electricity and the liquid from sewage (Left). Performance of electricity production of MFCs (Right).

References:

Merino-Jimenez I, Obata O, Pasternak G, Gajda I, Greenman J, Ieropoulos I. Effect of microbial fuel cell operation time on the disinfection efficacy of electrochemically synthesised catholyte from urine. Process Biochem. 2021 Feb;101:294-303. doi: 10.1016/j.procbio.2020.10.014.

Funding:

Mi-Hy is funded by the European Innovation Council (grant no. 101114746).

Website: http://www.mi-hy.eu/

40. An investigation into the combination of passive acoustic treatments and active structural acoustic control.

Charalampos Nikolaou, Jordan Cheer, Felix Langfeldt
University of Southampton

Project objectives and goals

The goal of this project is to enhance acoustic absorption performance in confined spaces by combining passive and active control methods. Traditional passive acoustic treatments, such as porous materials and micro-perforated panels (MPPs), face challenges in low-frequency noise attenuation. This project aims to integrate Active Structural Acoustic Control (ASAC) with different configurations of passive materials. The project focuses on optimizing the balance between passive and active components to maximize acoustic absorption across a broad frequency range while adhering to the practical constraints of compact systems.

Description of method and results

The system under investigation integrates several elements, including glass wool as a porous material, an actively actuated MPP, an actuated back panel, and an acoustic source for active control. The MPP, modeled as a flexible panel, is directly actuated, allowing it to improve acoustic performance by interacting with both the porous material and the air cavity behind it. This multi-layered sound-absorbing structure is designed to optimize the combined effect of both passive and active components for enhanced noise mitigation.

A comprehensive parametric sweep was conducted to systematically explore the influence of key design parameters. These parameters included the thickness of the porous material, the porosity and hole diameter of the MPP, and the positioning of the actuated back panel within the structure. Finite Element Modelling (FEM) simulations were used to evaluate the passive and active performance of various configurations. The results demonstrate that when active control is applied via the MPP and the actuated back panel, low-frequency absorption is significantly enhanced, particularly in comparison to systems relying solely on passive treatments. The combination of the MPP and ASAC showed an ability to broaden the frequency range over which the system achieves effective noise control.

Additionally, the study evaluated the combined effects of active and passive control, revealing that the inclusion of an actuated back panel behind the cavity, along with an acoustic source, provides new alternatives for controlling acoustic performance. The results highlight that an optimized system with combined active-passive control can achieve broadband absorption, offering reduced power consumption while maintaining high levels of acoustic efficiency.

Figure 1 – a) Geometry of the duct and active-passive sound absorber, showing the main dimensions that describe the system, the microphone positions,

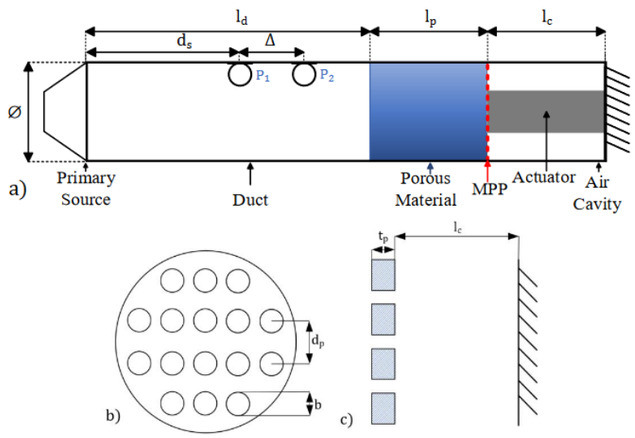

along with the initial active-passive arrangement. b) MPP geometry showing the main parameters that are utilised, where *dp* is the hole distance, *b* is hole diameter, and in c) *tp* is the thickness of the panel and *lc* is the cavity length.

Potential for application of results

The integration of ASAC with passive treatments offers a novel approach to acoustic performance enhancement, particularly in environments with spatial constraints. The findings of this research can be applied to the design of soundproofing systems in automotive, aerospace, and architectural applications, where low-frequency noise reduction is critical. The active-passive configurations investigated here offer a flexible and energy-efficient solution for acoustic control in challenging scenarios.

References:

Dah-You Maa (1998). Potential of microperforated panel absorber, Journal of the Acoustical Society of America 104(5): 2861-2866.

40. AN INVESTIGATION INTO THE COMBINATION OF PASSIVE ACOUSTIC TREATMENTS AND ACTIVE STRUCTURAL ACOUSTIC CONTROL.

41. Development of an in situ droplet microfluidic autonomous sensor for wide-range ocean alkalinity

Molly Phillips

Total alkalinity (TA) is the buffering capacity of the ocean, keeping the pH constant. High-frequency measurements are crucial for monitoring and maintaining the ocean's buffering system, particularly with increasing ocean acidification. In situ TA sensors allow us to measure rapidly changing alkalinity in marine environments like estuaries, quantifying ocean alkalinity enhancement (OAE) experiments, and assessing CO_2 seep impacts.

Currently, commercially available and academic in situ TA sensors have measurement range and sample frequency limitations. To address this, a droplet microfluidic sensor is being developed, utilizing lab-on-chip (LOC) technology to create discrete aqueous droplets suspended in hydrophobic oil. In each droplet, a single-point closed-cell titration occurs, sampling ~0.75 gL every 6 seconds. The small volume, high throughput nature of droplet flow improves on the limitations of current sensors, by taking measurements of each sample to increase the effective measurement ranges. This improves the analytical range and speed of analysis for in situ, high-frequency TA measurements.

Here I will present results from an initial closed-cell lab-based prototype sensor that proves the working principle. Measurements are in close agreement with those made by equivalent benchtop methods.

This technology will be tested in highly-variable settings, such as estuaries. When the increased analytical range is proven, this technology could offer a new and important tool in the analysis of the marine carbonate system in fast-changing environments.

This work is supported by Southampton Marine and Maritime Institute

Further Information:

Supervised by Adrian Nightingale A.Nightingale@soton.ac.uk, Allison Schaap Allison.Schaap@noc.ac.uk and Rachael James R.H.James@soton.ac.uk

42. Conversion of organic wastes into biodegradable plastics: a dual and synergistic solution in a circular economy

Seongbong Heo, Tararag Pincam, Yongqiang Liu
University of Southampton

Project objectives and goals

One of the largest organic waste such as sewage sludge can be converted into biogas and/or volatile fatty acids (VFAs) to promote waste valorisation and resource sustainability. VFAs can be used for bioplastics production, providing higher market value than the biogas, but its separation and purification from fermentation liquid are still a bottleneck. The direct use of mixed VFAs in fermentation liquid for production of polyhydroxyalkanoates (PHAs), a raw materials for bioplastic production, would be a great potential to not only recover high value from wastes, but also to combat with plastic pollution. This study, therefore, aimed to develop the integrated process of sludge fermentation and single-stage PHAs production in sequencing batch reactors (SBRs).

Description of method and results

Continuous fermentation of waste activated were conducted in two continuous stirring tank reactors (CSTR) under different temperatures (35 and 49 °C) and different pHs (pH 6 (without pH control), and pH controlled at 9 and 10). From fig. 1, it was observed that the highest VFA yield was achieved in fermentation under 49 °C and pH 9 and acetic acid was the major components. Without chemical addition for pH control, higher temperature also enhanced VFA yield by 43% and promote selectivity of butyric acid.

Fed-batch experiments were conducted to investigate the maximum PHB storage ability in the cultures enriched in single-stage SBRs employing different nutrient decoupling strategies. Synthetic wastewater with pure acetate and raw fermentation liquid were used as substrates. From fig. 2, the separated feeding of carbon and phosphorus in R3 was the most suitable conditions for one-stage PHB production in a SBR. The cultures fed with raw fermentation liquid achieved up to 45% of PHB contents in dry biomass, which was close to that fed with pure acetate in synthetic wastewater (54%wt).

Potential for application of results

This study provides the insight for process optimization of sludge fermentation and one-stage PHA production in SBR. The results suggested that thermophilic fermentation without pH control resulted in higher VFA yield and higher selectivity of butyrate. Over 45% of PHB content in dry biomass could be achieved in one-stage PHB production in SBR. Hence, feasibility of PHB production in one-stage reactor using unrefined VFA solution is validated, although it could achieved slightly lower PHB yield than when using pure acetate. Integrating sludge fermentation with PHA production from mixed VFA solutions offers a feasible strategy to valorise organic waste and address plastic pollution. To confirm the optimal technological route for this approach, life cycle environmental and economic assessment should be conducted.

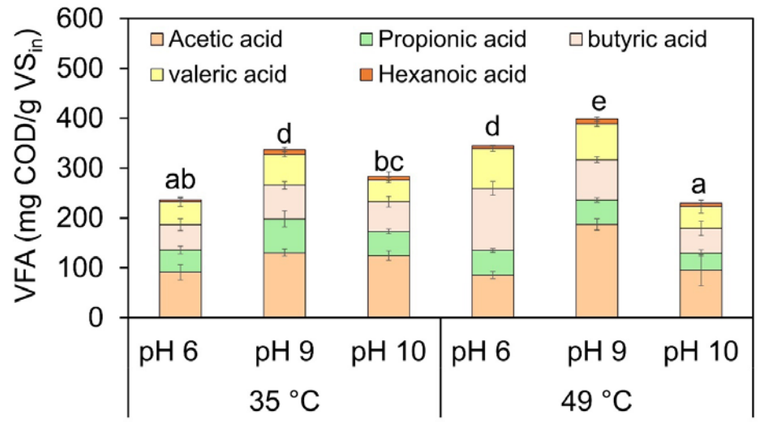

Fig. 1 Yields of VFA in fermentation of waste activated sludge under different temperatures and pHs.

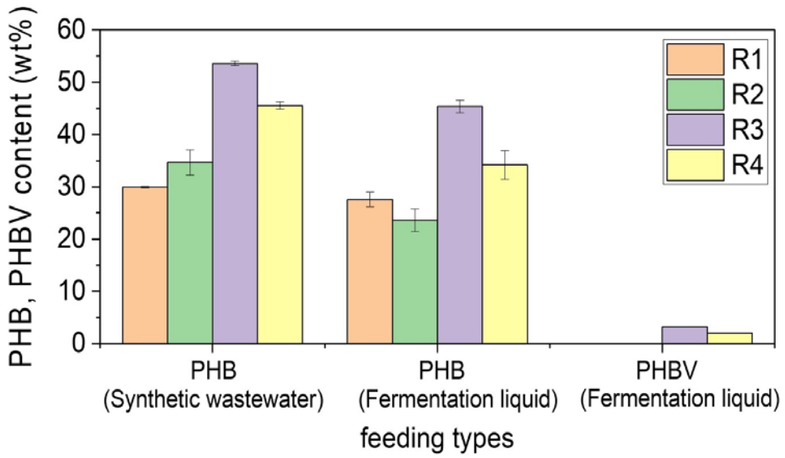

Fig. 2 Contents of polyhydroxybutyrate (PHB) and polyhydroxybutyrate-valerate (PHBV) in dry biomass from fed-batch experiment using synthetic wastewater and fermentation liquid. The cultures was enriched in SBRs employing four different nutrient decoupling strategies.

43. Abstract: Push-out tests on austenitic stainless steel and carbon steel welded shear studs

Rebecca Presswood
University of Southampton

Project objectives and goals

Steel-concrete composite beams are commonly used in bridge construction. The corrosion of the supporting steel beams is known to be a cause of deterioration of composite bridges. Stainless steel composite beams offer a viable solution to the steel corrosion problem in harsh environments. However, their design is outside the scope of the current international design standards due to a lack of reliable experimental data. This project aims to:

Investigate the push-out behaviour of austenitic EN 1.4301 stainless steel and carbon steel shear studs welded to lean duplex EN 1.4162 beams

Assess the applicability of international design code stud resistance predictions for stainless steel composite beams

Description of method and results

Eight push-out tests were conducted on lean duplex EN 1.4162 composite specimens: three with carbon steel studs in C100 concrete, three with austenitic EN 1.4301 studs in C100 concrete, and two with austenitic EN 1.4301 studs in C50 concrete. The shear resistances obtained from the push-out tests were compared to the predicted resistance by several international design codes, and to the resistance from push-out tests on carbon steel studs welded to carbon steel beams collected from the literature. Key results include:

Austenitic stainless steel studs achieved significantly larger capacity and ductility than carbon steel studs, and were able to meet the Eurocode 4 [1] ductility requirements

Carbon steel studs did not meet the Eurocode 4 ductility requirements. This was attributed to poor weld quality from stud welding the carbon steel studs to the lean duplex stainless steel plates, which has led to the conclusion that carbon steel studs should not be used in composite beams with lean duplex stainless steel sections.

The stud resistance equations given in Eurocode 4 and AASHTO [2] were found to provide safe-sided predictions, and the resistance performance of the austenitic stainless steel studs was found to be comparable to that of the carbon steel studs collected from the literature

Potential for application of results

No design codes currently exist for the design of stainless steel composite bridge structures; these results will assist in the development of new design guidance, ensuring optimal and efficient design of sustainable stainless steel composite bridges.

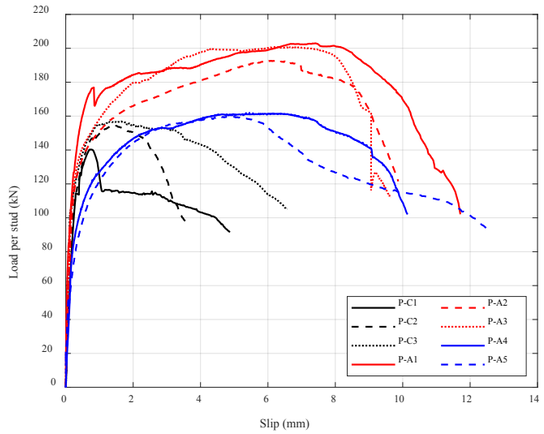

Fig. 1. Load-slip response of push-out tests: P-C indicates carbon steel studs in C100 concrete, P-A1 to P-A3 indicate austenitic EN 1.4301 stainless steel studs in C100 concrete and P-A4 and P-A5 indicate austenitic EN 1.4301 stainless steel studs in C50 concrete

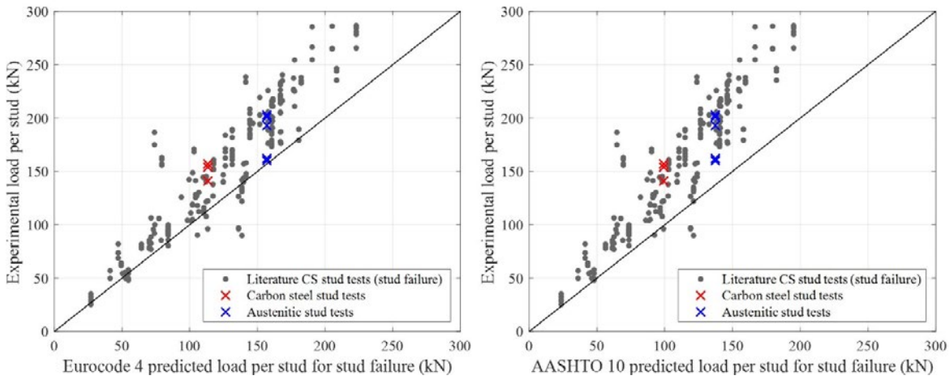

Fig. 2. Comparison of test results with Eurocode 4 and AASHTO 10 predicted stud resistance for carbon steel stud push-out tests reported in the literature and push-out tests from this study.

References:

[1] EN 1994-1-1:2004 Eurocode 4. Design of composite steel and concrete structures. General rules and rules for buildings, CEN, 2004.

[2] AASHTO LRFD bridge design specifications, American Association of State Highway and Transportation Officials, 2007.

44. Ultrasound propagation in materials with elongated grains and preferred orientation

Lucas Queiroz Machado[1], Michal Kalkowski[1], Mike Lowe[2]
[1]University of Southampton, [2]Imperial College

Project objectives and goals

Data interpretation of wave propagation in inhomogeneous materials remains a challenging task. This rises as a topic of interest in the nuclear industry, where the inspection of inhomogeneous thick section welds is vital to meet safety standards. Such welds are characterised by columnar grains with varying preferred orientations resultant of their complex solidification process. Consequently, conventional post-processing techniques of ultrasound data are imprecise, as the ultrasonic beam is distorted and attenuated, no longer following a straight path. Therefore, first we investigate how ultrasonic wave velocity and attenuation are affected by microstructure parameters such as grain morphology and crystallographic orientation. Second, we propose a procedure for determining an equivalent complex elastic tensor, given the wave propagation behaviour in varying columnar grain microstructures.

Description of methods and results

The analysis makes use of numerically generated microstructures, and ultrasound 3D grain-scale finite element simulations in Pogo (Huthwaite et al., 2014). Two materials are considered: stainless steel 316L and Inconel, both with cubic crystal structure and of interest in the nuclear industry. The grain morphology analysis considers the effect of the dominant grain orientation, size, and aspect ratio on the wave propagation. This enables a better understanding of the relationship between microstructure and wave propagation, given the relevant parameters. The crystal properties and Voigt averages are used for an initial estimate of the real component of the complex elastic tensor, setting the start for the parametric inversion process.

The parametric inversion is implemented with the use of the Particle Swarm Optimisation (PSO), yielding the real and imaginary components of the complex elastic tensor, given the attenuation and wave velocity obtained from three wave propagation modes, namely, quasi-longitudinal (qL), quasi-horizontal shear (qSH), and quasi-vertical shear (qSV). Fig.1 and Fig. 2 present the resultant wave velocity and attenuation profiles obtained from the homogenised tensor for Inconel.

Potential for application of results

Ultrasound data interpretation for defect location requires precise material information, which in conjunction with a propagation model can correct ultrasound images (Kalkowski et al., 2023). Additionally, the newly achieved capability has the potential for accurate modelling of signal loss in (semi) analytical ray models, which can be used to determine inspectability limits in safety-critical industries.

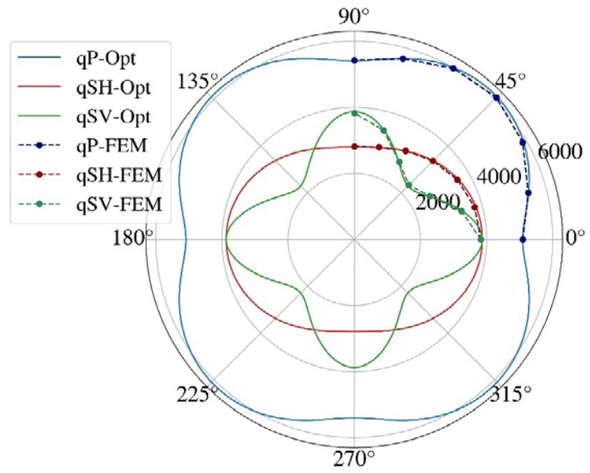

Fig. 1 Phase velocity.

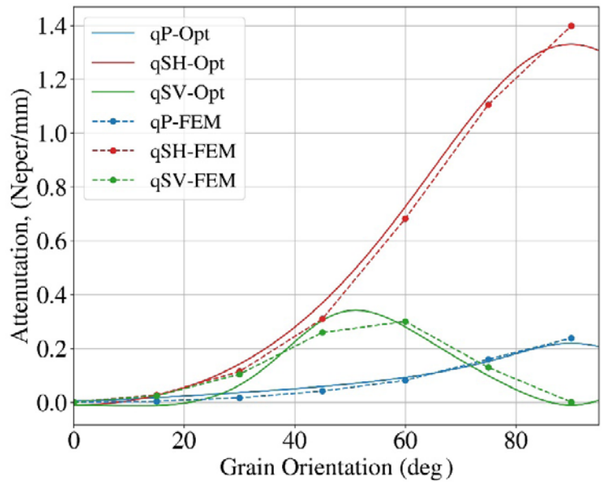

Fig. 2 Attenuation.

References:

P. Huthwaite, Accelerated finite element elastodynamic simulations using the gpu, J. Comput. Phys. 257 (PA) (2014) 687–707.

Kalkowski, M.K., Lowe, M.J.S., Samaitis,V., Schreyer, F., Robert, S., 2023. Weld map tomography for determining local grain orientations from ultrasound. Proceedings of the Royal Society A: Mathematical, Physical and Engineering Sciences, 479, 2277, 20230236.

Funding body

iWeld received funding from Euratom research and training programme 2021-2027 under grant agreement No 101061359. UK partners are funded by UK Research and Innovation (UKRI) under the UK government's Horizon Europe funding guarantee (grant numbers 10044428 and 10040812).

Further information

Lucas Machado (l.queiroz-machado@soton.ac.uk) - https://snetp.eu/portfolio-items/iweld/

45. Investigation into the mechanical performance of aluminium cold spray coated alloys

Rosemary Reed[1], Philippa Reed[1], Ali Alperen Bakir[2,3], Adrian Wei-Yee Tan[4]

[1] Materials Research Group, School of Engineering Sciences, University of Southampton, Highfield, Southampton SO17 1BJ, UK
[2] Faculty of Engineering and Computing, Coventry University, Coventry, CV15FB, UK
[3] NSIRC, TWI Ltd, Granta Park, Great Abington, Cambridge, CB21 6AL, UK
[4] Materials Research Group, School of Engineering Sciences, University of Southampton, 79200 Nusajaya, Johor, Malaysia

Aluminium alloys are commonly used in aerospace structures due to their high specific strength, durability, and machinability. However, these components can experience damage due to wear, corrosion, and cyclic loading. Cold spray (CS) technology presents an effective approach for repairing such components, utilising high-temperature compressed gases to accelerate powders onto damaged substrates at critical velocities (200-1500m/s). This process induces substantial plastic deformation in the impacting powder, facilitating deposition through metallurgical bonding and/or mechanical interlocking. However, attainable coating adhesion is contingent upon the material property combinations of both the feedstock powder and substrate, subsequently influencing the mechanical properties of the repaired material, thus their fatigue performance.

Fatigue is the most common mode of failure in aerospace components. The fatigue performance of CS deposition depends on the microstructure, porosity, residual stress distribution, which are closely related to the process parameters, powder, and substrate characteristics.

This work will focus on AA7075-T6, commonly used in aerospace structures. The microstructure of the alloy was characterised using optical and scanning electron microscopy (SEM), found to contain complex intermetallic systems. Electron backscatter diffraction (EBSD) was also used to evaluate grain structure and the mechanical variations within grains. Following characterisation, the short crack fatigue performance of the alloys was investigated using axial fatigue testing and in depth fractographic analysis using advanced microscopy methods and 3D reconstruction techniques.

This study lays the groundwork for preliminary investigations utilising Digital Image Correlation (DIC) to assess load transfer from the substrate to the CS coating and evaluate the impact of CS on the substrate material.

46. Predicting UK Domestic Electricity and Gas Consumption between Differing Demographic Household Compositions

Greg Sewell
University of Southampton

Project objectives and goals

This research examines the influence of building characteristics, occupant demographics and behaviour on gas and electricity consumption, differentiating between family groups; homes with children; homes with elderly; and homes with neither.

Description of method and results

Both regression and Lasso regression [1, 2] analyses are used to analyse data from a 2019 UK-based survey of 4358 homes (n = 1576 with children, n = 436 with elderly, n = 2330 with neither). Three models (building, occupants, behaviour) were tested against electricity and gas consumption for each group. The following Table 1 shows 'Model 1 variables' as an example of the analyses.

Predictors Model 1-Building	Categories (N) E = Electricity Model. G = Gas Model
Total floor area	E-N/A (continuous: M = 136m2, SD = 61m2) G-N/A (continuous: M = 135m2, SD = 59m2)
property type	E-Bungalow (212) Flat (204) House (1238) Maisonette (22) G-Bungalow (167) Flat (70) House (1030) Maisonette (12)
Local authority label	E-East Midlands (205) East England (216) London (147) Northeast (62) Northwest (136) Southeast (429) Southwest (171) Wales (64) West Midlands (131) Yorkshire and The Humber (115) G-East Midlands (160) East England (124) London (104) Northeast (48) Northwest (120) Southeast (349) Southwest (137) Wales (45) West Midlands (111) Yorkshire and The Humber (81)
Wall description	E-East Midlands (205) East England (216) London (147) Northeast (62) Northwest (136) Southeast (429) Southwest (171) Wales (64) West Midlands (131) Yorkshire and The Humber (115) G-East Midlands (160) East England (124) London (104) Northeast (48) Northwest (120) Southeast (349) Southwest (137) Wales (45) West Midlands (111) Yorkshire and The Humber (81)
Main fuel	E-Biogas (1) Electric (189) Gas (1284) LPG (20) NA (25) Oil (133) Solid Fuel (23) Waste Combustion (1) G-Electric (12) Gas (1251) LPG (2) NA (1) Oil (4) Solid Fuel (9)
Current energy efficiency (SAP Rating)	E-N/A (continuous: M = 61.0, SD = 14.2) G-N/A (continuous: M = 61.5, SD = 13.3)

Figure 1: Example of the first independent variables group 'Predictors Model 1—Building'.

Results indicated that homes without children or elderly consumed the least energy. Property Type emerged as the strongest predictor in the Building Model (except for homes with elderly), while Current Energy Efficiency was less significant, particularly for homes with elderly occupants. Homeownership and number of occupants were the most influential factors in the Occupants Model, though this pattern did not hold for homes with elderly.

Figure 2. Variable 'current energy efficiency' (EPC rating) vs. consumption

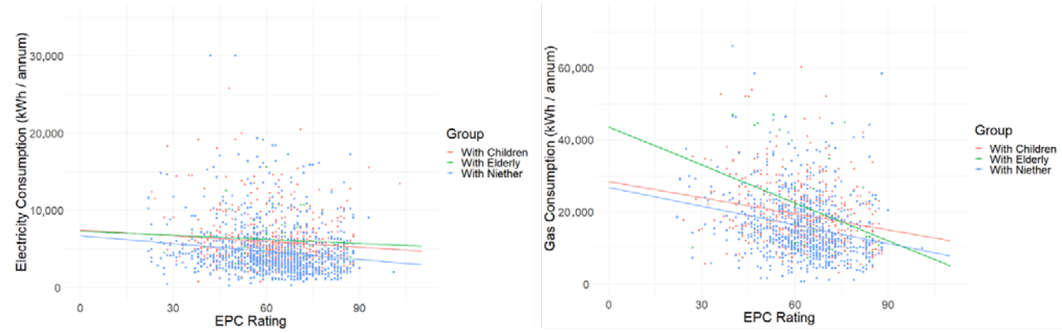

Figure 2 shows EPC Results against gas and electricity consumption. The regression lines suggest that the higher the score, the less energy is consumed, which is to be expected, but the shallowness of the line suggests the differences between the scores are small. Many occupant and behaviour variables are often considered 'unregulated energy' in calculations such as SAP and are thus typically disregarded. However, this study found these variables to be significant, especially as national standards improve. The findings suggest that incorporating occupant behaviour into energy modelling could help reduce the energy performance gap.

References:

Huebner, G.M.; Hamilton, I.; Chalabi, Z.; Shipworth, D.; Oreszczyn, T. Explaining domestic energy consumption—The comparative contribution of building factors, socio-demographics, behaviours and attitudes. Appl. Energy 2015, 159, 589–600.

Zhang, L.;Wei, X.; Lu, L.J.; Pan, J. Lasso regression: From explanation to prediction. Psychol. Sci. 2020, 28, 1777–1788.

Funding body

This work is part of the activities of the Energy and Climate Change Division and the Sustainability Energy Research Group at the University of Southampton (www.energy.soton.ac.uk, 1 September 2024). The work is supported by the EPSRC Project: Residential Heat as an Energy System Service (LATENT) (EP/T023074/1) with acknowledgement given to the wider project team for the collection and sharing of data used for the purpose of this study.

Collaborators

University of Southampton Energy and Climate Change Division - https://energy.soton.ac.uk/

46. PREDICTING UK DOMESTIC ELECTRICITY AND GAS CONSUMPTION BETWEEN DIFFERING DEMOGRAPHIC HOUSEHOLD COMPOSITIONS

47. Origami-inspired tubular multi-functional metamaterials

Aditi Sharma1*, Susmita Naskar[1] and Tanmoy Mukhopadhyay[1]
[1] University of Southampton, Southampton, UK

Project objectives and goals:

Mechanical metamaterials are a class of artificially engineered structures known for their exceptional mechanical properties, which are primarily determined by their geometric and structural configurations rather than the inherent characteristics of their constituent materials (Kundu et al., 2023, Sinha et al., 2023). A particularly promising approach to designing mechanical metamaterials is inspired by origami, the ancient art of paper folding. Origami offers a versatile framework for transforming simple 2D patterns into complex 3D structures, enabling precise control over mechanical properties through folding.

The objective and goal of the project is to:

- Investigate and characterize the mechanical response of a metamaterial featuring a waterbomb tubular structure under axial loading conditions.
- Explore how modifications in the fold dimensions, shapes, and arrangements can influence key mechanical properties such as stiffness, flexibility, and strength.
- Thoroughly examine the rigid foldability and motion behaviour of the waterbomb tube by analysing its displacement as axial force increases.

Methodology and results:

The waterbomb tube is an origami structure formed from a crease pattern created by tessellating the waterbomb bases in both longitudinal and circumferential directions. A typical waterbomb base consists of a six-crease pattern, which includes two collinear mountain creases and four diagonal valley creases that intersect at a common vertex (Ma et al., 2020, Mukhopadhyay et al., 2020).

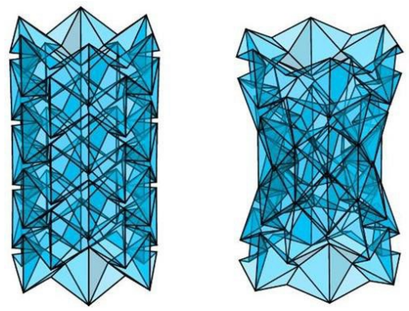

Figure 1: Shape modulation of waterbomb tube under compressive load

In modelling the waterbomb tube, the bar-hinge method is employed, with axial compressive loads applied to the top nodes of the structure. As shown in Figure 1, as the compressive load increases, the waterbomb creases contract, leading to the deformation of the tube. It is observed that with the increased compressive force, the tube begins to bulge inward, resulting in a concave bending. Furthermore, when a far-field compressive force is applied, the waterbomb tube achieves near-zero stiffness, demonstrating its tunability. Additionally, the stiffness of the waterbomb tube can be adjusted by altering its geometric configurations and material properties, highlighting its versatility in various applications.

Potential for application of results:

The waterbomb tube's tunable stiffness offers significant potential across various applications. These include adaptive structures for seismic resilience, shock absorption systems for protective gear and vehicles, and soft robotics that require compliant designs. Additionally, its properties could enhance biomedical devices like stents and lead to advancements in wearable technology, showcasing the versatility of this origami-inspired metamaterial.

References:

Kundu, D., Ghuku, S., Naskar, S. and Mukhopadhyay, T., 2023. Extreme Specific Stiffness Through Interactive Cellular Networks in Bi Level Micro Topology Architected Metamaterials. Advanced Engineering Materials, 25(8), p.2201407.

Sinha, P. and Mukhopadhyay, T., 2023. Programmable multi-physical mechanics of mechanical metamaterials. Materials Science and Engineering: R: Reports, 155, p.100745.

Ma, J., Feng, H., Chen, Y., Hou, D. and You, Z., 2020. Folding of tubular waterbomb. Research.

Mukhopadhyay, T., Ma, J., Feng, H., Hou, D., Gattas, J.M., Chen, Y. and You, Z., 2020. Programmable stiffness and shape modulation in origami materials: Emergence of a distant actuation feature. Applied Materials Today, 19, p.100537.

Collaborators

Department of Aeronautics and Astronautics at the University of Southampton

47. ORIGAMI-INSPIRED TUBULAR MULTI-FUNCTIONAL METAMATERIALS

48. Electricity generation in Microbial Fuel cell through Biofilm Immobilization Techniques

Aradhana Singh* and Ioannis Ieropoulos**
Water & Environmental Engineering Group, School of Engineering, University of Southampton
**Corresponding author email: i.ieropoulos@soton.ac.uk
*First author email: as3a23@soton.ac.uk

Objectives

1. A thorough review of studies on immobilization of microbial cells in microbial fuel cell (MFC).
2. Experimental comparison of power generation by free-living microbial consortium vs. immobilized cells in MFC.

Description of methods

Review:

Using the database 'Google Scholar', a thorough literature search was carried out from 2000–2024. "Immobilised microbes in microbial fuel cell" was the keyword. Boolean operators were employed to combine search terms.

Experiments:

MFCs consisting of plastic cylinders (acting as membrane) were used in this study. Anode was made up of carbon veil wrapped inside a carbon sleeve. Cathode electrode consisted of a mixture of activated carbon and a 60% polytetrafluoroethylene solution dispersed over a stainless-steel mesh. Ni-Cr wire was used for both the cathode and anode connections. Triplicate MFCs denoted as MFC-AS were then inoculated with activated sludge (20%) and mixture of tryptone (1%), yeast extract (0.5%) and sodium acetate (20 mM) (80%). Another triplicate MFCs denoted as MFC-IC were inoculated with 5 gram each, of immobilized bacterial cocktail in a powder form (a commercial product from an industrial company based in Thailand, SCG) and 150 mL of similar substrate. Polarisation tests were performed periodically to understand the maturity of microorganisms over the anode and the maximum power generation to compare the electrical performances of these MFCs.

Results and Discussions

In an immobilization technique, microbial cells are designed to become ensnared in or adhered to different matrices or supports, in non- viable state. The immobilisation technique used was rather uncommon (approximately 50) when compared to the numerous articles on microbial fuel cells (MFCs) that are published annually (7,055 journal publications alone in 2023). The findings of Lin et al. (2015) showed that MFCs with surface-attached and matrix-embedded cells as catalysts exhibited higher COD removal and power production efficiency than MFCs with freely suspended cells. We aim to reveal many details about these approaches, particularly their ease of use and sustainability in MFC, through this ongoing review.

The experimental findings indicate that, in comparison to MFC-AS, the initiation phase in MFC-IC took a bit longer. This is understandable as the microbial cells in MFC-IC were in non-viable state, hence it took extra time for the microbes to become active, however with time, the power and current production continued to be higher in MFC-IC with lower resistance compared to that of MFC-AS. The preliminary results are intriguing since they pave the way for an easily incorporated electrogenic microbial consortia that will thrive in the novel electrode system due to its increased resilience to operational instability and reduced non-electrogenic activity in the anode media.

Acknowledgments:

This work was funded by the Bill & Melinda Gates Foundation (Grant no. INV-042655).

References:

Lin, C.W., Wu, C.H., Huang, W.T. and Tsai, S.L., 2015. Evaluation of different cell-immobilization strategies for simultaneous distillery wastewater treatment and electricity generation in microbial fuel cells. *Fuel*, *144*, pp.1-8.

49. Using High-Speed Imaging and Digital Image Correlation to Compare Microbubble-Induced Deformation in Stiff and Soft Cells

Sam Sloan
University of Southampton

Project objectives and goals

Microbubbles are gas-filled lipid shells with a diameter <10gm. When stimulated with ultrasound, the microbubble will expand and contract rapidly. The rapid oscillation of microbubbles can cause increased permeabilisation of cells, known as sonoporation, allowing for a transfer of therapeutic molecules across the cell membrane. As such, ultrasound-stimulated microbubbles offer a promising minimally invasive, targeted drug delivery strategy. While sonoporation is a well-documented behaviour, it remains poorly understood how microbubbles induce cell strain and how this correlates with membrane permeabilisation and drug delivery. Here, we use high-speed imaging of microbubble-cell interactions alongside digital image correlation (DIC) to better elucidate the mechanical interactions between ultrasound-stimulated microbubbles and cells. Furthermore, we use this technique to determine the effect of the disruption of cytoskeletal structure in cells on stress cytoplasmic propagation.

Description of method and results

MG63 osteosarcoma cells were cultured on a glass slide integrated with a PDMS manifold (Fig. 1). Microbubbles, made through sonication of DSPC and PEG40s (9:1 molar ratio) lipid films, were then exposed to ultrasound generated using a 1MHz transducer (Precision Acoustics, Dorchester, UK). Imaging was performed using a Hypervision HPV-X high-speed camera (Shimadzu, Kyoto, Japan) attached to an Olympus XI-71 (Olympus, Tokyo, Japan) inverted microscope and captured at 5Mfps (Fig. 1). DIC was performed using MatchID 2D software to resolve the 2D displacement of the cells' surface between each frame. The displacement magnitude against time was then fitted to a sine curve, and parameters, such as displacement amplitude and phase change, can be mapped across the cell surface (Fig. 2).

Cell deformation decayed rapidly with increasing distance from the microbubble. Three possible strain decay models with distance from the microbubble were fit across all data sets, and R2 values were used to determine the model that most accurately captures the experimental behaviour. Exponential decay was found to fit the best, R2=0.71Ⓟ0.21, when compared to linear, R2=0.55Ⓟ0.19 ($p<0.0001$), and inverse square R2=0.65Ⓟ0.25 ($p<0.001$). "Half decay distance" (D1/2) was used as a measure of the rate of decay between untreated and cytochalasin-treated cells (Fig. 2). A significant decrease in D1/2 was observed in the cytochalasin-treated cells, D1/2=2.43Ⓟ0.60 gm (n=46), when compared to the untreated control cells, D1/2=2.95Ⓟ1.12 gm (n=42, $p<0.01$).

Potential for application of results

Microbubble-cell interactions can be imaged at 5Mfps with a high enough resolution and contrast to successfully resolve the 2D displacement of the cell surface using DIC. Further, displacement amplitude decays exponentially with distance from the microbubble, indicating that damping is the driving factor in the decay. Cell deformation in the cytochalasin-treated cells appears to decay quicker than in the untreated control group. These results could have a large impact in cell and tissue, targeting to optimise microbubble-enhanced ultrasound-mediated drug delivery.

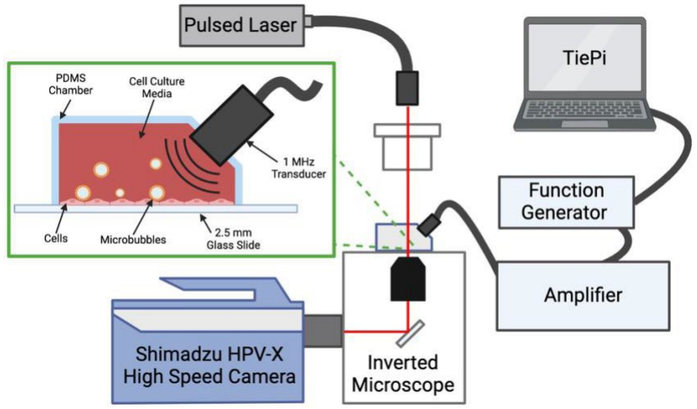

Fig 1: Schematic of high-speed imaging set-up and ultrasound-compatible cell culture chamber

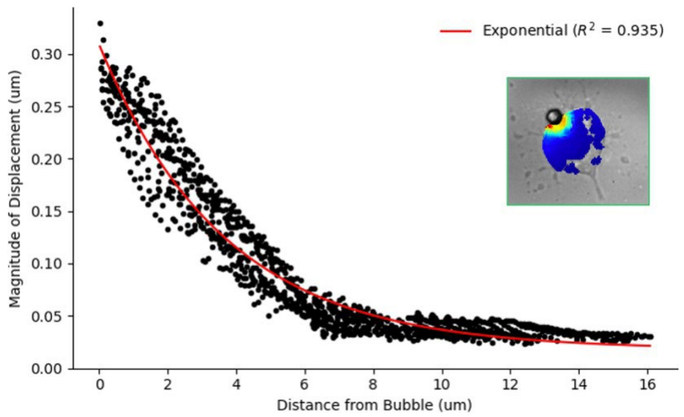

Fig 2: Displacement amplitude mapped across a cell and the corresponding decay.

Funding:

UKRI, Institute for Life Sciences

50. PhD Research Plan: Learning-Based Multi-Agent Marine Vessel Non-Causal Control and Distributed Optimization for Ship Rescue Operations

Yutong Song

Section 1: Introduction (Literature Review, Gaps, and Significance)

The maritime industry is facing increasingly complex challenges, particularly in ship rescue operations in offshore and congested waterways. Traditional control systems are limited in their ability to handle the high levels of uncertainty and nonlinear behaviors of marine vessels, especially during emergency maneuvers. Recent advances in multi-agent systems (MAS) and learning-based control offer promising solutions, yet gaps remain in the optimization and decentralized control of these systems. This PhD research aims to address these gaps by developing robust, distributed control architectures capable of optimizing multi-agent marine vessel operations in real-time, specifically for ship rescue missions. The research integrates quantum control concepts and ship dynamics, with a focus on decentralized leadership structures that are virtual and noncentric. The potential to drive this research towards quantum control could also unlock new capabilities in marine vessel coordination and autonomy.

Section 2: Objective Optimization and Decision Making

The first phase of the research focuses on optimizing the objectives of multi-agent marine vessels during rescue missions. This involves developing decision-making algorithms that can dynamically adapt to changes in the environment, such as sudden obstacles or adverse weather conditions. The research will employ advanced distributed optimization techniques, allowing each vessel in the multi-agent system to act autonomously while ensuring coordinated and efficient rescue operations. The optimization will be modeled to improve ship dynamics and efficiency during complex rescue maneuvers, ensuring that key mission goals such as speed, safety, and energy efficiency are met.

Section 3: Adaptive Dynamic Programming (ADP)

This section introduces adaptive dynamic programming (ADP) as a learning-based approach to improve the control of multi-agent systems. ADP will be used to develop non-causal control mechanisms for marine vessels, allowing them to predict and respond to future states rather than simply reacting to current conditions. The ADP framework will optimize control policies that minimize costs such as fuel consumption, time delays, and risks associated with collision or failure during rescue missions. The incorporation of ADP aims to advance autonomous decision-making processes within the multi-agent system.

Section 4: Model Predictive Control (MPC)

In this section, model predictive control (MPC) will be employed to further enhance the control strategies for multi-agent marine vessels. MPC provides a powerful framework for handling the nonlinear dynamics and multi-objective nature of ship rescue missions. The research will develop two distinct sets of MPC algorithms, focusing on both short-term path planning and long-term strategic mission execution. Each set of control algorithms will undergo rigorous simulation testing to ensure that they can handle the complex interplay between vessels in a distributed control system.

Section 5: Cloud Control and Decentralized Leadership

The final section of the research explores cloud-based control architectures and the decentralization of leadership within multi-agent systems. Traditional control systems oftenrely on a central leader, but this research proposes a noncentric, virtual leadership structure. By employing cloud control, where computation and decision-making are distributed among agents, this research aims to improve the resilience and adaptability of the system. The role of the leader becomes virtual, dynamically shifting based on the needs of the operation, ensuring a more flexible and robust control architecture that can handle unforeseen disruptions.

51. Assessing Vibration Risks For Medical Cargoes: A Comparative Analysis Of Electric And Combustion Engine Vans

Katherine Theobald [1*], Timothy Waters [2] and Thomas Cherrett [3]
[1] University of Southampton, United Kingdom, k.theobald@soton.ac.uk, [2] University of Southampton, United Kingdom, t.p.waters@soton.ac.uk, [3] University of Southampton, United Kingdom, t.j.cherrett@soton.ac.uk.
*Corresponding Author

Purpose

As part of the interdisciplinary £29m Future Transport Zones project taking place in in the Solent region of the UK, this study investigates the vibration profiles of electric and combustion engine vans during real-world transport scenarios to assess their potential impact on sensitive medical cargoes being carried for the NHS.

Research Approach

The vibration performance of an electric van and a traditional combustion engine van are compared using triaxial accelerometers affixed in strategic locations to compare variation across the van, e.g. across axels, as well as within the cargo. Both vans completed identical routes, equipped with the same instrumentation to record comprehensive vibration data throughout the vehicle. A comparative analysis was then conducted to identify key similarities and differences in the vibration profiles generated by each vehicle type. The key features of the vibration profile such as magnitude and frequency are compared across the vans as well as with the findings from other trials conducted by the authors which used the same methodology to quantify the effects of drone-induced vibration on the quality of cancer treatments.

Findings and Originality

This research presents an original comparison of the vibration characteristics of electric and combustion engine vans. Additionally, these have not been considered in the context of their impact on medical cargos, specifically monoclonal antibodies (mAbs), a type of cancer treatment. Our findings provide valuable insights into the potential vibration risks associated with each mode of transport.

Research Impact

The results will inform the development of evidence-based guidelines for selecting appropriate transportation methods for medical supplies, sensitive to vibration. This information will empower healthcare and logistics professionals to make informed decisions regarding the most suitable transportation method for various medical supplies based on their susceptibility to vibration, and will also contribute to the debate on how to best mitigate it.

Practical Impact

The findings contribute to the expansion of our existing vibration profile recording methodology, initially developed for drone deliveries, to encompass other modes of medical cargo transport. They also allow the comparison of vibration profiles to established benchmarks for safe transportation of medical supplies, demonstrating the suitability of specific modes of transport based on their similarity to existing, well-understood methods (e.g., traditional combustion engine vans).

Keywords

Medical Logistics, Vibration Analysis, Electric Vehicles, Cargo Safety, Drone Delivery

Project information

This work has been undertaken as part of the Soulent Future Transport Zone project. Further information about this project can be found at:

https://solent-transport.com/solent-future-transport-zone/

https://www.southampton.ac.uk/engineering/research/projects/solent-future-transport-zone-theme-1.page#%0A_____project_overview%0A_____

51. ASSESSING VIBRATION RISKS FOR MEDICAL CARGOES: A COMPARATIVE ANALYSIS OF ELECTRIC AND COMBUSTION ENGINE VANS

52. Estimation of the relative balance between the rotor and the OGV broadband noise in a turbofan engine

Ram Kumar Venkateswaran (PGR student)
Institute of Sound and Vibration Research (ISVR), University of Southampton

Background and objective of the research project:

The aeroengine is the loudest noise source in an aircraft. Large-scale commercial aircrafts are powered by turbofan engines, which include a fan stage comprising of a rotor (fan) and a stator (Outlet guide vane (OGV)) components as shown below in Fig. 1.

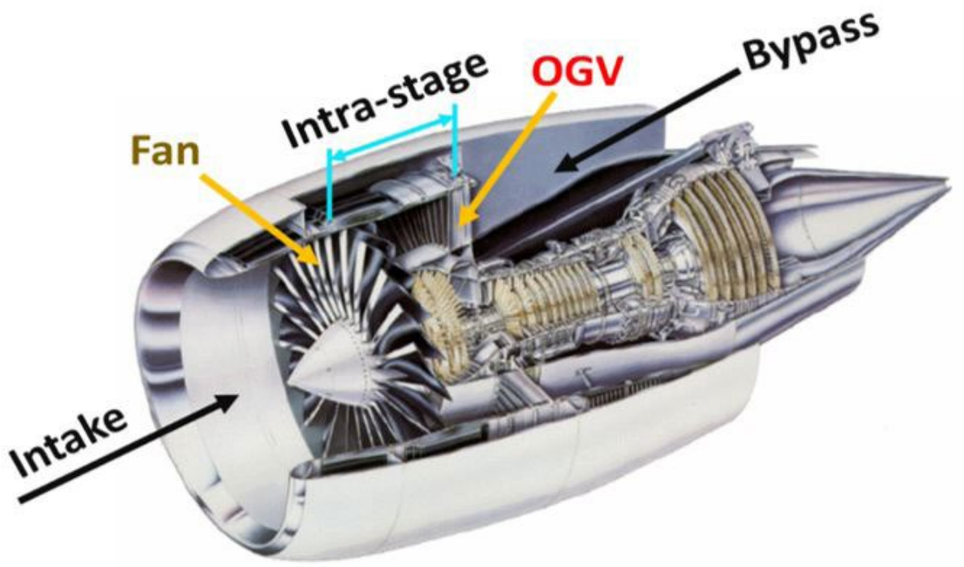

Fig. 1 A cutaway section of a modern high bypass ratio (HBR) turbofan engine showcasing the fan stage and its associated duct sections.

The broadband (BB) noise from this fan stage has been identified as the dominant contributor to the overall engine noise during the take-off and the landing phases. However, despite more than 50 years of research, the balance between the fan and the OGV BB noise sources has still not been established. The objective of this Ph.D. project is to develop a measurement technique for use in the engine intrastage, which is the duct section between the fan and the OGV, to separate the noise contributions due to the two BB noise sources and thereby determine the loudest component.

Challenges to overcome:

The engine intra-stage is a hostile environment for acoustic measurements owing to:

- the inherent space restriction to mount large microphone arrays,
- high turbulence levels,
- high levels of swirling flow, and
- high levels of background flow noise.

The measurement technique for the intra-stage is required to be robust enough to overcome these intrinsic complexities.

1-ring-1-mic technique for the engine intra-stage:

The measurement technique developed here comprises of a wall-mounted microphone ring and an axially-offset microphone and is named here as the "1-ring-1-mic technique". The technique proceeds as follows:

1. We estimate the coherence between the pressure signals sensed at the axially-offset microphone and the circumferential microphones.
2. This coherence is then inverse Fourier transformed (IFT) to estimate the relative mode amplitude distribution from which we predict the total noise levels of the upstream going acoustic modes (OGV-bound) and the downstream going acoustic modes (rotor-bound).

The broadband noise breakdown predicted by applying the foregoing method on the measured intrastage noise data of a 1/4th scaled model turbofan engine is shown below in Fig. 2. For more details, refer to the paper of Ram Kumar et al. (2023).

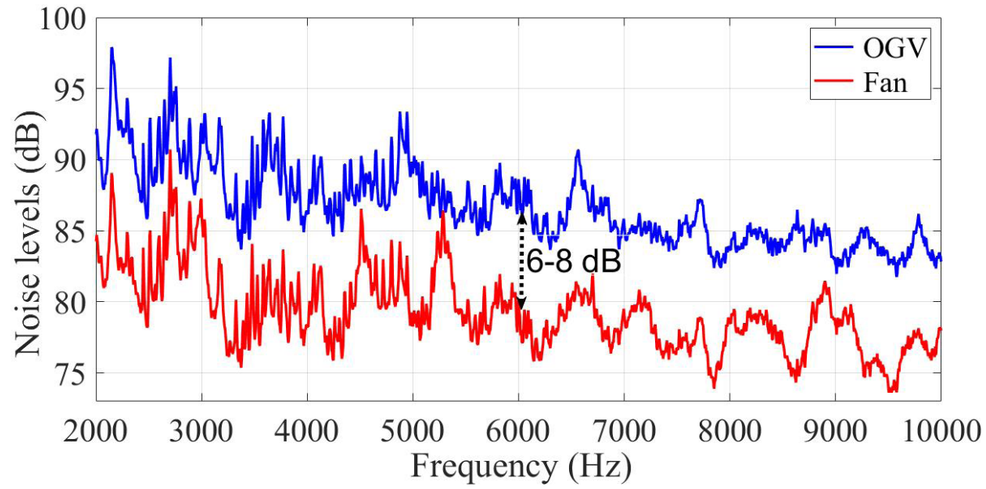

Fig. 2 Predicted BB noise levels of the fan and the OGV using the new 1-ring-1-mic technique.

The predicted breakdown of the fan stage noise sources suggests that the noise mitigation strategies must be targeted at the OGV to bring down the overall broadband noise levels.

Funding body:
This Ph.D. project is sponsored by Rolls-Royce PLC through the University Technology Centre in Propulsion Systems Noise at the ISVR, University of Southampton.

Collaborations:
Measured intra-stage noise data of different test rigs were requested and obtained from the NASA, the German Aerospace Center (DLR), and the Rolls-Royce PLC.

Contacts:
PGR student: Ram Kumar Venkateswaran (rkv1n20@soton.ac.uk)
Supervisors: Prof. Phillip Joseph (pfj@isvr.soton.ac.uk)
Associate Prof. Dr. Chaitanya Paruchuri (ccp1m17@soton.ac.uk)

References:
V. Ram Kumar, P. F. Joseph, and C. Paruchuri, Estimation of the relative balance between the rotor and the OGV broadband noise, AIAA Aviation Forum, San Diego (USA), 12-16 June (2023).

52. ESTIMATION OF THE RELATIVE BALANCE BETWEEN THE ROTOR AND THE OGV BROADBAND NOISE IN A TURBOFAN ENGINE

53. What information do road users actually need to know?

Delin Wang
University of Southampton

Project objectives and goals

This research explores the fundamental question of what information road users need to know when, in order to safely and efficiently negotiate an increasingly complex road environment.

In the near future, 'road users' will include not just human drivers, pedestrians, and cyclists, but also automated vehicles. Regardless of autonomy levels, all users, human or machine, will require information, such as static road layout information and dynamic interaction data to reduce uncertainty, increase capacity, and ensure safety.

While the rapid development of information technology has given road users the ability to obtain more data, additional data does not necessarily equal more useful information (VTRC, 2019). Indeed, excessive information generation and provision can overburden users (Lerner et al., 2003). It is therefore important to understand exactly what information is actually required by different road users in order to ensure that the right amount of information is provided to the right users in the right places at the right times. Therefore, this research hopes to establish a framework to analyse and define the information needs.

Based on this framework, this research will guide future road infrastructure development by optimizing information and infrastructure provision in order to avoid waste and insufficiency.

Description of method and results

This research adopts a multidimensional analysis framework to identify the fundamental information needs of different road users. The study begins with a comprehensive literature review, focusing on human drivers' information needs. By analysing the information needs across the journey progress and the hierarchy of information, this research develops a two-dimensional framework, as shown in Table 1.

Table 1 Information Needs Framework

	Steps	Strategic	Tactical	Immediate
Pre-Trip	a. Planning	1.Plan a route	2.Update the route	NA
In-Trip	b. Execution	3.Follow the route	4.Adapt instructions	5.Response events
	c. Manoeuvring	NA	6.Adjust operations	7.Complete interactions

It concludes that regardless of the travel mode, human or machine drivers need to know the fundamental seven types of information to meet journey needs, ensuring safety and efficiency. Missing this information in the pre-trip phase leaves road users unprepared and lacking it in the in-trip phase puts them at risk. While different mode drivers may adjust details in specific types of information, the need for route planning, plan execution, and vehicle manoeuvring information remains consistent.

According to this framework, enhancing single types of information provision alone is insufficient. Due to the present technical limitations of machine drivers, information acquisition cannot fully cover the seven types in the framework, so its capabilities are difficult approach those of competent human drivers. Comprehensive information within the framework throughout the journey is essential to human or machine drivers for true safety and efficiency.

References:

Lerner, N.D., Singer, J. and Huey, R. (2003) Additional Investigations on Driver Information Overload. Washington, D.C: National Academy Press (NCHRP report, 488).

VTRC (2019) Providing Traffic Control Device Information in a Connected and Automated Vehicle.

Supervisors

Dr. Ben Waterson and Dr. Simon Blainey

54. Data-driven stochastic model updating with conditional invertible neural networks (cINNs)

Tairan Wang[a] and Sifeng Bi[a]
[a] Department of Aeronautics & Astronautics, University of Southampton
E-mail: tairan.wang@soton.ac.uk; sifeng.bi@soton.ac.uk

This work aims to address the limitations of conventional Bayesian model updating approaches like (1) the curse of dimensionality, and (2) computing the discrepancy between two distributions efficiently, by developing a unique data-driven approach for stochastic model updating (Bi et al., 2023). The recently developed conditional invertible neural network (cINN) (Dinh, Sohl-Dickstein and Bengio, 2017; Ardizzone et al., 2019) is adopted in this study because its unique invertible characteristic enables its application in model updating as an inverse mapper. This allows for the direct prediction of nominal values of calibration parameters based on a set of newly available observation data. This is accomplished through the learning of an invertible probabilistic mapping that establishes a bijective transformation between input parameters and a simple distribution (i.e., latent distribution, normally a standard Gaussian distribution), conditioned on data from simulations/observations.

The cINN framework is composed of two primary components: the Invertible Neural Network (INN) and the Conditional Network. The INN is pivotal in establishing the bidirectional mapping between the model's inputs and latent space. The Conditional Network is capable of processing the raw data collected from simulations/observations to a fixed-size vector with the most informative statistics to be further used as the condition of INN. Both networks are trained jointly in the forward direction and can operate inversely to offer rapid and accurate predictions by given observation data. Once the cINN is well-trained, it can generate posterior distribution conditioned on the observation data without evaluating the likelihood function in the conventional Bayesian inference.

In this study, a novel stochastic model updating framework based on the cINN is developed, as shown in Fig . A classic 3 DOF (degree-of-freedom) spring-mass system was employed as the case study, as shown in Fig . All the springs in the system are assumed to follow Hooks's law and the linear elasticity assumption. The three stiffness coefficients k_1, k_2, and k_3 and the three masses m_1 , m_2 and m_3 are set to be constant variables. The other three stiffness coefficients k_4, k_5, and k_6 are random variables assumed independent with uncertainty to be investigated. The three natural frequencies f_1, f_2, and f_3 are the quantity of interest whose uncertainties are driven by the uncertain parameters. The three stiffness parameters are assumed to follow a pre-determined uniform distribution (prior distribution), and the target distributions are set to be Gaussian distributions with various means and standard deviations. In the training phase, the training data is generated from the prior distribution and the corresponding simulation output of the model. A well-trained cINN can run inversely given a sequence of synthetic observation data to predict the posterior distribution of the input parameter. The obtained posterior distributions are in good agreement with the target distribution and the inference process is very time efficient.

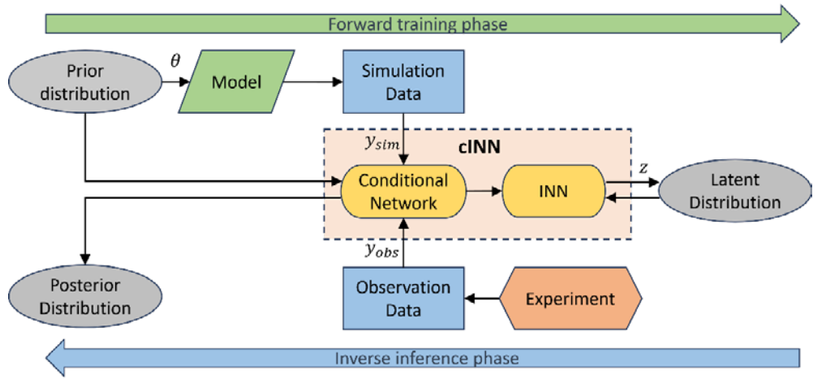

Fig.1 Framework of cINN-based model updating.

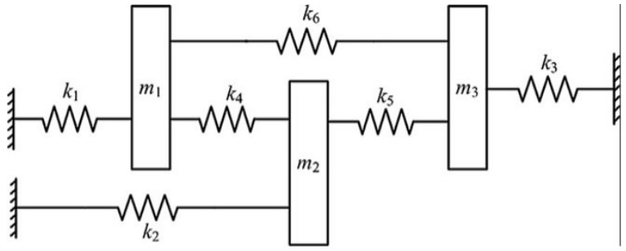

Fig.2 3 DOF spring-mass system.

References:

Ardizzone, L. et al. (2019) 'Guided Image Generation with Conditional Invertible Neural Networks'. arXiv. Available at: http://arxiv.org/abs/1907.02392 (Accessed: 10 November 2023).

Bi, S. et al. (2023) 'Stochastic Model Updating with Uncertainty Quantification: An Overview and Tutorial', Mechanical Systems and Signal Processing, 204, p. 110784. Available at: https://doi.org/10.1016/j.ymssp.2023.110784.

Dinh, L., Sohl-Dickstein, J. and Bengio, S. (2017) 'Density estimation using Real NVP'. arXiv. Available at: http://arxiv.org/abs/1605.08803 (Accessed: 5 November 2023).

55. Validation of Resin Embedding Protocols for Serial Block Face Scanning Electron Microscope of Human Tooth Dentine

Hao Yao Wong[1*], Richard B. Cook[1], Patricia Goggin[2] and James Thompson[2]

[1] Faculty of Engineering and Physical Sciences, University of Southampton, Southampton, UK
[2] Biomedical Imaging Unit, Faculty of Medicine, University of Southampton, Southampton, UK

Background

Dental hypersensitivity is caused by fluid flow triggering the pulpal nerves in open exposed dentinal tubules. Occluding the patent tubules to prevent fluid flow using active ingredients in dentifrices is an established method of treatment. Serial Block Face Scanning Electron Microscopy (SBF-SEM) is an advanced imaging technique used for efficacy evaluation of tubule occlusion levels and penetration depth of active ingredients.

Established protocols for preparing human dentine requires them to be embedded in resin, as this retains their structural integrity during SBF-SEM [1]. Resin embedding ensures that the tubule plugs are held in place during the block face slicing. Current protocols dictate that the samples are to be submerged in a 50/50 mixture of resin and solvent (acetonitrile) to ensure penetration into the tubules, which is then replaced with a full resin formulation prior to polymerization. Concerns were raised that the resin/solvent mix (mainly the acetonitrile) could "wash out" the plugs, and potentially dissolve some material in it.

Objectives and Goals

A small package of work was conducted to investigate the effects of sample preparation on the SBF-SEM results obtained in dentifrice treated dentine. This work should serve as a basis for future hard tissue preparation for SBF-SEM, through validating the need for resin embedding or vice versa.

Methods and Results

Human dentine samples (n=2) were brushed with a hypersensitivity formulation to form tubule occlusion plugs. Both samples were sectioned and divided into 3 preparation groups: (i) Samples embedded in resin as per protocol, (ii) Samples NOT embedded in resin, and (iii) Samples submerged in acetonitrile.

SBF-SEM images with 100nm slice thickness, totalling up to a depth of 40gm, were taken from groups (i) and (ii). This is followed by tubule occlusion comparisons at varying depths using novel image processing techniques. Surface SEM images of samples from group (iii) were taken before and after acetonitrile submersion, to validate the potential loss of material on the sample surface and within the tubules.

Results show no observable loss of material from the sample surface before and after acetonitrile submersion. SBF-SEM results from samples without resin showed a more sporadic spread of occlusion at varying depths. In conclusion, acetonitrile remains a reliable solvent and the study solidifies the need for resin embedding as the results suggest the possibility of debris falling into patent tubules during cutting of the block face.

Potential for Application of Results

The results validate the inherent need and the importance for resin embedding of hard tissue prior to SBF-SEM. The methodology and techniques (both image processing and sample preparation) applied in this work can serve as a basis for further improvements of future dentine occlusion studies.

References:

[1]P. Goggin, E. M. L. Ho, H. Gnaegi, S. Searle, R. O. C. Oreffo, and P. Schneider, "Development of protocols for the first serial block-face scanning electron microscopy (SBF SEM) studies of bone tissue," Bone, vol. 131, p. 115107, 2020/02/01/ 2020, doi: https://doi.org/10.1016/j.bone.2019.115107.

Funding

This project is funded by a CASE studentship with Haleon plc.

56. Metal organic framework-based microfluidic paper-based analytical devices for detecting nutrients in water

Niamh Yates, Dr Adrian Nightingale, Dr Darren Bradshaw and Dr Allison Schaap
University of Southampton
University Road, Southampton, Hampshire, England SO17 1BJ
niamh.yates1@gmail.com | nray1n18@soton.ac.uk

Project objectives and goals

Traditional methods of detecting nutrient levels in water by transporting a sample to a laboratory are limited by the cost and availability of transport (Mahmud et al., 2020). To overcome this, in-situ sensors such as electrochemical sensors can provide real-time and actionable data with a high degree of accuracy and sensitivity. However, in-situ sensors operate using a flow system where the storing of reagents and power can limit their operational lifetimes. In-situ sensors that utilise microfluidics minimise the sample and reagent and therefore minimize the energy required; an example of these is microfluidic paper-based analytical devices (gPADs) that possess additional benefits such as being simple to fabricate and are made of inexpensive materials.

The primary aim for this project is proposed:

To develop gPADs for the in-situ quantification of various nutrients in water, utilising a class of inorganic materials called metal organic frameworks (MOFs) as the detection method. The device should be user-friendly and should be capable of detecting nutrients at typical environmental concentrations.

Description of method and results

The detection of nitrite was chosen to begin this project as a result of the extensive literature utilising MOF-based detection. Deng et al., (2014) fabricated a novel fluorescent probe for the detection of nitrite in meat involving a dye, rhodamine 6G (Rh6G), encapsulated into a well-known water stable MOF, UiO-66-NH2. After successfully replicating the synthesis of the Rh6G@UiO-66-NH2, the ability of the dye@MOF as a sensor for NO2- was then established in solution, as displayed in Fig. 1. With increasing NO2- concentration, the fluorescence intensity ratio of Rh6G@UiO-66-NH2 was quenched.

The next developmental stage involved grafting Rh6G@UiO-66-NH2 onto filter paper; Chi et al., (2013) developed a grafting process by baking another dye@MOF, RhB@UiO-66-NH2, onto functionalised filter paper. A similar synthesis was replicated with Rh6G@UiO-66-NH2, resulting in pink strips of filter paper as displayed in Fig. 2. The response of the Rh6G@UiO-66-NH2 coated functionalised filter paper to nitrite is current, on-going research.

Potential for application of results

Nutrient ions such as nitrite are the foundations of the naturally occurring life cycles within the oceans and seas. However, an excess of these ions following from human activity such as agricultural run-off result in the formation of toxic algal blooms that pollute the coastal waters, often resulting in a loss of biodiversity. Therefore, measuring the concentration of these nutrient ions using gPADs are essential for the understanding and safeguarding against the pollution.

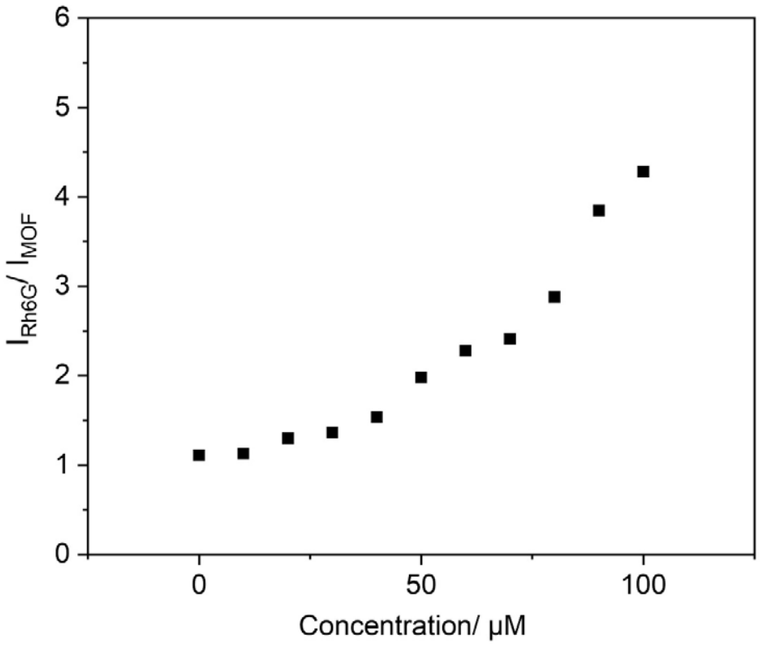

Fig. 1. The trend of fluorescence intensity ratio IRh6G/IMOF with changing nitrite concentration.

Fig. 2. Rh6G@UiO-66-NH2 grafted onto functionalised filter paper by baking in the oven at 60 °C for 30 minutes

References:

M A Parvez Mahmud, Fatemeh Ejeian, Shohreh Azadi, Matthew Myers, Bobby Pejcic, Rouzbeh Abbassi, Amir Razmjou, Mohsen Asadnia, (2020). Recent progress in sensing, nitrate, nitrite, phosphate and ammonium in aquatic environment, Chemosphere, 259:127492, 1-25.

Siyang Deng, Junmei Liu, Dong Han, Xinting Yang, Huan Liu, Chunhui Zhang, Christophe Blecker, (2024). Synchronous fluorescence detection of nitrite in meat products based on dual-emitting dye@MOF and its portable hydrogel test kit, Journal of Hazardous Materials, 463:132898, 1-12.

Jie Chi, Yanyan Song, Liang Feng, (2023). A ratiometric fluorescent paper sensor based on dye-embedded MOF for high-sensitive detection of arginine, 241:115666, 1-8.

Funding body

Southampton Maritime and Marine Institute

56. METAL ORGANIC FRAMEWORK-BASED MICROFLUIDIC PAPER-BASED ANALYTICAL DEVICES FOR DETECTING NUTRIENTS IN WATER

57. Bioproducing succinic acid from hydrolysate of biomass waste in a biofilm reactor

Muhammad Zalkifal
Primary supervisor: Dr Yongqiang Liu – University of Southampton
Co-Supervisor: Dr Mark Shepherd – University of Kent

Summary:

Succinic acid is an important platform chemical and has been identified as one of the top potential chemical building blocks for the future.

Succinic acid is currently manufactured mainly by petrochemical processes. A move from fossil fuel to renewable raw materials for sustainable development has been started for succinic acid fermentation towards a bioeconomy. However, the bioproduction of succinic acid is mainly restricted to conventional feedstock with a batch operation mode at the moment, resulting in low productivity and feedstock competition for food. To explore the economic and environmental feasibility of succinic acid bioproduction with widely available biomass waste, the key technical challenges such as inhibition from biomass hydrolysate and low productivity have to be overcome. Given the aggregation characteristics of some organic acid-producing species such as Actinobacillus succinogenes for succinic acid production under some conditions, this project aims to explore the aggregation potential of Actinobacillus succinogenes and develop either attached biofilm or self-aggregated microbial granules for continuous bioproduction of succinic acid from hydrolysate of biomass waste. The inhibition from hydrolysate and succinic acid in fermentation broth could be alleviated due to the three-dimensional structure formed by cell attachment to support or self-aggregation. Furthermore, this biofilm-based technology can not only retain higher biomass in reactors but also enable continuous fermentation with improved productivity. Apart from biofilm-based process development for continuous fermentation of succinic acid, the analysis of energy performance and CO_2 fixation in the succinic acid production process will be carried out in this project for the comparison with conventional suspended cells-based batch fermentation with glucose as well as the evaluation of the environmental sustainability of the newly developed process.

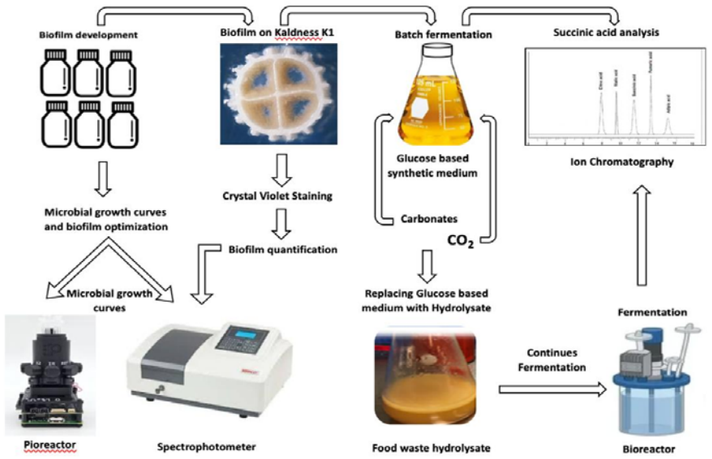

Funders:

UKRI, BBSRC, SoCoBio DTP

58. Probabilistic Assessments of Load Carrying Capacity of Corroded Metallic and Reinforced Concrete (RC) Railway Bridges

Ziliang Zhang
Infrastructure Group, Dept. of Civil, Maritime & Env. Eng., University of Southampton

Extended abstract

Accurate estimation of current/future load carrying capacity of railway bridges has prominent practical implications given the key role they play in transport network resilience. While state-of-the-practice bridge assessments typically do not incorporate degradation as a time-dependent phenomenon, abilities of bridges to safely withstand vertically/laterally exerted forces referencing various damage mechanisms are likely to deteriorate owing to ageing phenomena, e.g., corrosion. The problems studied herein thus focus on the exposure of railway bridges to moderate corrosive environments under Heavy Axle Weight (HAW) train or seismic loads.

Concerning HAW train accessibility, a probabilistic framework estimating future train load capacity (characterised on UK railways as Route Availability, or RA, number) is established and demonstrated on a three-span, half-through girder, metallic railway bridge built in 1903. Load tests carried out in the field assisted appropriate numerical idealisation of the bridge. A novel formulation referred to as Bridge Deterioration Equations (BDE) is proposed, estimating future RA capacity as a function of age and permissible train speed. An increasingly disproportionate impact of corrosion on RA capacity with respect to age is observed, attributing to: (a) nonlinearity in time-dependent corrosion depth models, (b) dependency of critical buckling load of Kirchhoff thin plates on a cubic term of plate-thickness, and (c) interaction between various failure (especially buckling) modes and their relative criticality in relation to nonuniform random spatial distribution of corrosion depth. BDE provides a straightforward information valuable in data-driven decision-making processes for rail infrastructure owners and freight operators.

Concerning seismic resistance, the impact of corrosion on the evolution of hysteretic behaviour, dynamic properties and lateral drift capacities of RC piers reinforced by carbon/stainless steel rebars is studied. Quasi-static cyclic tests carried out in laboratory on 5 large-scale circular RC piers provided physical evidence in developing well-calibrated, fibre-section, beam-column-element models, emphasising corrosion-induced nonuniform geometric-material degradation on critically located rebar and concrete segments. Simulated fibre responses offered explanations to: (a) the trends observed in cyclic degradation of lateral stiffness and natural frequency, and (b) physically observed damage mechanisms, including redistribution of compressive stresses between concrete and rebars, cover/core concrete crushing, and vertical reinforcement yielding/buckling/fracturing. A Matlab App is developed to provide quick references of critical drift ratios using Gaussian Process Regression models trained by datasets derived from a two-stage Latin Hypercube simulation of 175 differently configured hypothetical bridge columns. The impact of corrosion on drift capacity of RC piers, especially well-confined ones designed to modern seismic codes, is overwhelmingly pronounced at an early stage of their service life (e.g., 10-20 years) and can eventually lead to drift capacity reduction of ~70 % over 50 years. This highlights the potential over-boldness of accepting previously established drift limit recommendations, often neglecting age-dependency, in seismic assessment of seemingly young-aged RC bridges.

The gaps addressed herein highlight the importance of assessing age-dependent load carrying capacities of railway bridges with appropriate sophistication; and the established methodologies contribute to a future scope for ultimately moving towards the development of a machine-learning-based expert tool for quick estimations of future load carrying capacity of railway bridges.

Collaborators:

School of Geography and Env. Science, University of Southampton, https://www.southampton.ac.uk/about/faculties-schools-departments/school-of-geography-and-environmental-science

Rail Safety and Standards Board (RSSB), https://www.rssb.co.uk/

Network Rail Ltd., https://www.networkrail.co.uk/

59. Load transfer mechanisms for a transfemoral amputee during ambulation

Kunyi Zheng, Kirstie Devin, Jinghua Tang, Liudi Jiang
University of Southampton

Introduction:

Understanding load transfer mechanisms at lower limb amputee socket interfaces is crucial for socket design evaluations and comfort, leading to enhanced prosthetic limb functionality. To date, most studies have only focused on interface pressure (Paternò et al., 2023) with limited reports on shear, which is known to be associated with the dynamic residual interaction with the socket. This is due to a lack of sensing systems capable of producing multi-directional stresses. A thin and flexible tri-axial pressure and shear (TRIPS) sensing system has been developed and provides the platform to measure multi-directional stress at loaded body interfaces (Laszczak et al., 2016). This enabled the study of complex load transfer mechanism between the ground and socket interface.

Project objectives and goals

This study aims to investigate the relationship between ground reaction forces (GRFs) and interface stress on a transfemoral amputee.

Objectives:

- To measure GRFs and corresponding localised socket interface pressure, and shear, using a TRIPS sensing system, during level walking.
- To evaluate interface stresses and GRFs as a function of gait cycle.

Description of method and results

A left-sided transfemoral amputee participated in this study. Seven level walking trials for the amputee were conducted. A trial is defined as the prosthetic side making contact with a force plate (Fig. 1 inset). TRIPS sensors were mounted to the inner socket wall at key load-bearing sites (Fig. 2 inset). Direction conventions for circumferential shear (SC) and longitudinal shear (SL) are also indicated.

TRIPS sensors and force plate were synchronised and normalised, enabling evaluation of interface pressure and shear and GRFs as a function of gait cycles. Mean and one standard deviation were calculated and analysed.

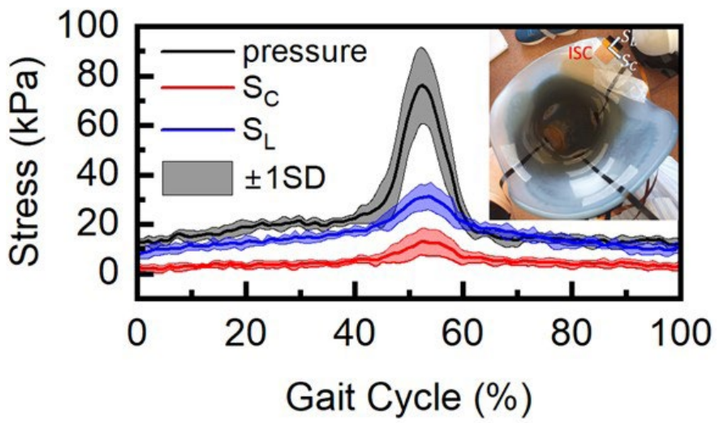

Fig. 1: GRFs as a function of gait cycle. Inset: prosthetic side making contact with force plate.

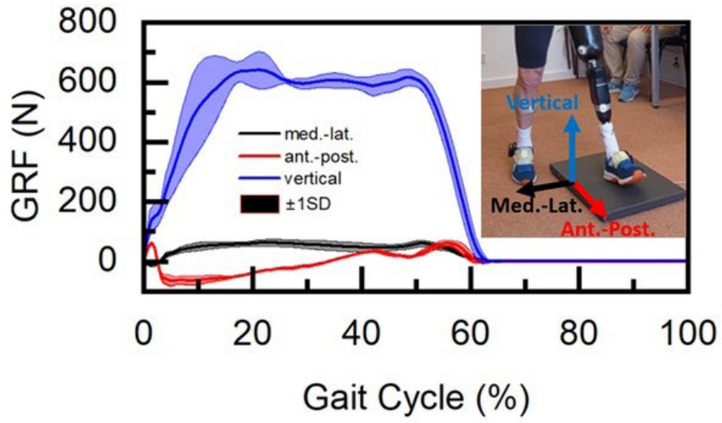

Fig. 2 Pressure-shear as function of gait cycle. Inset: location of the TRIPS sensor.

Fig. 1 shows peak vertical GRF of 728N occurred during weight acceptance phase, while the peak for anterior-posterior and medial-lateral GRFs of 119N and 75N were obtained at initial contact, respectively.

Fig. 2 shows, at ischial seat region, negligible change in stress was observed in most of the stance phase, while 96kPa, 24kPa and 41kPa of peak pressure, SC and SL were obtained, respectively.

Potential for application of results

This preliminary study demonstrated that interface stress adds additional biomechanical insights on how localised anatomical landmark interacts with a socket over a gait cycle, which could not be revealed using a conventional force platform. This underpins the prosthetic limb and socket designs, all leading to enhanced rehabilitation outcomes.

References:

Laszczak, P. et al., (2016). A pressure and shear sensor system for stress measurement at lower limb residuum/socket interface. Medical Engineering & Physics, 38(7), pp.695-700. doi:10.1016/j.medengphy.2016.04.007.

Paternò, L. et al., (2023). Quantitative analysis of interface pressures in transfemoral prosthetic sockets, Prosthetics & Orthotics International, 48(2), pp. 176–183. doi:10.1097/pxr.0000000000000251.

Further information

Kunyi Zheng (E: kz4n20@soton.ac.uk)

Find out more:
www.southampton.ac.uk/engineering

www.linkedin.com/company/school-of-engineering-university-of-southampton